Validation of RNA interference as technique to study CNS anti-obesity drug targets

Margriet van Gestel

Colofon

Cover design Proefschriftmaken.nl || Uitgeverij BOXPress
Cover illustration 'Sweet Dreams' by El van Leersum
Printing & Lay Out Proefschriftmaken.nl || Uitgeverij BOXPress

ISBN: 978-94-6295-154-9

The research described in this thesis was performed at
Brain Center Rudolf Magnus, Department of Translational Neuroscience, University Medical Center Utrecht, Utrecht, the Netherlands

This research was financially supported by
Top Institute Pharma (project T5-210)

Validation of RNA interference as technique to study CNS anti-obesity drug targets

Validatie van RNA interferentie als methode om CZS anti-obesitas doelwitten voor geneesmiddelen te bestuderen

(met een samenvatting in het Nederlands)

Proefschrift

ter verkrijging van de graad van doctor aan de Universiteit Utrecht
op gezag van de rector magnificus, prof.dr. G.J. van der Zwaan,
ingevolge het besluit van het college voor promoties
in het openbaar te verdedigen op

donderdag 30 april 2015 des middags te 12.45 uur

door

Marguérite Alexandra van Gestel

geboren op 26 augustus 1980 te Delft

Promotor: Prof.dr. R.A.H. Adan

Table of contents

CHAPTER 1

General introduction

Based on:
Pharmacological manipulations in animal models of anorexia and binge eating in relation to humans.

van Gestel MA, Kostrzewa E, Adan RA, Janhunen SK

Br J Pharmacol. 2014 Oct;171(20):4767-84

RNA interference

Large-scale genome-wide association studies (GWAS) have dramatically increased the pace of genomic discovery, resulting in the discovery of at least 75 obesity susceptibility loci.[1,2] One next step is to explore the biological function of these associated risk genes. In mice, this is accomplished by homologous recombination in embryonic stem cells. Although it succeeds in complete gene silencing, there are important limitations to the use of the gene knockout technique. If a gene is removed during early development, compensatory mechanisms can mask development of a phenotype as observed in agouti-related protein and neuropeptide Y knockout mice.[3] To overcome this limitation, gene knockdown can be applied, since this can be performed in adult animals. This technique uses the principle of RNA interference (RNAi) to decrease (knockdown) expression of the gene of interest. Gene knockdown has some important advantages compared to the gene knockout technique. It is applicable to multiple species, the extent of knockdown is controllable, it is relatively inexpensive, there is spatial and temporal control and there is no compensation during development by related genes.

RNAi is an evolutionary conserved post-transcriptional gene regulatory mechanism mediated by small, non-coding, inhibitory RNA molecules.[4,5] The introduction of double-stranded (ds) RNA into the cell cytoplasm can trigger a cascade of events resulting in sequence-specific degradation of endogenous mRNAs leading to a reduction in protein levels.[6] Since its discovery in C. Elegans and in mammalian cells, RNAi has become a very powerful and indispensable technique for both determination of gene function and drug target validation.[6,7] The highly specific and selective post-transcriptional gene silencing, which can be applied in a variety of eukaryotic organisms and cultured cells, has allowed for the design of precise targeting tools. This thesis focuses on the optimization of RNA interference using adeno-associated virus (AAV) and its application in drug target discovery in the brain for the development of novel anti- obesity therapies. I will first introduce the principle of RNAi and the use of AAV as vehicle. Next a brief introduction to some basics of regulation of energy balance and how it is measured (in particular feeding behavior) will follow. Finally the outline of this thesis will be described.

Adeno-associated virus (AAV)-mediated RNAi delivery to the central nervous system

The mechanism of RNA interference

RNAi can be elicited endogenously, from transcription of RNA-coding genes in the genome (primary (pri) microRNAs), or exogenously, with a viral infection or with chemically synthesized small interfering RNAs (siRNAs). Direct transfection of chemically synthesized siRNA duplexes will result in a transient effect of RNAi, therefore long-term studies prefer the use of vector-based siRNA delivery. After transfection of the vector, the DNA insert will express a short hairpin (sh) RNA. In contrast to siRNAs, shRNAs are synthesized in the nucleus of cells and are presumably processed similar to the microRNA biogenesis pathway (Figure 1). The primary transcript contains a hairpin like stem-loop structure that is processed by the microprocessor complex containing the RNase III enzyme Drosha and the double-stranded RNA-binding domain protein DGCR8 (Figure 1).[8] The Drosha/DGCR8 complex cleaves the initially transcribed shRNA into export-ready pre-shRNAs with a 2 nucleotide 3' overhang.[9] The pre-shRNA is then transported from the nucleus to the cytoplasm by the RanGTP-dependent dsRNA-binding protein Exportin 5 (Figure 1).[10,11] Cytoplasmic pre-shRNA is then bound by the RNase III enzyme Dicer as part of the RNA-induced silencing complex (RISC) Loading Complex (RLC) including the regulatory domain TRBP and argonaute 2 (Ago2) (Figure 1).[12–14] Dicer cleaves the pre-shRNA loop and processes the pre-shRNA into mature ~21-23 nucleotide shRNA duplexes with short 2 nt 3' overhangs.[15–17] The mature shRNA enters the RISC and binds complementary stretches within the 3'UTR of the target mRNA. RISC-bound mRNA transcripts are suppressed by direct Ago2-catalysed endonucleolytic cleavage of its mRNA target or by triggering deadenylation and decapping.[18–23]

Adeno-associated virus

There are some important limitations to the delivery of dsRNA molecules into the RNAi pathway at the level of Dicer. The main limitations are delivery to different cell types, longevity and the activation of an innate immune response. As mentioned earlier, vector-based siRNA delivery provides a means to study long-term phenotypes. Adeno-associated virus (AAV) currently is one of the most attractive gene transfer tools for RNAi. AAV has been classified as a dependovirus as efficient replication of the AAV genome requires the presence of helper viruses, such as adenovirus, herpesvirus or vaccinia virus.[25–27] Despite estimates that up to 80-90% of humans are seropositive for AAV2, no known pathology is associated with the wild-type virus. The defective replication, persistency and non-pathogenic nature of wild-type AAVs make them an attractive viral vector system for the use of RNAi.

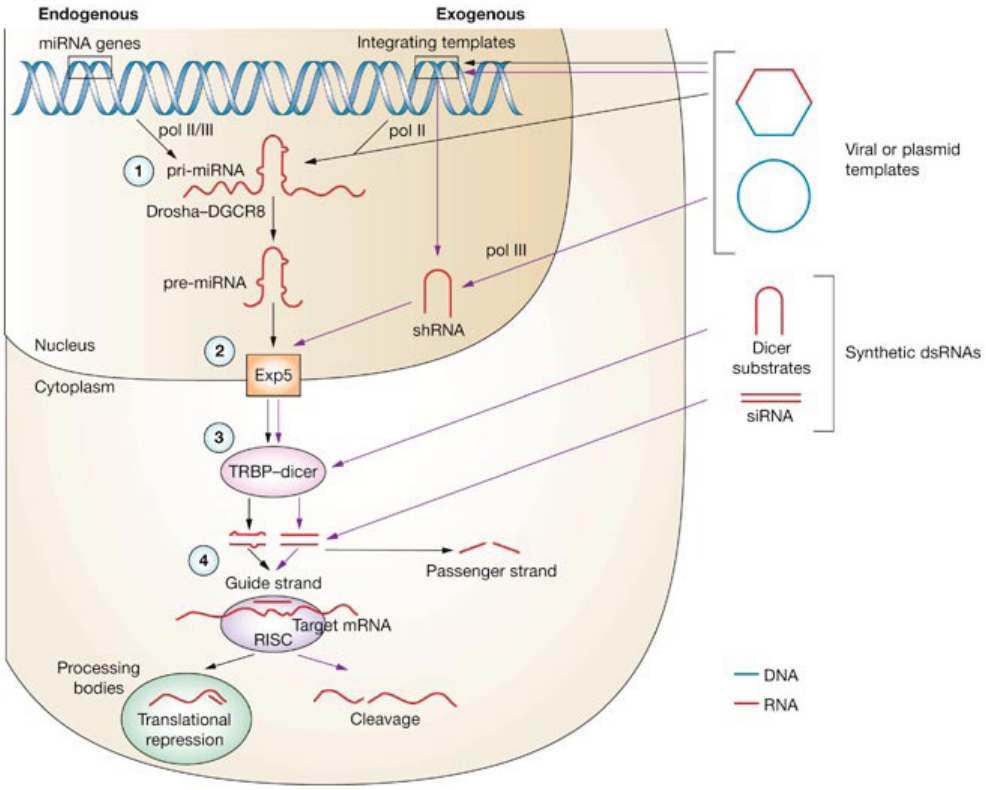

Figure 1. The process of RNA interference and its manipulation

Whereas some nuclear events are unique to the endogenous or the exogenous RNA interference (RNAi) pathway, many nuclear processing steps (1,2) and all cytoplasmic processing steps (3,4) are shared by both pathways. Exogenous RNAi-mediating molecules can follow the miRNA pathway (black arrows) or the siRNA pathway (purple arrows), entering the pathways at different points depending on the specific molecule and delivery vehicle employed. Most endogenous miRNA genes are transcribed by RNA polymerase II before nuclear processing by the Drosha/DGCR8 complex (1). Exogenous miRNAs can be engineered as pri-miRNAs, thereby following the same steps, or as shRNA templates that enter the nucleus but are transcribed by RNA polymerase III, thereby bypassing the nuclear transcriptional and processing machinery employed by the endogenous pathway. All nuclear RNAi-mediating constructs converge in the nuclear export event (2). Once in the cytoplasm, dsRNAs still joined by a loop, whether derived from nuclear processing events or from exogenous delivery as synthetic Dicer substrates, require processing by TRBP–Dicer (3), resulting in separation into two strands. Exogenous siRNAs do not need Dicer processing, and therefore bypass steps 1–3. All dsRNAs converge in loading the guide strand into RISC (4), whereas endogenous miRNAs mostly lead to translational repression, and exogenous dsRNAs to target cleavage. Modified from Gonzalez-Alegre and Paulson, 2007.[24]

AAV belongs to the parvovirus family with a linear single-stranded DNA genome of approximately 4.7-kilobases with two inverted terminal repeats (ITRs) of 145 nucleotides.[28] The ITRs flank two open reading frames - rep (replication) and cap (capsid), encoding non-structural and structural proteins, respectively. The Rep proteins are critical in all aspects of AAV biology. *Rep* encodes four proteins (Rep 78,

Rep 68, Rep 52 and Rep 40), which are controlled by two promoters. The large Rep proteins (Rep 78 and its splice variant Rep 68) are transcribed from the p5 promoter and are essential for replication, transcriptional control and site-specific integration. The small Rep proteins (Rep 52 and its splice variant Rep 40) are controlled by the p19 promoter and are essential for accumulation of viral DNA used for packaging.[29–31] *Cap* encodes three capsid proteins (VP1, VP2 and VP3), which are controlled by the p40 promoter. Although they share the stop codon, they differ because of different splicing and different start codons.[30]

The terminal 125 nucleotides of each ITR form a palindrome, which enables the ITR to form a T-shaped hairpin structure by folding upon itself via base paring.[32] This way the ITR contributes to a self-priming act by providing a 3'OH onto which the DNA polymerase can synthesize a second strand. In addition, the ITRs contain Rep binding sites (RBS) and a specific cleavage site for the bound Rep, a terminal resolution site (TRS).[33,34] Rep 78 and 68 can bind the RBS and exert ATPase, helicase, and strand-specific/site-specific endonuclease activities. The TRS is identical to a sequence in human chromosome 19 (AAVS1) and facilitates integration of the viral genome.

AAV Tropism

AAV2 is the most widely used serotype to transduce the central nervous system. AAV2-based vectors mediate stable and long-term gene expression in both dividing and non-dividing mammalian cells.[35,36] However, major drawbacks of AAV2-based vectors are the selective tissue tropism, the limited transduction efficacy and the high prevalence of neutralizing antibodies.[37–39] To overcome these disadvantages, the AAV2 vector has been pseudotyped with viral capsids from different AAV serotypes. In recent years numerous AAV serotypes have been described with variable tropism. The general genome organization has been conserved across the different serotypes, which primarily differ in capsid surface properties.[40–42] AAV 1-9 share less than 45% homology in the amino acid sequence of the capsid proteins.[43–47] This capsid is a critical determinant of differential cell tropism and transduction efficiency because of its interaction with host cell factors, including cell surface receptors and co-receptors. AAV2 and 3 bind primarily to heparin sulfate proteoglycans and co-receptors, including aVb integrin, fibroblast or hepatocyte growth factor receptors and a laminin receptor, enhance internalization of AAV2.[48–52] The laminin receptor is also known to interact with AAV3, 8 and 9.[52] AAV1, 4, 5 and 6 lack heparin binding animo acids and utilize sialic acid-containing glycoproteins for binding and transduction.[53–58] The platelet-derived growth factor receptor has been shown to serve as a co-receptor for AAV5.[59] AAV9 binds primarily to terminal N-linked galactose.[60]

To optimize AAV-mediated RNAi in the brain, AAV serotypes have been studied extensively for their tropism and transduction efficiency. Different serotypes have been shown to effectively transduce the hypothalamus,[61] striatum,[41,62–64] hippocampus,[41,62,65–67] substantia nigra[62,65,67,68] and red nucleus[69].

Recombinant AAV

Recombinant AAV (rAAV) vector production is relatively straightforward owing to the simplicity of the AAV genome. The ITRs flanking the two viral genes of the wildtype virus are the only *cis*-acting elements necessary for genome rescue and virus replication and encapsidation.[70,71] Expression cassettes of ~5 kb, containing a promoter and a gene of interest, can be introduced between the ITRs after removal of the rep and cap open reading frames.[72] The foreign DNA flanked by parental ITRs can be rescued upon exposure to a helper virus or plasmid containing the original viral genes for replication and packaging. The recombinant viral genome can be replicated and encapsidated into AAV viral particles as long as the helper virus provides AAV rep en cap gene products in *trans*.[71] These viral particles will be replication deficient, because their genome lacks the genes necessary for replication and packaging. Recombinant AAV vectors will remain predominantly episomal because of the removal of the *rep* and *cap* open reading frames.

Neurobiology of energy balance

Overweight and obesity are increasingly major health problems worldwide. According to the World Health Organization about 1.4 billion people are overweight and approximately one third of them are obese. Between 1980 and 2008, the worldwide prevalence of obesity has nearly doubled.[73] Food intake and energy expenditure, consisting of resting metabolism, physical activity and the thermogenic effect of food, need to be in balance to maintain a stable and normal body weight. In obesity, this balance is shifted by an excessive food intake and decreased energy expenditure. Lesioning and electrical stimulation studies have indicated that separate, partly overlapping, neural circuits of the hypothalamus and brainstem regulate meal initiation and termination, respectively.[74–83] Although it is evident that environmental factors play an important role in the increasing prevalence of obesity, individuals may show different responses to obesogenic environmental conditions due to genetic variation. Two genes that are implicated in obesity are the leptin receptor gene, *lepr*, and the fat mass and obesity-associated gene, *FTO*.

Leptin Receptor (LepR)

Energy homeostasis is regulated by a negative feedback system from humoral adiposity signals and the brain can adjust energy intake in response to changing energy requirements. A key hormone in energy balance is the adiposity-derived hormone leptin, which circulates in the blood in proportion to the adipose mass.[84,85] Leptin acts

via neurons involved in the regulation of energy balance[86,87] to decrease food intake and to increase energy expenditure.[88–90] Impaired central leptin signaling will result in hyperphagia and obesity.[84,91–93] Leptin is transported across the blood brain barrier and binds to the leptin receptor (LepR). Alternative splicing of the *lepr* gene generates six LepR isoforms (LepRa-f). The long LepRb is the only isoform containing functional Janus kinase-2 (JAK2) and signaling transducer and activator of transcription-3 (STAT3) binding sites. Injection of leptin into the ventral tegmental area (VTA) leads to increased levels of phosphorylated STAT3 and activation of JAK2 signaling pathways.[94,95] Leptin binding to LepRb leads to the recruitment and activation of JAK2 to promote the phosphorylation of JAK2 and three tyrosine residues (985, 1077 and 1138); each of these phosphorylation sites mediates a different aspect of downstream LepR signaling with distinct physiological leptin functions.

Leptin acts directly on the arcuate nucleus of the hypothalamus, the VTA within the midbrain and the nucleus of the solitary track within the hindbrain. Although leptin action in hypothalamic regions is firmly established, identification of the physiological function of leptin in the VTA midbrain has long been understudied. Mesolimbic dopamine neurons in the VTA, which project to limbic regions including the amygdala, nucleus accumbens and prefrontal cortex, play an important role in the regulation of emotion and reward. The LepR is expressed in the VTA and 75-90% of the LepR-positive neurons are dopaminergic.[96–98] Leptin injections in the ventricle and in the VTA result in decreased food intake and body weight, while overall locomotor activity is unchanged.[94,99,100] Ventricular leptin injections decrease response rates on a progressive ratio task, indicating a decreased motivation for food reward.[101] rAAV-mediated overexpression of leptin in the rat VTA resulted in a lower bodyweight gain compared to controls.[102] Divergent results are seen after decreased VTA leptin signaling. rAAV-mediated knockdown of leptin in the VTA increases food intake, locomotor activity and sensitivity to highly palatable foods.[96] Knockout animals lacking the LepR in dopaminergic neurons in the VTA show no changes in body weight, food intake, food reward or locomotor activity. The discrepancies might be explained by technical differences between these studies. rAAV-mediated knockdown is not restricted to the dopaminergic neurons. Furthermore, species differences or compensatory mechanisms can account for the different results. The specific role of LepR signaling in mesolimbic dopamine neurons in the regulation of energy balance still needs to be unraveled.

Fat mass and obesity-associated gene (FTO)

The fat mass and obesity-associated gene *(FTO)* is a large gene located on human chromosome 16 with nine exons. In 2007, *FTO* was identified as the first GWAS-identified obesity-susceptibility gene.[103–105] The common variants in the first intron of *FTO* were originally discovered through a GWAS of type 2 diabetes mellitus.[103] Correcting

for BMI eliminated the association of the single nucleotide polymorphisms with type 2 diabetes, indicating that the association between *FTO* and type 2 diabetes was mediated through obesity. An increased BMI of approximately 0.4 kg/m2 per risk allele results from these common variants.[103] FTO has been predicted to be a 2-oxoglutarate (2-OG) Fe(II) dependent nucleic acid demethylase of DNA and RNA.[106,107] *In vitro* studies have shown, that FTO can catalyze the demethylation of thymidine and uracil.[106,107] It is suggested that FTO may influence the expression of genes implicated in energy balance by nucleic acid repair or modification.[106]

FTO is widely expressed throughout peripheral tissues and the brain, especially in the hypothalamic arcuate (ARC), paraventricular, dorsomedial (DMH) and ventromedial (VMH) nuclei[106,108] and expression is affected by nutritional status[106,109–111]. FTO-deficient mice and mice with a missense mutation in the mouse *FTO* gene are protected from high fat diet-induced obesity by a higher level of energy expenditure.[112,113] Recent studies, however, suggest that the involvement of *FTO* in a disturbed energy balance in humans is due to changes in mechanisms underlying energy intake and not energy expenditure.[114–124]

Interestingly, fasting results in decreased hypothalamic FTO mRNA expression in mice,[109] but increased mRNA levels in rats[111]. These differences might be explained by interspecies differences or by a different timing in sample collection. If a period of fasting results in upregulation of *FTO* in rats, this suggests that FTO stimulates food intake. However, overexpression of FTO in the rat ARC results in decreased food intake, while AAV-mediated knockdown of FTO increases food intake.[110] These contradictory findings might be explained by the fact that *FTO* manipulations are restricted to the ARC, indicating the need to study gene function in different areas of the brain.

Monitoring feeding behavior

Concepts of food intake

Richter's classic experiments indicates that food and water intake in all mammals is episodic, not continuous.[125] Episodes of feeding and drinking result from ongoing interactive mechanisms, which either stimulate these behaviors (hunger, thirst) or restrain them (satiety and satiation). In rats, daily food intake occurs in series of meals separated by intermeal intervals and overall intake consists of two components, meal size and meal frequency.[126] These two components can be separately manipulated, suggesting regulation via separate physiological processes.[126]

Rats display a circadian rhythm in active feeding behavior and the majority of intake occurs during the dark period, after which food intake is minimal until occasional meals are again consumed during the latter part of the light phase (Figure 2).[126,127] Meal size

is positively correlated with the duration of postmeal interval.[79,128] This postprandial correlation is thought to reflect the action of meal-initiated metabolic events on the induction and maintenance of intermeal satiety.

Monitoring feeding behavior in animals

Feeding behavior can be monitored automatically and continuously every few seconds or minutes or by weighing food pellets or mash manually at selected time-points once or twice per day. Automated monitoring improves throughput and accuracy of measurements and reduces manual work and stress caused by human interference. Large numbers of animals can be monitored over long periods of time under conditions supporting animals' normal stress-free behavior.

Unlike manual recording, automatic monitoring records meal patterning, consisting of meal size and meal frequency for each individual animal. Various automated monitoring methods have been used to study feeding behavior in rodents. There are (1) operant methods, in which the animal presses a bar to obtain the food[129,130]; (2) devices which record the presence of either the whole animal inside a feeding chamber[131,132] or the animal's head over the food cup[133]; (3) devices which detect the animal's contact with the food, commonly known as eatometers[134–136]; (4) pellet-detecting eatometers which deliver a pellet each time one is eaten[135,136]; and (5) electronic balances which continuously measure the weight of the food and relay the information to a computer[127,137–139.]

The automated electronic food weighing system in rats gives continuous data from an animal's food intake and meal patterning.[127,139–143] A meal is defined as a feeding episode, e.g. with a minimal consumption of 0.5g chow and a 5min intermeal interval, and information is sent every 12sec to a computer. Figure 2 shows an example of 24h data from a rat whose feeding, drinking and locomotor behavior and core body temperature were automatically recorded. A lickometer, which monitors contact with the nipple of a water bottle, was combined with the food weighing system to investigate the animal's drinking behavior (Figure 2). Telemetric transmitters in the intraperitoneal cavity simultaneously monitored locomotor activity and core body temperature (Figure 2). Feeding behavior consisted of meals of different sizes and meals were followed by varying intermeal intervals (Figure 2). Figure 2 shows that most feeding behavior occurred during the dark period and drinking behavior often followed a meal. The rat was most active during the dark period and particularly at the time when it consumed a meal. Core body temperature rose after these active feeding periods (Figure 2). Automated systems can be used for the monitoring of different components of energy expenditure after various acute or chronic drug treatments[127,139,144] or local injections of compounds in the activity-based anorexia model[145].

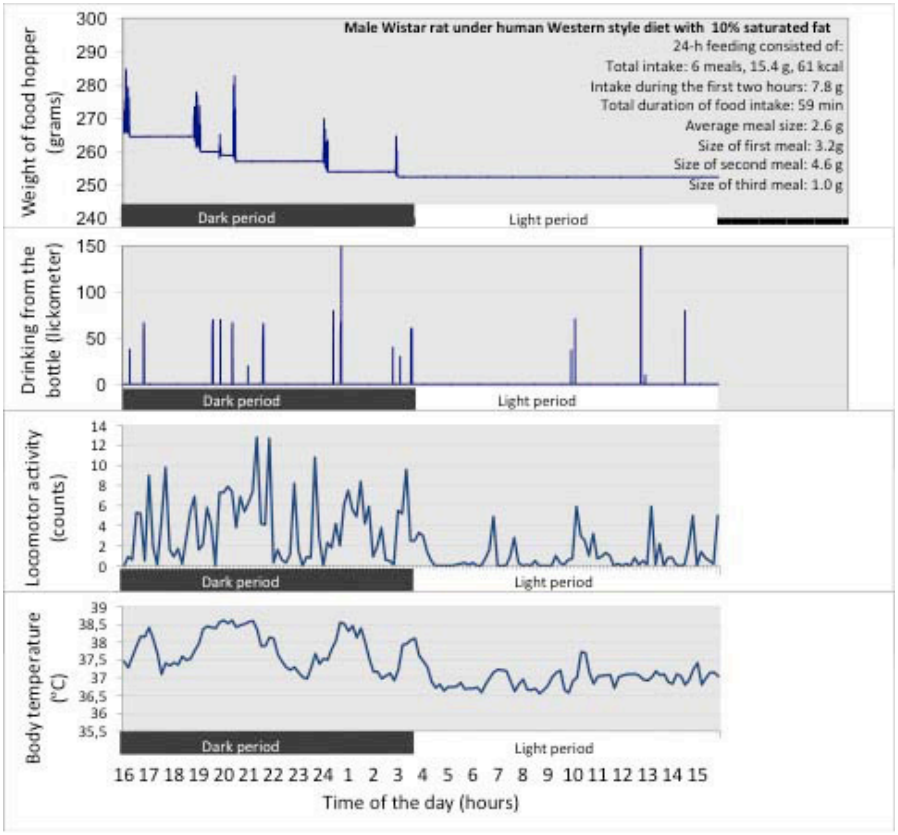

Figure 2. 24h behavioral data from one naïve male Wistar rat using automated monitoring system.

Food intake was detected by automated weighing of the food hopper and water intake was measured by recording the animal's contact with bottle nipple by lickometer. Each burst represents a meal or drinking session. Locomotor activity (counts) and core body temperature (degrees Celsius) were measured by telemetric transmitters. All data were recorded to a computer. Dark bar represents the dark period (lights off, 16:00-04:00) and light bar represents the light period (lights on, 04:00-16:00).

Aims and outlines of this study

RNA interference offers the opportunity to unravel the roles of genes in a specific area of the brain. Genes implicated in energy balance are perfect targets for the application of RNA interference as their phenotypes can be easily monitored and the neural circuits involved in energy homeostasis are well described. Energy homeostasis is here studied in a rat model, since recording of feeding in rats is more accurate than in mice and the size of the rat's brain allows more precise injection into brain areas. The overall aim of this thesis was to optimize AAV-mediated knockdown of obesity-associated genes.

In order to achieve this goal different AAV serotypes commonly used to transfect the brain were injected into the VMH to determine transduction efficiency. To evaluate

biosafety, half-life was calculated after injection of the AAV serotypes in the blood. These experiments are described in **chapter two**.

Unfortunately, the AAV-mediated delivery of shRNAs to the central nervous system resulted in toxicity. To elucidate the cause of the observed toxicity, rats received a unilateral injection with an AAV carrying an shRNA and a control AAV on the other side. In situ hybridization on microRNA-124 was performed to investigate the consequences of shRNA delivery to a neuron for microRNA expression. This study shows an shRNA-mediated oversaturation of the microRNA pathway and the results are described in **chapter three**.

As AAV-mediated knockdown has become a common method to determine gene function, it is important to determine whether the observed toxicity can result in a false phenotype. **Chapter four** describes how an AAV encoding an shRNA targeting the LepR results in a false phenotype.

A solution to the shRNA-mediated oversaturation of the microRNA pathway is to place the shRNA in a microRNA background. Using this technique, the role of *FTO* in the VMH in the regulation of energy balance was studied. Results from this study are described in **chapter five**.

Finally, **chapter six** summarizes and discusses the main findings of these studies.

References

1. Day, F. R. & Loos, R. J. F. Developments in obesity genetics in the era of genome-wide association studies. *J. Nutr. Nutr.* **4,** 222–238 (2011).
2. Lu, Y. & Loos, R. J. Obesity genomics: assessing the transferability of susceptibility loci across diverse populations. *Genome Med.* **5,** 55 (2013).
3. Qian, S. *et al.* Neither agouti-related protein nor neuropeptide Y is critically required for the regulation of energy homeostasis in mice. *Mol. Cell. Biol.* **22,** 5027–5035 (2002).
4. Meister, G. & Tuschl, T. Mechanisms of gene silencing by double-stranded RNA. *Nature* **431,** 343–349 (2004).
5. Hannon, G. J. & Rossi, J. J. Unlocking the potential of the human genome with RNA interference. *Nature* **431,** 371–378 (2004).
6. Elbashir, S. M. *et al.* Duplexes of 21-nucleotide RNAs mediate RNA interference in cultured mammalian cells. *Nature* **411,** 494–498 (2001).
7. Fire, A. *et al.* Potent and specific genetic interference by double-stranded RNA in Caenorhabditis elegans. *Nature* **391,** 806–811 (1998).
8. Lee, Y. *et al.* The nuclear RNase III Drosha initiates microRNA processing. *Nature* **425,** 415–419 (2003).
9. Zhang, H., Kolb, F. A., Brondani, V., Billy, E. & Filipowicz, W. Human Dicer preferentially cleaves dsRNAs at their termini without a requirement for ATP. *EMBO J.* **21,** 5875–5885 (2002).
10. Yi, R., Qin, Y., Macara, I. G. & Cullen, B. R. Exportin-5 mediates the nuclear export of pre-microRNAs and short hairpin RNAs. *Genes Dev.* **17,** 3011–3016 (2003).
11. Lund, E., Güttinger, S., Calado, A., Dahlberg, J. E. & Kutay, U. Nuclear export of microRNA precursors. *Science* **303,** 95–98 (2004).
12. Chendrimada, T. P. *et al.* TRBP recruits the Dicer complex to Ago2 for microRNA processing and gene silencing. *Nature* **436,** 740–744 (2005).
13. Gregory, R. I., Chendrimada, T. P., Cooch, N. & Shiekhattar, R. Human RISC couples microRNA biogenesis and posttranscriptional gene silencing. *Cell* **123,** 631–640 (2005).
14. Maniataki, E. & Mourelatos, Z. A human, ATP-independent, RISC assembly machine fueled by pre-miRNA. *Genes Dev.* **19,** 2979–2990 (2005).
15. Hutvágner, G. *et al.* A cellular function for the RNA-interference enzyme Dicer in the maturation of the let-7 small temporal RNA. *Science* **293,** 834–838 (2001).
16. Ketting, R. F. *et al.* Dicer functions in RNA interference and in synthesis of small RNA involved in developmental timing in C. elegans. *Genes Dev.* **15,** 2654–2659 (2001).
17. Lee, Y. S. *et al.* Distinct roles for Drosophila Dicer-1 and Dicer-2 in the siRNA/miRNA silencing pathways. *Cell* **117,** 69–81 (2004).
18. Chen, C.-Y. A., Zheng, D., Xia, Z. & Shyu, A.-B. Ago-TNRC6 triggers microRNA-mediated decay by promoting two deadenylation steps. *Nat. Struct. Mol. Biol.* **16,** 1160–1166 (2009).
19. Braun, J. E., Huntzinger, E., Fauser, M. & Izaurralde, E. GW182 proteins directly recruit cytoplasmic deadenylase complexes to miRNA targets. *Mol. Cell* **44,** 120–133 (2011).
20. Chekulaeva, M. *et al.* miRNA repression involves GW182-mediated recruitment of CCR4-NOT through conserved W-containing motifs. *Nat. Struct. Mol. Biol.* **18,** 1218–1226 (2011).
21. Fabian, M. R. *et al.* miRNA-mediated deadenylation is orchestrated by GW182 through two conserved motifs that interact with CCR4-NOT. *Nat. Struct. Mol. Biol.* **18,** 1211–1217 (2011).
22. Piao, X., Zhang, X., Wu, L. & Belasco, J. G. CCR4-NOT deadenylates mRNA associated with RNA-induced silencing complexes in human cells. *Mol. Cell. Biol.* **30,** 1486–1494 (2010).

23. Behm-Ansmant, I. *et al.* mRNA degradation by miRNAs and GW182 requires both CCR4:NOT deadenylase and DCP1:DCP2 decapping complexes. *Genes Dev.* **20,** 1885–1898 (2006).
24. Gonzalez-Alegre, P. & Paulson, H. L. Technology Insight: therapeutic RNA interference—how far from the neurology clinic? *Nat. Clin. Pract. Neurol.* **3,** 394–404 (2007).
25. Hoggan, M. D., Blacklow, N. R. & Rowe, W. P. Studies of small DNA viruses found in various adenovirus preparations: physical, biological, and immunological characteristics. *Proc. Natl. Acad. Sci. U. S. A.* **55,** 1467–1474 (1966).
26. Buller, R. M. L., Janik, J. E., Sebring, E. D. & Rose, J. A. Herpes Simplex Virus Types 1 and 2 Completely Help Adenovirus-Associated Virus Replication. *J. Virol.* **40,** 241–247 (1981).
27. Schlehofer, J. R., Ehrbar, M. & zur Hausen, H. Vaccinia virus, herpes simplex virus, and carcinogens induce DNA amplification in a human cell line and support replication of a helpervirus dependent parvovirus. *Virology* **152,** 110–117 (1986).
28. Srivastava, A., Lusby, E. W. & Berns, K. I. Nucleotide sequence and organization of the adeno-associated virus 2 genome. *J. Virol.* **45,** 555–564 (1983).
29. Grimm, D. Production methods for gene transfer vectors based on adeno-associated virus serotypes. *Methods* **28,** 146–157 (2002).
30. Büning, H. *et al.* Receptor targeting of adeno-associated virus vectors. *Gene Ther.* **10,** 1142–1151 (2003).
31. Balagúe, C., Kalla, M. & Zhang, W. W. Adeno-associated virus Rep78 protein and terminal repeats enhance integration of DNA sequences into the cellular genome. *J. Virol.* **71,** 3299–3306 (1997).
32. Russell, D. W. & Kay, M. A. Adeno-Associated Virus Vectors and Hematology. *Blood* **94,** 864–874 (1999).
33. Young, S. M., McCarty, D. M., Degtyareva, N. & Samulski, R. J. Roles of adeno-associated virus Rep protein and human chromosome 19 in site-specific recombination. *J. Virol.* **74,** 3953–3966 (2000).
34. Young, S. M. & Samulski, R. J. Adeno-associated virus (AAV) site-specific recombination does not require a Rep-dependent origin of replication within the AAV terminal repeat. *Proc. Natl. Acad. Sci. U. S. A.* **98,** 13525–13530 (2001).
35. Kaplitt, M. G. *et al.* Long-term gene expression and phenotypic correction using adeno-associated virus vectors in the mammalian brain. *Nat. Genet.* **8,** 148–154 (1994).
36. McCown, T. J., Xiao, X., Li, J., Breese, G. R. & Jude Samulski, R. Differential and persistent expression patterns of CNS gene transfer by an adeno-associated virus (AAV) vector. *Brain Res.* **713,** 99–107 (1996).
37. Chirmule, N. *et al.* Immune responses to adenovirus and adeno-associated virus in humans. *Gene Ther.* **6,** 1574–1583 (1999).
38. Erles, K., Sebökovà, P. & Schlehofer, J. R. Update on the prevalence of serum antibodies (IgG and IgM) to adeno-associated virus (AAV). *J. Med. Virol.* **59,** 406–411 (1999).
39. Moskalenko, M. *et al.* Epitope Mapping of Human Anti-Adeno-Associated Virus Type 2 Neutralizing Antibodies: Implications for Gene Therapy and Virus Structure. *J. Virol.* **74,** 1761–1766 (2000).
40. Zincarelli, C., Soltys, S., Rengo, G. & Rabinowitz, J. E. Analysis of AAV serotypes 1-9 mediated gene expression and tropism in mice after systemic injection. *Mol. Ther. J. Am. Soc. Gene Ther.* **16,** 1073–1080 (2008).
41. Cearley, C. N. & Wolfe, J. H. Transduction Characteristics of Adeno-associated Virus Vectors Expressing Cap Serotypes 7, 8, 9, and Rh10 in the Mouse Brain. *Mol. Ther.* **13,** 528–537 (2006).
42. Wu, Z., Asokan, A. & Samulski, R. J. Adeno-associated virus serotypes: vector toolkit for human gene therapy. *Mol. Ther. J. Am. Soc. Gene Ther.* **14,** 316–327 (2006).

43. Chiorini, J. A., Yang, L., Liu, Y., Safer, B. & Kotin, R. M. Cloning of adeno-associated virus type 4 (AAV4) and generation of recombinant AAV4 particles. *J. Virol.* **71,** 6823–6833 (1997).
44. Rutledge, E. A., Halbert, C. L. & Russell, D. W. Infectious clones and vectors derived from adeno-associated virus (AAV) serotypes other than AAV type 2. *J. Virol.* **72,** 309–319 (1998).
45. Chiorini, J. A., Kim, F., Yang, L. & Kotin, R. M. Cloning and characterization of adeno-associated virus type 5. *J. Virol.* **73,** 1309–1319 (1999).
46. Gao, G.-P. *et al.* Novel adeno-associated viruses from rhesus monkeys as vectors for human gene therapy. *Proc. Natl. Acad. Sci. U. S. A.* **99,** 11854–11859 (2002).
47. Gao, G. *et al.* Clades of Adeno-associated viruses are widely disseminated in human tissues. *J. Virol.* **78,** 6381–6388 (2004).
48. Summerford, C. & Samulski, R. J. Membrane-associated heparan sulfate proteoglycan is a receptor for adeno-associated virus type 2 virions. *J. Virol.* **72,** 1438–1445 (1998).
49. Summerford, C., Bartlett, J. S. & Samulski, R. J. V 5 integrin: a co-receptor for adeno-associated virus type 2 infection. *Nat. Med.* **5,** 78–82 (1999).
50. Qing, K. *et al.* Human fibroblast growth factor receptor 1 is a co-receptor for infection by adeno-associated virus 2. *Nat. Med.* **5,** 71–77 (1999).
51. Kashiwakura, Y. *et al.* Hepatocyte growth factor receptor is a coreceptor for adeno-associated virus type 2 infection. *J. Virol.* **79,** 609–614 (2005).
52. Akache, B. *et al.* The 37/67-kilodalton laminin receptor is a receptor for adeno-associated virus serotypes 8, 2, 3, and 9. *J. Virol.* **80,** 9831–9836 (2006).
53. Rabinowitz, J. E. *et al.* Cross-Packaging of a Single Adeno-Associated Virus (AAV) Type 2 Vector Genome into Multiple AAV Serotypes Enables Transduction with Broad Specificity. *J. Virol.* **76,** 791–801 (2002).
54. Negishi, A. *et al.* Analysis of the interaction between adeno-associated virus and heparan sulfate using atomic force microscopy. *Glycobiology* **14,** 969–977 (2004).
55. Walters, R. W. *et al.* Binding of Adeno-associated Virus Type 5 to 2,3-Linked Sialic Acid Is Required for Gene Transfer. *J. Biol. Chem.* **276,** 20610–20616 (2001).
56. Kaludov, N., Brown, K. E., Walters, R. W., Zabner, J. & Chiorini, J. A. Adeno-Associated Virus Serotype 4 (AAV4) and AAV5 Both Require Sialic Acid Binding for Hemagglutination and Efficient Transduction but Differ in Sialic Acid Linkage Specificity. *J. Virol.* **75,** 6884–6893 (2001).
57. Chen, S. *et al.* Efficient Transduction of Vascular Endothelial Cells with Recombinant Adeno-Associated Virus Serotype 1 and 5 Vectors. *Hum. Gene Ther.* **16,** 235–247 (2005).
58. Wu, Z., Miller, E., Agbandje-McKenna, M. & Samulski, R. J. Alpha2,3 and alpha2,6 N-linked sialic acids facilitate efficient binding and transduction by adeno-associated virus types 1 and 6. *J. Virol.* **80,** 9093–9103 (2006).
59. Pasquale, G. D. *et al.* Identification of PDGFR as a receptor for AAV-5 transduction. *Nat. Med.* **9,** 1306–1312 (2003).
60. Shen, S., Bryant, K. D., Brown, S. M., Randell, S. H. & Asokan, A. Terminal N-linked galactose is the primary receptor for adeno-associated virus 9. *J. Biol. Chem.* **286,** 13532–13540 (2011).
61. De Backer, M. W. A., Brans, M. A. D., Luijendijk, M. C., Garner, K. M. & Adan, R. A. H. Optimization of adeno-associated viral vector-mediated gene delivery to the hypothalamus. *Hum. Gene Ther.* **21,** 673–682 (2010).
62. Burger, C. *et al.* Recombinant AAV Viral Vectors Pseudotyped with Viral Capsids from Serotypes 1, 2, and 5 Display Differential Efficiency and Cell Tropism after Delivery to Different Regions of the Central Nervous System. *Mol. Ther.* **10,** 302–317 (2004).

63. Sondhi, D. *et al.* Enhanced survival of the LINCL mouse following CLN2 gene transfer using the rh.10 rhesus macaque-derived adeno-associated virus vector. *Mol. Ther. J. Am. Soc. Gene Ther.* **15,** 481–491 (2007).

64. Reimsnider, S., Manfredsson, F. P., Muzyczka, N. & Mandel, R. J. Time course of transgene expression after intrastriatal pseudotyped rAAV2/1, rAAV2/2, rAAV2/5, and rAAV2/8 transduction in the rat. *Mol. Ther. J. Am. Soc. Gene Ther.* **15,** 1504–1511 (2007).

65. Klein, R. L. *et al.* Efficient neuronal gene transfer with AAV8 leads to neurotoxic levels of tau or green fluorescent proteins. *Mol. Ther. J. Am. Soc. Gene Ther.* **13,** 517–527 (2006).

66. Klein, R. L., Dayton, R. D., Tatom, J. B., Henderson, K. M. & Henning, P. P. AAV8, 9, Rh10, Rh43 vector gene transfer in the rat brain: effects of serotype, promoter and purification method. *Mol. Ther. J. Am. Soc. Gene Ther.* **16,** 89–96 (2008).

67. Taymans, J.-M. *et al.* Comparative analysis of adeno-associated viral vector serotypes 1, 2, 5, 7, and 8 in mouse brain. *Hum. Gene Ther.* **18,** 195–206 (2007).

68. McFarland, N. R., Lee, J.-S., Hyman, B. T. & McLean, P. J. Comparison of transduction efficiency of recombinant AAV serotypes 1, 2, 5, and 8 in the rat nigrostriatal system. *J. Neurochem.* **109,** 838–845 (2009).

69. Ehlert, E. M., Eggers, R., Niclou, S. P. & Verhaagen, J. Cellular toxicity following application of adeno-associated viral vector-mediated RNA interference in the nervous system. *BMC Neurosci.* **11,** 20 (2010).

70. Samulski, R. J., Srivastava, A., Berns, K. I. & Muzyczka, N. Rescue of adeno-associated virus from recombinant plasmids: Gene correction within the terminal repeats of AAV. *Cell* **33,** 135–143 (1983).

71. Samulski, R. J., Chang, L. S. & Shenk, T. A recombinant plasmid from which an infectious adeno-associated virus genome can be excised in vitro and its use to study viral replication. *J. Virol.* **61,** 3096–3101 (1987).

72. Muzyczka, N. Use of adeno-associated virus as a general transduction vector for mammalian cells. *Curr. Top. Microbiol. Immunol.* **158,** 97–129 (1992).

73. Finucane, M. M. *et al.* National, regional, and global trends in body-mass index since 1980: systematic analysis of health examination surveys and epidemiological studies with 960 country-years and 9·1 million participants. *Lancet* **377,** 557–567 (2011).

74. Hetherington, A. W. & Ranson, S. W. Hypothalamic lesions and adiposity in the rat. *Anat. Rec.* **78,** 149–172 (1940).

75. Brobeck, J. R., Tepperman, J. & Long, C. N. H. Experimental Hypothalamic Hyperphagia in the Albino Rat. *Yale J. Biol. Med.* **15,** 831–853 (1943).

76. Anand, B. K. & Brobeck, J. R. Hypothalamic Control of Food Intake in Rats and Cats. *Yale J. Biol. Med.* **24,** 123–140 (1951).

77. Hoebel, B. G. & Teitelbaum, P. Weight regulation in normal and hypothalamic hyperphagic rats. *J. Comp. Physiol. Psychol.* **61,** 189–193 (1966).

78. Herberg, L. J. & Blundell, J. E. Lateral hypothalamus: hoarding behavior elicited by electrical stimulation. *Science* **155,** 349–350 (1967).

79. Thomas, D. W. & Mayer, J. Meal taking and regulation of food intake by normal and hypothalamic hyperphagic rats. *J. Comp. Physiol. Psychol.* **66,** 642–653 (1968).

80. Olney, J. W. Brain lesions, obesity, and other disturbances in mice treated with monosodium glutamate. *Science* **164,** 719–721 (1969).

81. Leibowitz, S. F., Hammer, N. J. & Chang, K. Hypothalamic paraventricular nucleus lesions produce overeating and obesity in the rat. *Physiol. Behav.* **27,** 1031–1040 (1981).

82. Seeley, R. J., Grill, H. J. & Kaplan, J. M. Neurological dissociation of gastrointestinal and metabolic contributions to meal size control. *Behav. Neurosci.* **108,** 347–352 (1994).

83. Choi, S. & Dallman, M. F. Hypothalamic Obesity: Multiple Routes Mediated by Loss of Function in Medial Cell Groups. *Endocrinology* **140,** 4081–4088 (1999).
84. Zhang, Y. *et al.* Positional cloning of the mouse obese gene and its human homologue. *Nature* **372,** 425–432 (1994).
85. Considine, R. V. *et al.* Serum immunoreactive-leptin concentrations in normal-weight and obese humans. *N. Engl. J. Med.* **334,** 292–295 (1996).
86. Baskin, D. G., Breininger, J. F. & Schwartz, M. W. Leptin receptor mRNA identifies a subpopulation of neuropeptide Y neurons activated by fasting in rat hypothalamus. *Diabetes* **48,** 828–833 (1999).
87. Elmquist, J. K., Bjørbaek, C., Ahima, R. S., Flier, J. S. & Saper, C. B. Distributions of leptin receptor mRNA isoforms in the rat brain. *J. Comp. Neurol.* **395,** 535–547 (1998).
88. Campfield, L. A., Smith, F. J., Guisez, Y., Devos, R. & Burn, P. Recombinant mouse OB protein: evidence for a peripheral signal linking adiposity and central neural networks. *Science* **269,** 546–549 (1995).
89. Grill, H. J. *et al.* Evidence that the caudal brainstem is a target for the inhibitory effect of leptin on food intake. *Endocrinology* **143,** 239–246 (2002).
90. Pelleymounter, M. A. *et al.* Effects of the obese gene product on body weight regulation in ob/ob mice. *Science* **269,** 540–543 (1995).
91. Bahary, N., Leibel, R. L., Joseph, L. & Friedman, J. M. Molecular mapping of the mouse db mutation. *Proc. Natl. Acad. Sci. U. S. A.* **87,** 8642–8646 (1990).
92. Phillips, M. S. *et al.* Leptin receptor missense mutation in the fatty Zucker rat. *Nat. Genet.* **13,** 18–19 (1996).
93. Takaya, K. *et al.* Nonsense mutation of leptin receptor in the obese spontaneously hypertensive Koletsky rat. *Nat. Genet.* **14,** 130–131 (1996).
94. Morton, G. J., Blevins, J. E., Kim, F., Matsen, M. & Figlewicz, D. P. The action of leptin in the ventral tegmental area to decrease food intake is dependent on Jak-2 signaling. *Am. J. Physiol. Endocrinol. Metab.* **297,** E202–210 (2009).
95. Fulton, S. *et al.* Leptin regulation of the mesoaccumbens dopamine pathway. *Neuron* **51,** 811–822 (2006).
96. Hommel, J. D. *et al.* Leptin Receptor Signaling in Midbrain Dopamine Neurons Regulates Feeding. *Neuron* **51,** 801–810 (2006).
97. Figlewicz, D. P., Evans, S. B., Murphy, J., Hoen, M. & Baskin, D. G. Expression of receptors for insulin and leptin in the ventral tegmental area/substantia nigra (VTA/SN) of the rat. *Brain Res.* **964,** 107–115 (2003).
98. Leshan, R. L. *et al.* Ventral tegmental area leptin receptor neurons specifically project to and regulate cocaine- and amphetamine-regulated transcript neurons of the extended central amygdala. *J. Neurosci. Off. J. Soc. Neurosci.* **30,** 5713–5723 (2010).
99. Krügel, U., Schraft, T., Kittner, H., Kiess, W. & Illes, P. Basal and feeding-evoked dopamine release in the rat nucleus accumbens is depressed by leptin. *Eur. J. Pharmacol.* **482,** 185–187 (2003).
100. Bruijnzeel, A. W., Corrie, L. W., Rogers, J. A. & Yamada, H. Effects of insulin and leptin in the ventral tegmental area and arcuate hypothalamic nucleus on food intake and brain reward function in female rats. *Behav. Brain Res.* **219,** 254–264 (2011).
101. Figlewicz, D. P., Bennett, J. L., Naleid, A. M., Davis, C. & Grimm, J. W. Intraventricular insulin and leptin decrease sucrose self-administration in rats. *Physiol. Behav.* **89,** 611–616 (2006).
102. Matheny, M., Shapiro, A., Tümer, N. & Scarpace, P. J. Region-specific diet-induced and leptin-induced cellular leptin resistance includes the ventral tegmental area in rats. *Neuropharmacology* **60,** 480–487 (2011).

103. Frayling, T. M. *et al.* A common variant in the FTO gene is associated with body mass index and predisposes to childhood and adult obesity. *Science* **316,** 889–894 (2007).

104. Dina, C. *et al.* Variation in FTO contributes to childhood obesity and severe adult obesity. *Nat. Genet.* **39,** 724–726 (2007).

105. Scuteri, A. *et al.* Genome-Wide Association Scan Shows Genetic Variants in the FTO Gene Are Associated with Obesity-Related Traits. *PLoS Genet* **3,** e115 (2007).

106. Gerken, T. *et al.* The obesity-associated FTO gene encodes a 2-oxoglutarate-dependent nucleic acid demethylase. *Science* **318,** 1469–1472 (2007).

107. Jia, G. *et al.* Oxidative demethylation of 3-methylthymine and 3-methyluracil in single-stranded DNA and RNA by mouse and human FTO. *FEBS Lett.* **582,** 3313–3319 (2008).

108. McTaggart, J. S. *et al.* FTO Is Expressed in Neurones throughout the Brain and Its Expression Is Unaltered by Fasting. *PLoS ONE* **6,** e27968 (2011).

109. Stratigopoulos, G. *et al.* Regulation of Fto/Ftm gene expression in mice and humans. *Am. J. Physiol. Regul. Integr. Comp. Physiol.* **294,** R1185–1196 (2008).

110. Tung, Y.-C. L. *et al.* Hypothalamic-Specific Manipulation of Fto, the Ortholog of the Human Obesity Gene FTO, Affects Food Intake in Rats. *PLoS ONE* **5,** e8771 (2010).

111. Fredriksson, R. *et al.* The obesity gene, FTO, is of ancient origin, up-regulated during food deprivation and expressed in neurons of feeding-related nuclei of the brain. *Endocrinology* **149,** 2062–2071 (2008).

112. Fischer, J. *et al.* Inactivation of the Fto gene protects from obesity. *Nature* **458,** 894–898 (2009).

113. Church, C. *et al.* A mouse model for the metabolic effects of the human fat mass and obesity associated FTO gene. *PLoS Genet.* **5,** e1000599 (2009).

114. Cecil, J. E., Tavendale, R., Watt, P., Hetherington, M. M. & Palmer, C. N. A. An obesity-associated FTO gene variant and increased energy intake in children. *N. Engl. J. Med.* **359,** 2558–2566 (2008).

115. Haupt, A. *et al.* Variation in the FTO gene influences food intake but not energy expenditure. *Exp. Clin. Endocrinol. Diabetes Off. J. Ger. Soc. Endocrinol. Ger. Diabetes Assoc.* **117,** 194–197 (2009).

116. Speakman, J. R., Rance, K. A. & Johnstone, A. M. Polymorphisms of the FTO gene are associated with variation in energy intake, but not energy expenditure. *Obes. Silver Spring Md* **16,** 1961–1965 (2008).

117. Timpson, N. J. *et al.* The fat mass- and obesity-associated locus and dietary intake in children. *Am. J. Clin. Nutr.* **88,** 971–978 (2008).

118. Wardle, J., Llewellyn, C., Sanderson, S. & Plomin, R. The FTO gene and measured food intake in children. *Int. J. Obes. 2005* **33,** 42–45 (2009).

119. Tanofsky-Kraff, M. *et al.* The FTO gene rs9939609 obesity-risk allele and loss of control over eating. *Am. J. Clin. Nutr.* **90,** 1483–1488 (2009).

120. Berentzen, T. *et al.* Lack of association of fatness-related FTO gene variants with energy expenditure or physical activity. *J. Clin. Endocrinol. Metab.* **93,** 2904–2908 (2008).

121. Do, R. *et al.* Genetic variants of FTO influence adiposity, insulin sensitivity, leptin levels, and resting metabolic rate in the Quebec Family Study. *Diabetes* **57,** 1147–1150 (2008).

122. Goossens, G. H. *et al.* Several obesity- and nutrient-related gene polymorphisms but not FTO and UCP variants modulate postabsorptive resting energy expenditure and fat-induced thermogenesis in obese individuals: the NUGENOB study. *Int. J. Obes. 2005* **33,** 669–679 (2009).

123. Hakanen, M. *et al.* FTO genotype is associated with body mass index after the age of seven years but not with energy intake or leisure-time physical activity. *J. Clin. Endocrinol. Metab.* **94,** 1281–1287 (2009).

124. Liu, G. *et al.* FTO variant rs9939609 is associated with body mass index and waist circumference, but not with energy intake or physical activity in European- and African-American youth. *BMC Med. Genet.* **11,** 57 (2010).

125. Richter, C. P. A Behavioristic Study of the Activity of the Rat. *Comp. Psychol. Monogr.* 1922, 56 (2012).

126. Rosenwasser, A. M., Boulos, Z. & Terman, M. Circadian organization of food intake and meal patterns in the rat. *Physiol. Behav.* **27,** 33–39 (1981).

127. Janhunen, S. K., van der Zwaal, E. M., la Fleur, S. E. & Adan, R. A. H. Inverse agonism at 2A adrenoceptors augments the hypophagic effect of sibutramine in rats. *Obes. Silver Spring Md* **19,** 1979–1986 (2011).

128. Smith, G. P. The controls of eating: a shift from nutritional homeostasis to behavioral neuroscience. *Nutr. Burbank Los Angeles Cty. Calif* **16,** 814–820 (2000).

129. Anliker, J. & Mayer, J. An Operant Conditioning Technique for Studying Feeding-Fasting Patterns in Normal and Obese Mice. *J. Appl. Physiol.* **8,** 667–670 (1956).

130. Snowdon, C. T. Motivation, regulation, and the control of meal parameters with oral and intragastric feeding. *J. Comp. Physiol. Psychol.* **69,** 91–100 (1969).

131. Milner, M. & De Caire, E. An improved photo-electric switching circuit for monitoring the feeding behaviour of rats which have the choice of several feeding troughs. *S. Afr. J. Med. Sci.* **30,** 37–39 (1965).

132. Madrid, J. A., Salido, G. M., Muñoz-Arrebola, P. & Martínez de Victoria, E. Circadian rhythms of food intake in gastroduodenally-ulcerated rats: effects of three anti-ulcer drugs. *Chronobiol. Int.* **6,** 321–328 (1989).

133. Madrid, J. A., Lopez-Bote, C. & Martín, E. Effect of neonatal androgenization on the circadian rhythm of feeding behavior in rats. *Physiol. Behav.* **53,** 329–335 (1993).

134. Fallon, D. Eatometer: a device for continuous recording of free-feeding behavior. *Science* **148,** 977–978 (1965).

135. Kissileff, H. R. Free feeding in normal and 'recovered lateral' rats monitored by a pellet-detecting eatometer. *Physiol. Behav.* **5,** 163–173 (1970).

136. Madrid, J. A., Matas, P., Sánchez-Vázquez, F. J. & Cuenca, E. M. A contact eatometer for automated continuous recording of feeding behavior in rats. *Physiol. Behav.* **57,** 129–134 (1995).

137. Pokrovsky, V. & Le Magnen, J. [Design of a device for continuous and automatic graphic recording of food consumption by the white rat]. *J. Physiol. (Paris)* **55,** 318–319 (1963).

138. Hulsey, M. G. & Martin, R. J. A system for automated recording and analysis of feeding behavior. *Physiol. Behav.* **50,** 403–408 (1991).

139. Janhunen, S. K., la Fleur, S. E. & Adan, R. A. H. Blocking alpha2A adrenoceptors, but not dopamine receptors, augments bupropion-induced hypophagia in rats. *Obes. Silver Spring Md* (2013). doi:10.1002/oby.20581

140. Tiesjema, B., Adan, R. A. H., Luijendijk, M. C. M., Kalsbeek, A. & la Fleur, S. E. Differential effects of recombinant adeno-associated virus-mediated neuropeptide Y overexpression in the hypothalamic paraventricular nucleus and lateral hypothalamus on feeding behavior. *J. Neurosci. Off. J. Soc. Neurosci.* **27,** 14139–14146 (2007).

141. De Backer, M. W. A. *et al.* Neuropeptide delivery to the brain: a von Willebrand factor signal peptide to direct neuropeptide secretion. *BMC Neurosci.* **11,** 94 (2010).

142. La Fleur, S. E., Luijendijk, M. C. M., van der Zwaal, E. M., Brans, M. A. D. & Adan, R. A. H. The snacking rat as model of human obesity: effects of a free-choice high-fat high-sugar diet on meal patterns. *Int. J. Obes. 2005* (2013). doi:10.1038/ijo.2013.159

143. Merkestein, M. *et al.* GHS-R1a signaling in the DMH and VMH contributes to food anticipatory activity. *Int. J. Obes. 2005* (2013). doi:10.1038/ijo.2013.131

144. Van der Zwaal, E. M., Luijendijk, M. C. M., Adan, R. A. H. & la Fleur, S. E. Olanzapine-induced weight gain: chronic infusion using osmotic minipumps does not result in stable plasma levels due to degradation of olanzapine in solution. *Eur. J. Pharmacol.* **585,** 130–136 (2008).

145. Verhagen, L. A. W., Luijendijk, M. C. M., Hillebrand, J. J. G. & Adan, R. A. H. Dopamine antagonism inhibits anorectic behavior in an animal model for anorexia nervosa. *Eur. Neuropsychopharmacol. J. Eur. Coll. Neuropsychopharmacol.* **19,** 153–160 (2009).

CHAPTER 2

Recombinant adeno-associated virus: efficient transduction of the rat VMH and clearance from blood

van Gestel MA
Boender AJ
de Vrind VA
Garner KM
Luijendijk MC
Adan RA

PLoS One. 2014 May 23;9(5):e97639

Abstract

To promote the efficient and safe application of adeno-associated virus (AAV) vectors as a gene transfer tool in the central nervous system (CNS), transduction efficiency and clearance were studied for serotypes commonly used to transfect distinct areas of the brain. As AAV2 was shown to transduce only small volumes in several brain regions, this study compares the transduction efficiency of three AAV pseudotyped vectors, namely AAV2/1, AAV2/5 and AAV2/8, in the ventromedial nucleus of the hypothalamus (VMH). No difference was found between AAV2/1 and AAV2/5 in transduction efficiency. Both AAV2/1 and AAV2/5 achieved a higher transduction rate than AAV2/8. One hour after virus administration to the brain, no viral particles could be traced in blood, indicating that no or negligible numbers of virions crossed the blood-brain barrier. In order to investigate survival of AAV in blood, clearance was determined following systemic AAV administration. The half-life of AAV2/1, AAV2/2, AAV2/5 and AAV2/8 was calculated by determining virus clearance rates from blood after systemic injection. The half-life of AAV2/2 was 4.2 minutes, which was significantly lower than the half-lives of AAV2/1, AAV2/5 and AAV2/8. With a half-life of more than 11 hours, AAV2/8 particles remained detectable in blood significantly longer than AAV2/5. We conclude that application of AAV in the CNS is relatively safe as no AAV particles are detectable in blood after injection into the brain. With a half-life of 1.67 hours of AAV2/5, a systemic injection with 1×10^9 genomic copies of AAV would be fully cleared from blood after 2 days.

Introduction

Viral vector gene delivery is currently among the most widely used gene transfer tools for gene delivery in the central nervous system (CNS). Recombinant adeno-associated virus (rAAV) vectors mediate stable and long-term gene expression in both dividing and non-dividing cells without eliciting a significant immune response, making them an attractive viral vector system.[1,2] rAAV vectors are easily designed because of the simplicity of the AAV genome. The inverted terminal repeats (ITRs) flanking the two viral genes *rep* (replication) and *cap* (capsid) of the wild type virus are the only elements necessary for virus replication and encapsidation. To design a rAAV vector, *rep* and *cap* are replaced by a promoter followed by the gene of interest or short hairpin RNA (shRNA) and subsequently provided *in trans* from a plasmid without ITRs.

For the determination of gene function in distinct areas of the brain it is of importance to optimize the AAV-mediated transfer and expression of genes or shRNAs. For this purpose AAV serotypes have been studied for their transduction efficiency in the brain. AAV2 is the most widely used serotype to transduce the CNS.[1,2] Since different serotypes infect different and overlapping types of cells, the AAV2 vector has been pseudotyped in capsids from different AAV serotypes. AAV2/1, AAV2/5 and AAV2/8 have been shown to effectively transduce rat hypothalamus,[3] striatum,[4,5] hippocampus,[4,6,7] substantia nigra[4,6,8] and red nucleus[9].

This study focused on transduction of the ventromedial nucleus of the hypothalamus (VMH) in the rat brain, which is involved in energy homeostasis[10], fear[11] and female reproductive behavior[12]. AAV2/1, AAV2/5 and AAV2/8 transduction efficiency was compared in the rat VMH. We did not consider AAV2/2, because previously it was demonstrated that AAV2/1, AAV2/5 and AAV2/8 more effectively transduce neurons in rat hypothalamus, striatum, hippocampus and substantia nigra than AAV2/2.[3,4,8]

The use of different serotypes with their own receptor tropism may have implications for the viral particle biodistribution. An evaluation of the biodistribution for every serotype and for every route of administration is relevant to biosafety with respect to the use of AAV. Several AAVs have been shown to effectively cross the mouse blood-brain barrier after intravascular delivery.[13,14] It is not known whether AAV delivery in the brain results in the introduction of viral particles in the bloodstream. This study therefore focused on AAV vector transfer to the blood after AAV2/1, AAV2/2, AAV2/5 or AAV2/8 transduction of the VMH, as these serotypes are commonly used to transfect the brain.

Working with AAVs has been assigned to Biosafety Level 2 in most countries. For optimal conductance of behavioral experiments, transfer of genetically modified animals

to a Biosafety Level 1 laboratory might be required. To indicate when animals injected with AAV can be safely handled at Biosafety Level 1, blood clearance rates were assessed after systemic injection.

Material and Methods

Ethics statement

All experimental procedures were approved by the Committee for Animal Experimentation of the University of Utrecht (Utrecht, the Netherlands). Human Embryonic Kidney (HEK) 293T cells used in this study were purchased from ATCC.

Cell lines

HEK293T cells were cultured in growth medium (Dulbecco's modified Eagle medium, DMEM) (Invitrogen, USA) supplemented with 10% fetal calf serum (FCS) (Lonza, Switzerland), 2mM glutamine (PAA, Germany), 100Uml^{-1} penicillin (PAA, Germany), 100Uml^{-1} streptomycin (PAA, Germany) and non-essential amino acids (PAA, Germany) at 37°C with 5% CO_2.

Virus production and purification

Virus was generated and purified as previously described.[15] HEK293T cells were co-transfected with pAAV-LepR (a kind gift from R.J. DiLeone[16]) and pDP1, pDP2, pDP5 or pAR-8 + pXX6 (Plasmid factory, Germany) in fifteen 15 x 15 cm dishes using PEI. Sixty hours after transfection, cells were collected, pelleted and resuspended in ice-cold buffer (150mM NaCl, 50mM Tris, pH 8.4). Cells were lysed by three freeze-thaw cycles and incubated for 30min at 37°C with 50Uml^{-1} benzonase (Sigma, The Netherlands). The lysate was loaded onto a 15%, 25%, 40%, and 60% iodixanol gradient. After centrifugation at 70.000rpm for 60min at 18oC, the 40% layer was extracted and used for ion-exchange chromatography. AAV positive fractions were determined by quantitative PCR (qPCR) on GFP (forward primer 5'-CACATGAAGCAGCACGACTT; reverse primer 5'-GAAGTTCACCTTGATGCCGT) and concentrated using an Amicon Ultra 15ml filter (Millipore). Titer was determined by qPCR on GFP.

Animal studies

Male Wistar rats (Charles River, Germany) were housed in filter top cages in a temperature- and humidity-controlled room (temperature 21±2°C and humidity 55±5%) with a 12h light/dark cycle. AAV2/1, AAV2/2, AAV2/5 or AAV2/8 was administered either stereotactically in the VMH (see: surgical procedure) or systemically via the tail vein. Blood samples from animals injected in the VMH were collected via a tail cut one hour after injection. Blood samples from systemically injected animals were

collected 1min, 10min, 20min, 40min, 1h, 4h and 24h after injection via a tail cut in heparin-coated capillary tubes.

Surgical procedures

Rats were anesthetized using fentanyl/fluanisone and midazolam and mounted onto a stereotaxic apparatus. Virus was administered by placing a syringe needle into the VMH (coordinates from Bregma: -2.1 AP, +1.5 ML, -9.9 DV, at a 5° angle). A total of 1,5µl of virus (7 x 10^{11} genomic copies (gc)ml^{-1} AAV2/1, AAV2/5 or AAV2/8; 1.5 x 10^{11} $gcml^{-1}$ AAV2/2) was injected at a rate of 0.2$\mu lmin^{-1}$.

Viral DNA isolation from blood and real-time PCR

Viral DNA was isolated from blood using the High Pure Viral Nucleic Acid Kit according to the manufacturer's instructions (Roche, Germany). Briefly, 200µl of binding buffer supplemented with carrier RNA and 50µl of Proteinase K solution were added to 200µl of plasma. After mixing, the samples were incubated for 10min at 72°C. 100µl of binding buffer was added and samples were mixed. Next, samples were transferred to a High Pure Filter Tube and centrifuged at 8000 x g for 1min. 500µl Inhibitor Removal Buffer was added to the filter tube followed by centrifugation. The filter was washed twice with 450µl Wash Buffer followed by centrifugation. To elute viral nucleic acids, 50µl Elution Buffer was added to the filter tube and samples were centrifuged. PCR was performed on each sample for the GFP gene (forward primer 5'- CACATGAAGCAGCACGACTT; reverse primer 5'- GAAGTTCACCTTGATGCCGT) with the Roche Lightcycler according to the manufacturer's instructions. Viral DNA was assayed for copy number of the GFP gene using the SYBR-Green I (Roche, Germany). AAV plasmid at 1 x 10^4gc, 1 x 10^6gc and 1 x 10^8gc was used as copy number controls. AAV plasmids were dissolved in blood and purified using the High Pure Viral Nucleic Acid Kit (Roche, Germany) as previously described. The lower limit of quantification was 100$gc\mu l^{-1}$.

In situ hybridization

For the in situ hybridization (ISH), cryostat sections of 20µm thickness from fresh frozen brains were mounted onto slides. Brains were sliced from Interaural: 7.28mm, Bregma: -1.72mm to Interaural: 5.64 mm, Bregma: -3.36mm and the VMH was localized using the atlas 'The Rat Brain' (Paxinos and Watson, 6th edition). Sections were fixed in 4% paraformaldehyde (PFA) for 20min, washed in phosphate buffered saline (PBS), acetylated for 10min and washed again. Sections were pre hybridized in hybridization solution (50% formamide, 5 x SSC, 5 x Denhardts, 250μgml^{-1} tRNA Baker's yeast, 500μgml^{-1} sonicated salmon sperm DNA) for 2h at room temperature. The hybridization solution containing 400 $ngml^{-1}$ 720bp long digoxigenin (DIG)-labeled enhanced green fluorescent protein (eGFP) riboprobe (antisense to NCBI gene DQ768212) was then applied to the slides followed by overnight incubation at 68°C.

After a quick wash in 68°C pre warmed 2 x SSC, slides were transferred to 68°C pre warmed 0.2 x SSC for 2h. DIG was detected with an alkaline phosphatase labeled antibody (1:5000, Roche, Germany) after overnight incubation at room temperature using NBT/BCIP as a substrate. Sections were dehydrated in ethanol, cleared in xylene and embedded in Entellan.

ImageJ Software was used to quantify the spread of GFP mRNA expression in the VMH.

Statistical analyses

All data were presented as means ± SEM. The significance of differences in the comparison of transduction area, blood clearance rate and half-life was evaluated by a Kruskal-Wallis analysis, followed by Mann-Whitney U-test using GraphPad Prism 5 software. A P-value of <0.05 was considered to be significant.

Results

Transduction efficiency and biodistribution of AAV2/1, AAV2/5 and AAV2/8

A vector containing AAV2 terminal repeats flanking a shRNA targeting the leptin receptor and an enhanced green fluorescent protein (eGFP) expression cassette was packaged with an AAV1, AAV5 or AAV8 capsid. To determine transduction efficiency, rats (n=6) received an injection of 1 x 10^9gc AAV2/1, AAV2/5 or AAV2/8 in the VMH and their brains were analyzed six weeks after injection. AAV2 transduction was not studied for its transduction efficiency as other serotypes have been shown to more efficiently transduce distinct areas of the CNS.[3,4,8] A GFP in situ hybridization (ISH) to detect GFP mRNA was performed to precisely identify the transduced area and to analyze transduction efficiency. Both AAV2/1 and AAV2/5 efficiently transduced the VMH (Figure 1a, b and e) and distributed over a significantly larger area (0,51±0,05mm^2 and 0,40±0,05mm^2, respectively) than AAV2/8 (0,21±0,04mm^2) within the VMH (Figure 1c, d and e) ($P<0.01$ and $P<0.05$, respectively). No difference in transduction efficiency was observed between AAV2/1 and AAV2/5.

AAV biodistribution after administration to the brain

To examine AAV biodistribution after virus administration to the brain, serotypes commonly used to transfect the brain were injected into the VMH. Rats (n=6) received an injection of 3 x 10^8gc AAV2/2 or 1 x 10^9gc AAV2/1, AAV2/5 or AAV2/8 in the VMH. Blood samples were collected from the tail one hour after virus administration. No genomic copies were detectable by quantitative PCR in blood samples collected one hour after virus administration.

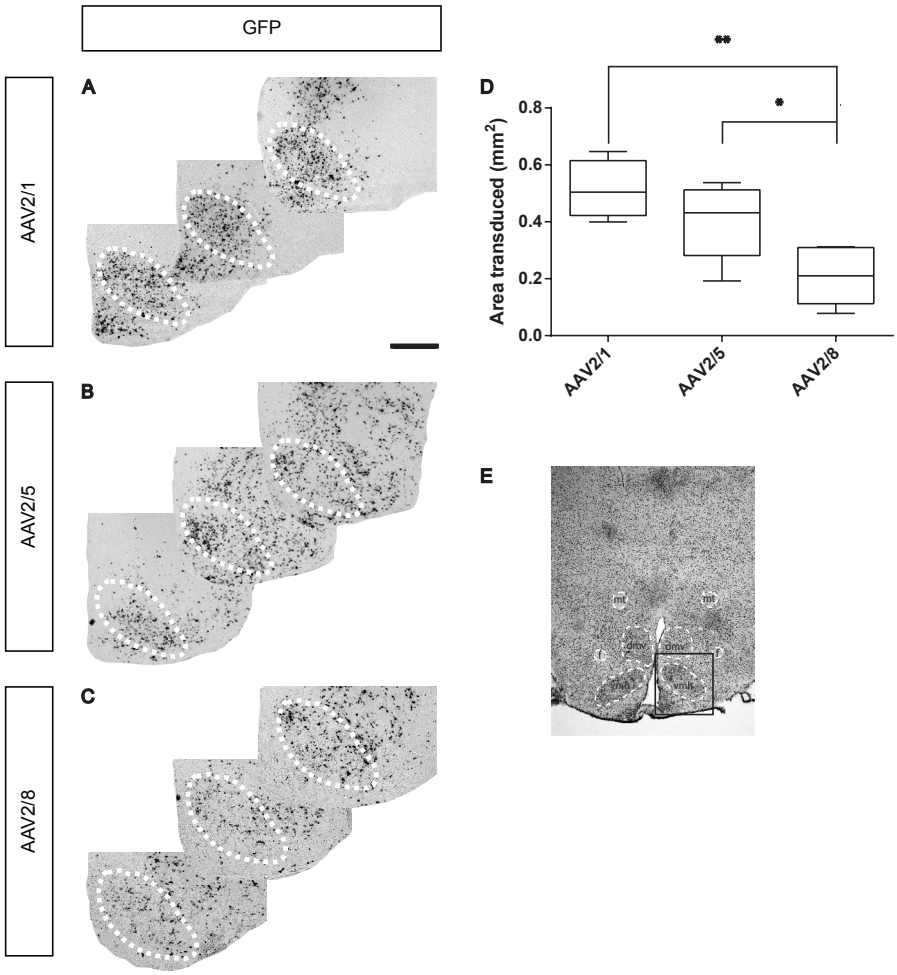

Figure 1 Comparison of transduction efficiency of serotype AAV2/1, AAV2/5 and AAV2/8 in the VMH.

Rats (n=6) were injected with 1 x 10^9 genomic copies of AAV2/1, AAV2/5 or AAV2/8 in the VMH. The transduced area was identified using ISH on GFP. AAV2/1 and AAV2/5 were equally efficient in transducing the VMH (A, B, D) and performed significantly better than AAV2/8 (C, D) ($P<0.01$ and $P<0.05$, respectively). The VMH area is indicated by a dotted line. Figure E depicts the hypothalamic area. The square indicates the area that is enlarged in Figures A, B and C. mt = mammillary tract; f = fornix; dmh = dorsomedial hypothalamus; vmh = ventromedial hypothalamus. Scale bar: 500µm

AAV clearance from blood

To quantify the half-life of AAV, blood clearance rates of AAV serotypes commonly used to transfect the brain (AAV1, AAV2, AAV5 and AAV8) were determined. Blood samples were collected 1min, 10min, 20min, 40min, 1h, 4h and 24h after systemic injection of 1 x 10^9gc into adult rats (n=6). A very rapid blood clearance rate was found for AAV2/2 compared to the other serotypes (Figure 2). Ten minutes after injection,

AAV2/2 exhibited a higher decrease in blood concentration than AAV2/1, AAV2/5 and AAV2/8 ($p<0.01$). Since there was some variability between rats in plasma AAV concentration one minute after systemic injection, we calculated the relative changes in concentrations. Concentrations below 3% were found for AAV2/1 and AAV2/2 four hours after injection. In contrast, AAV2/8 particles showed a relatively slow blood clearance rate, with a concentration above 10% one day after injection, which is significantly higher than the blood concentration of AAV2/5 ($p<0.01$).

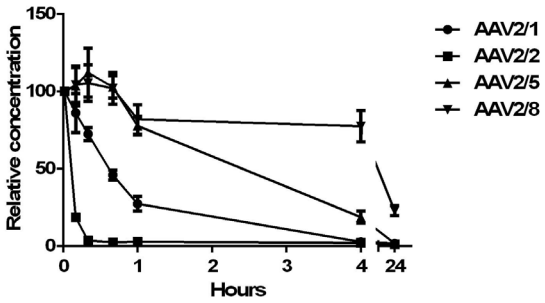

Figure 2 Blood clearance kinetics of AAV2/1, AAV2/2, AAV2/5 and AAV2/8 after systemic administration.

Rats (n=6) received a systemic injection of 1 x 10^9 AAV2/1, AAV2/2, AAV2/5 or AAV2/8 and blood samples were collected 10min, 20min, 40min, 1h, 4h and 24h after injection. AAV2/2 showed a significantly faster clearance rate than AAV2/1, AAV2/5 and AAV2/8. Four hours after injection, less than 3% of the starting material of AAV2/1 and AAV2/2 could be traced. AAV2/8 showed a delayed clearance rate. One day after injection still more than 20% of the starting material was present in the circulation.

Half-life was calculated for each serotype (Table 1). A half-life of 4,2 minutes was found for AAV2/2, which was significantly lower than the half-lives of AAV2/1, AAV2/5 and AAV2/8 ($P<0.01$). AAV2/8 showed a significantly prolonged half-life compared to AAV2/5 ($p<0.01$).

Serotype	Half-life (hours)
1	0.55±0.08
2	0.07±0.00
5	1.67±0.21
8	11.40±1.09

Table 1 Half-life of AAV2/1, AAV2/2, AAV2/5 and AAV2/8.

Half-life in blood was calculated after systemic AAV administration in rats (n=6).

Discussion

The use of AAV as a tool to manipulate gene expression in the central nervous system has shown much promise. The aim of the present study was to contribute to the efficient and safe use of AAV serotypes commonly used to transduce the mammalian brain.

A comparison of different AAV serotypes in the brain area of interest contributes to the optimization of gene or shRNA transfer. We have already demonstrated that AAV2/1 results in higher levels of gene delivery in the hypothalamic area compared to AAV2/2 and AAV2/8.[3] This study confirms a more efficient transduction of AAV2/1 compared to AAV2/8 in the VMH. As AAV2/5 is shown to effectively transduce other brain structures,[4,8,9] this serotype was examined for its transduction efficiency in the VMH. AAV2/5 was found to be equally effective in transducing the VMH as AAV2/1, which corresponds to Burger et al., who compared these serotypes in rat striatum, hippocampus and substantia nigra.[4]

The observed divergence in cellular uptake of the AAV serotypes might be explained by their mode of entrance (receptor type) into cells. Cell surface receptors mediating the cellular entry of AAV2 are best known. AAV2 attachment is mediated by heparan sulfate proteoglycans, while co-receptors, including aVb integrin, fibroblast or hepatocyte growth factor receptors and a laminin receptor, enhance internalization.[17–21] The laminin receptor is also known to interact with AAV8.[21] AAV1 and AAV5 lack heparan binding amino acids and subsequently do not use surface heparan sulfate proteoglycans as a receptor for infection.[22,23] Both utilize sialic acid-containing glycoproteins for efficient binding and transduction.[24–27] For AAV5, the platelet-derived growth factor receptor has been shown to serve as a co-receptor.[28] Besides binding and entry, other steps in the AAV infection pathway influence the transduction process, including intracellular viral trafficking, nuclear transport, uncoating and second strand DNA synthesis.[29–31]

When applying AAV-mediated gene transfer to study the functions of a gene in a certain brain area, it is important to take serotype specific biodistribution into account. If the AAV, which is administered to the brain, is able to cross the blood-brain barrier, its content might exert unwanted side effects in the periphery. It has been reported that AAV2/2 and AAV2/5 are not able to cross the blood-brain barrier both *in vitro*[32] and *in vivo*[14,33] in mice and rats. However, in nonhuman primates, that received AAV2/2 or 2/5, vector DNA could be traced in the spleen and in the liver and spleen, respectively.[34,35] No peripheral tissue was transduced in animals receiving lower doses and no genomic copies were detected in the blood.[34] In another study using nonhuman primates, viral DNA was detected in the serum as soon as one hour after intracerebral administration of AAV2/1, 2/2 and 2/5.[36] Systemically injected AAV2/1 and AAV2/8 have been shown to efficiently cross the blood-brain barrier and subsequently transduce neurons in

hypothalamus, cerebellum and spinal cord in the neonatal mouse brain.[14,37] This study shows that one hour after administration of AAV2/1, AAV2/2, AAV2/5 and AAV2/8 in the VMH no viral particles could be traced in the blood. This indicates that AAVs are not crossing the blood-brain barrier after injection in the brain or that the number is too low to detect by qPCR on blood samples. If the latter is the case, then probably the number of genomic copies crossing is too low to induce an effect. All serotypes have been shown to be able to cross the blood-brain barrier. Interspecies differences in blood-brain barrier composition, titer, age, time after injection and different sites of injection might explain these contradicting outcomes. We cannot rule out that injection with higher titers will result in (detectable) viral particles in the blood.

Blood clearance kinetics of AAV2/1, AAV2/2, AAV2/5 and AAV2/8 were assessed after systemic injection. AAV2/1 and AAV2/2 showed a rapid clearance with less than 3% of the starting material left after 4 hours. This is in accordance to results obtained in mice.[38,39] However, in contrast to previous results,[39] AAV2/8 showed a significantly delayed clearance compared to the other serotypes. The observed differences in AAV serotype clearance might be explained by the number of genomic copies lost to the phagocytic cells in the liver, Kupffer cells, and serotype-specific transcytosis of AAV across the endothelial cells.[32,40]

This study aimed to optimize the safe and efficient use of AAV-mediated gene transfer to the VMH of the rat brain. Efficient transduction of the VMH was achieved using AAV2/1 and AAV2/5. No genomic copies could be found in blood one hour after AAV administration to the brain and both serotypes exhibit a relatively fast clearance from blood. This minimizes the risk for transduction of peripheral organs, which could potentially influence phenotypic results.

References

1. Kaplitt MG, Leone P, Samulski RJ, Xiao X, Pfaff DW, O'Malley KL, et al. Long-term gene expression and phenotypic correction using adeno-associated virus vectors in the mammalian brain. Nat Genet. 1994 Oct;8(2):148–54.
2. McCown TJ, Xiao X, Li J, Breese GR, Jude Samulski R. Differential and persistent expression patterns of CNS gene transfer by an adeno-associated virus (AAV) vector. Brain Res. 1996 Mar 25;713(1–2):99–107.
3. De Backer MWA, Brans MAD, Luijendijk MC, Garner KM, Adan RAH. Optimization of adeno-associated viral vector-mediated gene delivery to the hypothalamus. Hum Gene Ther. 2010 Jun;21(6):673–82.
4. Burger C, Gorbatyuk OS, Velardo MJ, Peden CS, Williams P, Zolotukhin S, et al. Recombinant AAV Viral Vectors Pseudotyped with Viral Capsids from Serotypes 1, 2, and 5 Display Differential Efficiency and Cell Tropism after Delivery to Different Regions of the Central Nervous System. Mol Ther. 2004 Aug;10(2):302–17.
5. Reimsnider S, Manfredsson FP, Muzyczka N, Mandel RJ. Time course of transgene expression after intrastriatal pseudotyped rAAV2/1, rAAV2/2, rAAV2/5, and rAAV2/8 transduction in the rat. Mol Ther J Am Soc Gene Ther. 2007 Aug;15(8):1504–11.
6. Klein RL, Dayton RD, Leidenheimer NJ, Jansen K, Golde TE, Zweig RM. Efficient neuronal gene transfer with AAV8 leads to neurotoxic levels of tau or green fluorescent proteins. Mol Ther J Am Soc Gene Ther. 2006 Mar;13(3):517–27.
7. Klein RL, Dayton RD, Tatom JB, Henderson KM, Henning PP. AAV8, 9, Rh10, Rh43 vector gene transfer in the rat brain: effects of serotype, promoter and purification method. Mol Ther J Am Soc Gene Ther. 2008 Jan;16(1):89–96.
8. McFarland NR, Lee J-S, Hyman BT, McLean PJ. Comparison of transduction efficiency of recombinant AAV serotypes 1, 2, 5, and 8 in the rat nigrostriatal system. J Neurochem. 2009 May;109(3):838–45.
9. Blits B, Derks S, Twisk J, Ehlert E, Prins J, Verhaagen J. Adeno-associated viral vector (AAV)-mediated gene transfer in the red nucleus of the adult rat brain: comparative analysis of the transduction properties of seven AAV serotypes and lentiviral vectors. J Neurosci Methods. 2010 Jan 15;185(2):257–63.
10. Satoh N, Ogawa Y, Katsuura G, Tsuji T, Masuzaki H, Hiraoka J, et al. Pathophysiological significance of the obese gene product, leptin, in ventromedial hypothalamus (VMH)-lesioned rats: evidence for loss of its satiety effect in VMH-lesioned rats. Endocrinology. 1997 Mar;138(3):947–54.
11. Trogrlic L, Wilson YM, Newman AG, Murphy M. Context fear learning specifically activates distinct populations of neurons in amygdala and hypothalamus. Learn Mem Cold Spring Harb N. 2011;18(10):678–87.
12. Mathews D, Edwards DA. The ventromedial nucleus of the hypothalamus and the hormonal arousal of sexual behaviors in the female rat. Horm Behav. 1977 Feb;8(1):40–51.
13. Foust KD, Nurre E, Montgomery CL, Hernandez A, Chan CM, Kaspar BK. Intravascular AAV9 preferentially targets neonatal neurons and adult astrocytes. Nat Biotechnol. 2009 Jan;27(1):59–65.
14. Zhang H, Yang B, Mu X, Ahmed SS, Su Q, He R, et al. Several rAAV vectors efficiently cross the blood-brain barrier and transduce neurons and astrocytes in the neonatal mouse central nervous system. Mol Ther J Am Soc Gene Ther. 2011 Aug;19(8):1440–8.
15. Backer MWA de, Brans M a D, Rozen AJ van, Zwaal EM van der, Luijendijk MCM, Garner KG, et al. Suppressor of cytokine signaling 3 knockdown in the mediobasal hypothalamus: counterintuitive effects on energy balance. J Mol Endocrinol. 2010 Nov 1;45(5):341–53.
16. Hommel JD, Trinko R, Sears RM, Georgescu D, Liu Z-W, Gao X-B, et al. Leptin Receptor Signaling in Midbrain Dopamine Neurons Regulates Feeding. Neuron. 2006 Sep 21;51(6):801–10.

17. Summerford C, Samulski RJ. Membrane-associated heparan sulfate proteoglycan is a receptor for adeno-associated virus type 2 virions. J Virol. 1998 Feb;72(2):1438–45.

18. Summerford C, Bartlett JS, Samulski RJ. V 5 integrin: a co-receptor for adeno-associated virus type 2 infection. Nat Med. 1999 Jan;5(1):78–82.

19. Qing K, Mah C, Hansen J, Zhou S, Dwarki V, Srivastava A. Human fibroblast growth factor receptor 1 is a co-receptor for infection by adeno-associated virus 2. Nat Med. 1999 Jan;5(1):71–7.

20. Kashiwakura Y, Tamayose K, Iwabuchi K, Hirai Y, Shimada T, Matsumoto K, et al. Hepatocyte growth factor receptor is a coreceptor for adeno-associated virus type 2 infection. J Virol. 2005 Jan;79(1):609–14.

21. Akache B, Grimm D, Pandey K, Yant SR, Xu H, Kay MA. The 37/67-kilodalton laminin receptor is a receptor for adeno-associated virus serotypes 8, 2, 3, and 9. J Virol. 2006 Oct;80(19):9831–6.

22. Rabinowitz JE, Rolling F, Li C, Conrath H, Xiao W, Xiao X, et al. Cross-Packaging of a Single Adeno-Associated Virus (AAV) Type 2 Vector Genome into Multiple AAV Serotypes Enables Transduction with Broad Specificity. J Virol. 2002 Jan 15;76(2):791–801.

23. Negishi A, Chen J, McCarty DM, Samulski RJ, Liu J, Superfine R. Analysis of the interaction between adeno-associated virus and heparan sulfate using atomic force microscopy. Glycobiology. 2004 Nov;14(11):969–77.

24. Walters RW, Yi SMP, Keshavjee S, Brown KE, Welsh MJ, Chiorini JA, et al. Binding of Adeno-associated Virus Type 5 to 2,3-Linked Sialic Acid Is Required for Gene Transfer. J Biol Chem. 2001 Jun 8;276(23):20610–6.

25. Kaludov N, Brown KE, Walters RW, Zabner J, Chiorini JA. Adeno-Associated Virus Serotype 4 (AAV4) and AAV5 Both Require Sialic Acid Binding for Hemagglutination and Efficient Transduction but Differ in Sialic Acid Linkage Specificity. J Virol. 2001 Aug 1;75(15):6884–93.

26. Chen S, Kapturczak M, Loiler SA, Zolotukhin S, Glushakova OY, Madsen KM, et al. Efficient Transduction of Vascular Endothelial Cells with Recombinant Adeno-Associated Virus Serotype 1 and 5 Vectors. Hum Gene Ther. 2005 Feb;16(2):235–47.

27. Wu Z, Miller E, Agbandje-McKenna M, Samulski RJ. Alpha2,3 and alpha2,6 N-linked sialic acids facilitate efficient binding and transduction by adeno-associated virus types 1 and 6. J Virol. 2006 Sep;80(18):9093–103.

28. Pasquale GD, Davidson BL, Stein CS, Martins I, Scudiero D, Monks A, et al. Identification of PDGFR as a receptor for AAV-5 transduction. Nat Med. 2003 Oct;9(10):1306–12.

29. Hauck B, Zhao W, High K, Xiao W. Intracellular Viral Processing, Not Single-Stranded DNA Accumulation, Is Crucial for Recombinant Adeno-Associated Virus Transduction. J Virol. 2004 Dec 15;78(24):13678–86.

30. Thomas CE, Storm TA, Huang Z, Kay MA. Rapid Uncoating of Vector Genomes Is the Key to Efficient Liver Transduction with Pseudotyped Adeno-Associated Virus Vectors. J Virol. 2004 Mar 15;78(6):3110–22.

31. Ferrari FK, Samulski T, Shenk T, Samulski RJ. Second-strand synthesis is a rate-limiting step for efficient transduction by recombinant adeno-associated virus vectors. J Virol. 1996 May 1;70(5):3227–34.

32. Di Pasquale G, Chiorini JA. AAV transcytosis through barrier epithelia and endothelium. Mol Ther J Am Soc Gene Ther. 2006 Mar;13(3):506–16.

33. Fitzsimons HL, Riban V, Bland RJ, Wendelken JL, Sapan CV, During MJ. Biodistribution and safety assessment of AAV2-GAD following intrasubthalamic injection in the rat. J Gene Med. 2010 Apr;12(4):385–98.

34. Cunningham J, Pivirotto P, Bringas J, Suzuki B, Vijay S, Sanftner L, et al. Biodistribution of Adeno-associated Virus Type-2 in Nonhuman Primates after Convection-enhanced Delivery to Brain. Mol Ther J Am Soc Gene Ther. 2008 Jul;16(7):1267–75.

35. Colle M-A, Piguet F, Bertrand L, Raoul S, Bieche I, Dubreil L, et al. Efficient intracerebral delivery of AAV5 vector encoding human ARSA in non-human primate. Hum Mol Genet. 2010 Jan 1;19(1):147–58.

36. Ciron C, Cressant A, Roux F, Raoul S, Cherel Y, Hantraye P, et al. Human alpha-iduronidase gene transfer mediated by adeno-associated virus types 1, 2, and 5 in the brain of nonhuman primates: vector diffusion and biodistribution. Hum Gene Ther. 2009 Apr;20(4):350–60.

37. Miyake N, Miyake K, Yamamoto M, Hirai Y, Shimada T. Global gene transfer into the CNS across the BBB after neonatal systemic delivery of single-stranded AAV vectors. Brain Res. 2011 May 10;1389:19–26.

38. Zincarelli C, Soltys S, Rengo G, Rabinowitz JE. Analysis of AAV serotypes 1-9 mediated gene expression and tropism in mice after systemic injection. Mol Ther J Am Soc Gene Ther. 2008 Jun;16(6):1073–80.

39. Kotchey NM, Adachi K, Zahid M, Inagaki K, Charan R, Parker RS, et al. A Potential Role of Distinctively Delayed Blood Clearance of Recombinant Adeno-associated Virus Serotype 9 in Robust Cardiac Transduction. Mol Ther. 2011 Jun;19(6):1079–89.

40. Alemany R, Suzuki K, Curiel DT. Blood clearance rates of adenovirus type 5 in mice. J Gen Virol. 2000 Nov;81(Pt 11):2605–9.

CHAPTER 3

shRNA-induced saturation of the microRNA pathway in the rat brain

van Gestel MA
van Erp S
Sanders LE
Brans MA
Luijendijk MC
Merkestein M
Pasterkamp RJ
Adan RA

Gene Ther. 2014 Feb;21(2):205-11

Abstract

RNA interference (RNAi) is a powerful strategy for unraveling gene function and for drug target validation, but exogenous expression of short hairpin RNAs (shRNAs) has been associated with severe side effects. These may be caused by saturation of the microRNA pathway. This study shows degenerative changes in cell morphology and intrusion of blood vessels after transduction of the ventromedial hypothalamus (VMH) of rats with a shRNA expressing adeno-associated viral (AAV) vector. To investigate whether saturation of the microRNA pathway has a role in the observed side effects, expression of neuronal microRNA miR-124 was used as a marker. Neurons transduced with the AAV vector carrying the shRNA displayed a decrease in miR-124 expression. The decreased expression was unrelated to shRNA sequence or target and observed as early as 1 week after injection. In conclusion, this study shows that the tissue response after AAV-directed expression of an shRNA to the VMH is likely to be caused by shRNA-induced saturation of the microRNA pathway. We recommend controlling for miR-124 expression when using RNAi as a tool for studying (loss of) gene function in the brain as phenotypic effects caused by saturation of the RNAi pathway might mask true effects of specific downregulation of the shRNA target.

Introduction

RNA interference (RNAi) has become a very powerful and widely used technique for both determination of gene function and drug target validation. The specificity of post-transcriptional gene silencing has allowed for the design of precise targeting tools. Despite the successful application of RNAi to animal models of disease, there is emerging evidence linking high-level short hairpin RNA (shRNA) expression to cellular toxicity. An increasing number of reports reveal dramatic adverse effects after shRNA delivery *in vivo* regardless of tissue type or animal species. Adverse effects of shRNAs have been described in dog heart[1], in mouse liver[2–4], in several mouse brain regions such as striatum[5,6] and cerebellum[7] and in rat ventral tegmental area/substantia nigra[8,9] and red nucleus[10]. These toxic effects have been attributed to activation of innate immunity via induction of an interferon response[11], off target effects[12] and saturation of the microRNA pathway[2].

Viral vector-mediated overexpression or knockdown of genes is also a promising approach to unravel the role of genes implicated in energy balance. We have gained novel insights into the role of genes in bodyweight regulation by overexpressing the neuropeptides agouti-related peptide and neuropeptide Y using adeno-associated virus (AAV).[13,14] AAV expression constructs were also developed for stable expression of shRNAs targeting obesity-related genes, including the fat mass and obesity-associated protein *(FTO)*.[15] In order to address whether this specific approach induces toxicity, we performed a morphological analysis of neuronal degeneration using cresyl violet staining. We show the importance of using expression of neuron-specific microRNA miR-124 as tool to investigate whether toxic effects are due to saturation of the microRNA pathway.

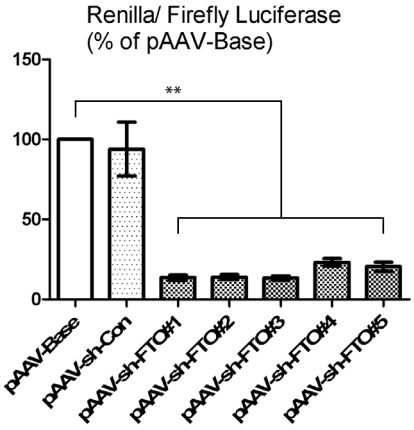

Figure 1 *In vitro* knockdown of FTO. FTO was efficiently down regulated by pAAV-sh-FTO#1 to #5 relative to the empty construct pAAV-Base. Transfection with the non-targeting pAAV-sh-Con did not result in knockdown of FTO.

Results and Discussion

The aim of the present study was to examine putative adverse effects of viral vector-mediated RNAi and to find a reliable method to determine toxicity due to saturation of the microRNA pathway. Five different *FTO*-targeting shRNA sequences were cloned into an AAV2 vector. A dual luciferase assay was performed to measure *FTO* knockdown by the different pAAV-sh-FTO constructs *in vitro* (Figure 1). pAAV-sh-FTO#1 (further referred to as pAAV-sh-FTO) was selected for further study because of its 87% silencing efficacy ($P<0.01$).

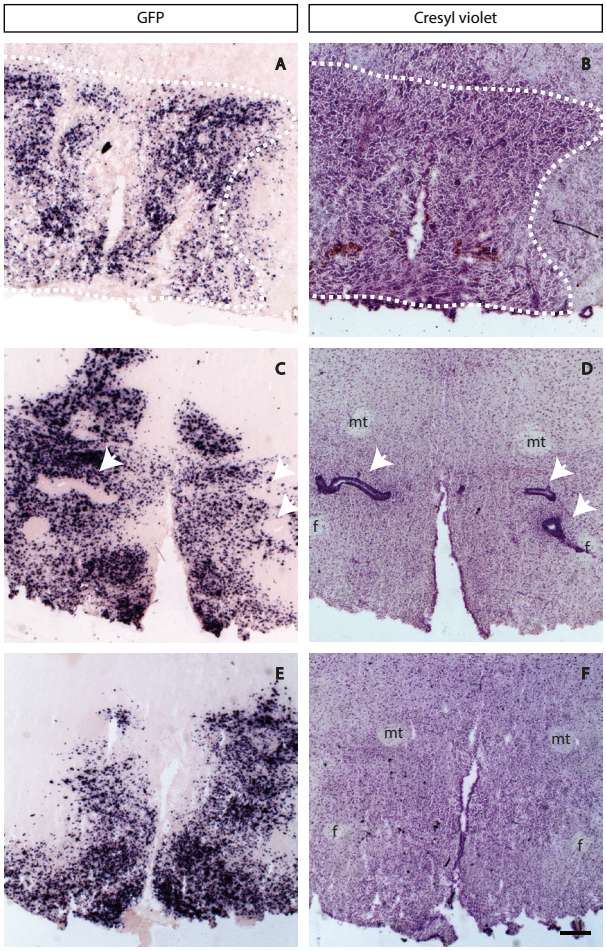

Figure 2 Toxicity following AAV-sh-FTO injection into the VMH. Rats received a bilateral injection with AAV-sh-FTO and were killed 6 weeks after injection. The VMH area was efficiently transduced as shown by ISH of GFP (A, C and E). A cresyl violet staining was performed to reveal potential toxicity. Toxicity manifested itself in most of the brains either by degenerative changes in tissue morphology (n=3) (B, within dotted line) or by bloodvessels (n=3) (D, arrow heads). Few brains showed no signs of toxicity (n=2) (F). mt, mammillothalamic tract; f, fornix. Scalebar: 500µm

pAAV-sh-FTO was encapsidated into an AAV1 coat and stereotactically injected into the ventromedial hypothalamus (VMH). Eight animals received AAV-sh-FTO and their brains were analyzed six weeks after injection. The viral vector contained a green fluorescent protein (GFP) cassette allowing the transduced area to be precisely

identified. An *in situ* hybridization (ISH) to detect GFP mRNA expression and a cresyl violet staining were used to analyze transduction efficiency and to detect potential toxicity, respectively. Analysis of GFP expression indicated that the hypothalamic area was efficiently transduced by AAV-sh-FTO (Figures 2a, c and e). However, cresyl violet staining revealed an adverse tissue reaction in the VMH in response to the injection of AAV-sh-FTO, as indicated by the degenerative changes in tissue morphology (n=3) (Figure 2b) or by intrusion of blood vessels (n=3) (Figure 2d). This was similar to Ehlert et al.[10] who used shRNAs targeting neuropilins in the red nucleus. Surprisingly, some brains of rats injected with the same amount of particles of the same viral prep appeared not to display an adverse tissue reaction (n=2) (Figure 2f), indicating that either the AAV-sh-FTO did not always induce toxicity or it was not always visible after cresyl violet staining. The observed differences in morphological changes might be explained by variation in the number of genomic copies that transduced the cells. Higher copy numbers could lead to increased toxicity.

Adverse effects after exogenous shRNA expression have been attributed to induction of an interferon response, massive off-target effects and saturation of the microRNA pathway.[2,11,12,16] As there were signs of toxicity, we focused on the saturation of the microRNA pathway as a possible cause of the observed adverse tissue reaction. It has been reported that viral vector-mediated expression of shRNAs may lead to downregulation of endogenous microRNAs both *in vitro*[17] and *in vivo*.[2,3] Expression of the endogenous neuronal microRNA miR-124 was analyzed to determine whether shRNA expression lead to saturation of the microRNA pathway. Cells transduced by AAV-sh-FTO showed a 62% decrease in miR-124 expression (Figures 3a and b). The sites where GFP was expressed, indicating infected cells, do not express miR-124, whereas there was ubiquitous expression of miR-124 in non-infected regions. To exclude the possibility that the observed toxicity is due to off-target effects by pAAV-sh-FTO or due to *FTO* knockdown, the non-targeting pAAV-sh-Con was also included. The overexpression construct pAAV-GFP was used to investigate whether AAV infection or GFP expression could result in toxicity. Animals receiving AAV-sh-Con (n=8) and AAV-GFP (n=4) were killed six weeks after injection. No decrease in miR-124 was observed after transduction with AAV-GFP (Figures 3c and d, Figure 4), indicating that GFP expression and AAV transduction were not responsible for the observed decrease in miR-124 expression. A loss of miR-124 expression (67%) was also detected in animals receiving the AAV-sh-Con (Figures 3e and f), suggesting that loss of miR-124 did not result from knockdown of the target gene. NeuN staining revealed some clear neuronal loss in areas targeted by AAV-sh-Con (Figure 3 f', Figure 5). Neurons that survived the ectopic expression of shRNAs showed a decrease in miR-124 expression. To exclude the possibility that only miR-124 was affected by the presence of shRNAs, a locked nucleic acid (LNA) ISH was

performed on miR-138. A decrease in miR-138 expression was observed in infected cells expressing GFP and the shRNA (Figure 6).

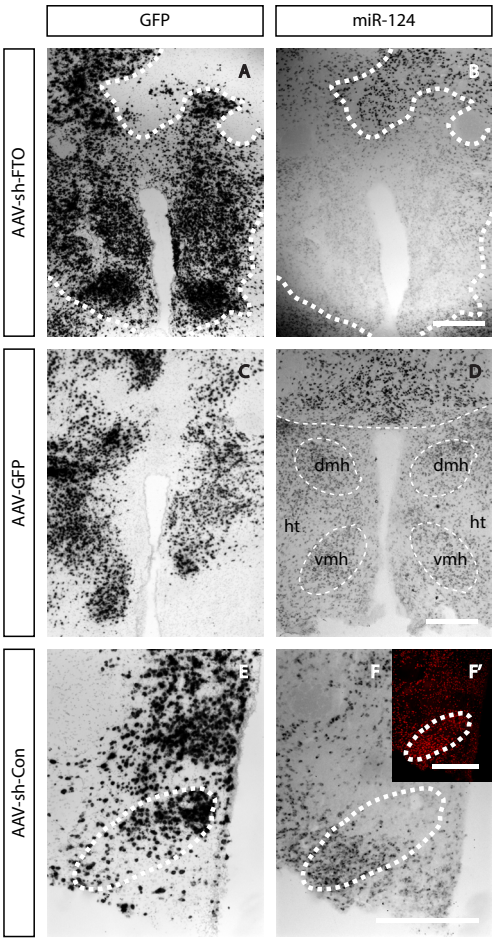

Figure 3 shRNA induced oversaturation of the microRNA pathway. Rats received a bilateral injection with AAV-sh-FTO, AAV-GFP or AAV-sh-Con and were killed 6 weeks after injection. GFP ISH was used to localize the viruses (AAV-sh-FTO (A), AAV-GFP (C) or AAV-sh-Con (E)). Expression of miR-124 was decreased within the areas transduced by shRNA carrying viruses AAV-sh-FTO (B) or AAV-sh-Con (F). MiR-124 expression in neurons transduced by overexpression virus AAV-GFP was not affected (D). Transduction by AAV-sh-Con (within dotted line (F')) resulted in some neuronal degeneration in the upper part of the VMH. ht, hypothalamic area; dmh, dorsomedial hypothalamic nucleus; vmh, ventromedial hypothalamic nucleus. Scalebar: 500µm

To learn more about shRNA-induced saturation of the microRNA pathway and its timeline, six rats received a unilateral injection of AAV-sh-FTO in the VMH. AAV-GFP was injected in the other side, so rats could serve as their own control. Rats were killed 1, 2 and 5 weeks after injection and their brains were analyzed for miR-124 and NeuN expression. After injection of AAV-sh-FTO in the VMH, a trend towards decreased miR-124 expression could be observed after only 1 week (Figure 7b). At 5 weeks miR-124 expression was decreased to 9±7.9% of control side (Figures 7h and j). Expression of *FTO* shRNA correlated strongly with reduction in miR-124 expression (Figures 7c, f and i).

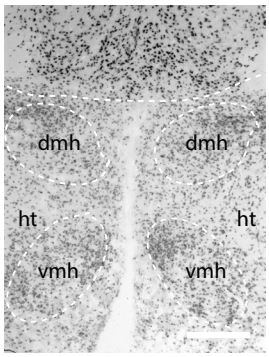

Figure 4 MiR-124 expression in the hypothalamic area of a non-transfected rat brain. ht, hypothalamic area; dmh, dorsomedial hypothalamic nucleus; vmh, ventromedial hypothalamic nucleus. Scalebar: 500µm

In none of the rats injected with AAV-sh-FTO or AAV-sh-Con into the VMH, body weight or food intake was affected (data not shown). This is in contrast to Tung et al.[18] who showed that expression of FTO shRNA in mice resulted in increased food intake. They targeted the arcuate nucleus, which is in close proximity to the VMH, and this may be a more important site for FTO to have a physiological role in energy balance than the VMH. However, Tung et al. did not report on toxicity, and the control used consisted of a scrambled shRNA.

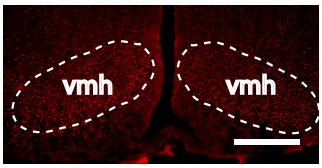

Figure 5 NeuN expression in the ventromedial hypothalamic nucleus of a non-transfected rat brain. vmh, ventromedial hypothalamic nucleus. Scalebar: 500µm

Our findings provide further evidence that the endogenous microRNA machinery is perturbed by shRNA overexpression. Consistent with previous findings, this decrease in endogenous microRNA expression is unrelated to shRNA sequence or target and is not observed after GFP overexpression.[10] Some studies report neuronal degeneration upon shRNA delivery[6], whereas others report a decrease in microRNA expression.[2] This study demonstrates that within one animal both neuronal degeneration, assessed by loss of NeuN staining, and a decrease in microRNA expression in surviving neurons, assessed by miR-124 staining, can be observed (Figures 3f and f'). Whether a neuron survives the saturation of the microRNA pathway might be dependent on the variation in number of genomic copies in transduced cells and the activity of the endogenous miRNA pathway.[17] These results indicate that the oversaturation of the microRNA machinery is progressive and precedes neuronal degeneration. Therefore, we cannot exclude that the lack of histologically visible toxicity after shRNA overexpression (such as shown in Figure 2) is due to a modest interference of endogenous microRNA expression that may develop over time.

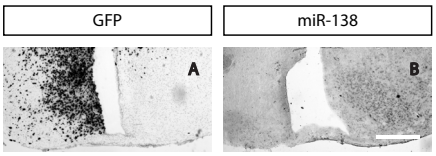

Figure 6 Decreased miR-138 expression following AAV-sh-FTO injection into the VMH. Rats received a bilateral injection with AAV-sh-FTO. GFP ISH was used to localize AAV-sh-FTO (A). MiR-138 expression was decreased in neurons transduced by AAV-sh-FTO (B). Scalebar: 500μm

As the downregulation of endogenous microRNAs is also seen in brains without morphological changes, these results indicate that lack of morphological changes or neuronal loss does not implicate that shRNA expression does not cause severe side effects. MicroRNAs function by targeting a variety of 3' untranslated regions of genes. Depending on the specific role of microRNAs in a given cell, a certain phenotypic effect will be induced. This effect might subsequently be attributed to the downregulation of the shRNA target. Besides cresyl violet and NeuN staining, expression of endogenous microRNAs appears to be a good marker for neuronal health after expression of shRNAs. We propose to use tissue-specific endogenous microRNAs as markers to exclude saturation of the microRNA pathway in studies of shRNA-mediated knockdown of genes. Care should be taken in interpreting results obtained from studies lacking these controls.[19–21]

Based on *in vitro* studies, Exportin-5 and Argonaute-2 are most likely the two components of the microRNA pathway to be saturated by exogenous shRNA expression. The karyopherin Exportin-5 is responsible for nuclear export of both shRNAs and pre-miRNAs.[22,23] Exogenous shRNAs can compete with pre-miRNAs for binding Exportin-5 leading to inhibition of miRNA function.[17] The consequences of this saturation can be relieved by overexpression of Exportin-5, enhancing both shRNA- and microRNA-induced RNAi *in vitro*[17,24] and *in vivo*.[2] As Exportin-5 expression is relatively low in the brain,[17] it is proposed that this makes this organ particularly sensitive to saturation of Exportin-5.[10] Within the cytoplasm, RNAi-induced silencing complex component Argonaute-2 is responsible for microRNA biogenesis and binding and cleavage of target mRNA. Overexpression of Argonaute-2 results in enhanced RNAi mediated by shRNAs and miRNAs.[24]

The specificity of RNAi allows for the design of very precise targeting tools, which may have the potential to be used as a therapeutic strategy. It is of importance in the use of RNAi for clinical applications to prevent saturation of the microRNA pathway by shRNAs without comprising their therapeutic efficacy. Possible strategies to relieve the saturation of microRNA pathways by exogenous shRNA expression include lowering the dose[8,10], the use of a less efficient or regulatable promoter[25], changing viral vector serotype[10] or placing the shRNA into a microRNA background.[5,7]

In summary, this study demonstrates the presence of an adverse tissue response after AAV1 administration to the VMH, which is likely to be caused by shRNA-induced saturation of the microRNA pathway. Decreased expression of endogenous microRNAs is evident 1 week after injection of the virus, and this decrease aggravates in time. In animal models of disease, these lowered levels of microRNA expression might lead to an incorrect interpretation of results. It is therefore important to carefully examine the expression of tissue-specific endogenous microRNAs as markers to be able to exclude potential toxicity due to saturation of the microRNA pathway.

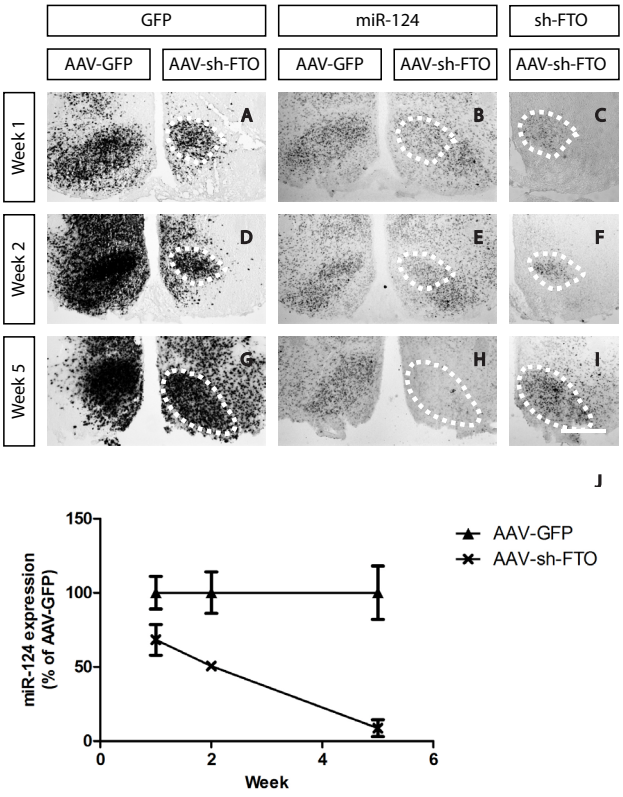

Figure 7 Toxicity timeline. Rats received a unilateral injection with AAV-GFP (left) and a unilateral injection with AAV-sh-FTO (right). Rats were killed 1, 2 or 5 weeks after injection. Presence of both viruses was localized using GFP ISH (A, D and G) and a LNA ISH on the FTO shRNA (C, F and I). MiR-124 expression decreased in time at the side of AAV-sh-FTO injection (right) and was unaffected at the side injected with AAV-GFP (left) (B, E and H). Graph (J) shows the average amount of miR-124 on the AAV-sh-FTO side relative to the AAV-GFP side of two different rats per time point. The relative difference in amount of miR-124 increased in time. Scalebar: 500µm

Material & Methods

Cell lines

Human Embryonic Kidney (HEK) 293T cells were cultured at 37ºC with 5% CO2 in Dulbecco's modified Eagle medium (DMEM) (Invitrogen, Carlsbad, CA, USA) supplemented with 10% fetal calf serum (FCS) (Lonza, Basel, Switzerland), 2 mM glutamine (PAA, Cölbe, Germany), 100 units/ml penicillin (PAA), 100 units/ml streptomycin (PAA) and non-essential amino acids (PAA).

AAV plasmids

All pAAV-shRNA constructs were designed by cloning oligonucleotides into the AAV2 vector pAAV-Base. The viral vector contained a GFP cassette to precisely identify the transduced area. Experiments were conducted using shRNAs targeting *FTO* (pAAV-sh-FTO), a control shRNA without an endogenous mRNA target (pAAV-sh-Con) and a GFP expression vector without shRNA (pAAV-GFP). pAAV-Base and pAAV-sh-Con were a kind gift from RJ DiLeone.[21] pAAV-sh-FTO plasmids were cloned as previously described.[26] Bioinformatics tools from Biopredsi (Qiagen, Valencia, CA, USA) and Invitrogen were used to identify shRNA sequences targeting *FTO*. Five sets of oligonucleotides were synthesized for cloning (Table 1). The oligonucleotides had XbaI and SapI overhangs to allow for ligation into the pAAV-Base. Cloning of AAV-GFP was previously described.[27] All constructs were verified by sequencing.

cDNA-renilla fusion construct

Rat *FTO* cDNA was obtained by PCR-amplification using B1 and B2 gateway primers on hypothalamic rat cDNA (Table 1). The cassette was recombined with pDONR201 (Invitrogen) to generate pENTR201-FTO. This construct was subsequently recombined with pBabe-puro (Invitrogen) containing Renilla Luciferase cDNA to generate the cDNA-Renilla fusion plasmid pBabe-FTO-Renilla. All constructs were verified by sequencing.

Luciferase assay

HEK293T cells in a 24-well plate were transfected with 5 ng pcDNA4/TO-luc, 500 ng pBabe-FTO-Renilla and 1500 ng pAAV-shRNA or pAAV-Base using polyethylenimine (Polysciences, Eppelheim, Germany). Three days after transfection, cells were lysed, and Renilla Luciferase activity was assessed. Values were corrected for transfection efficiency using Firefly Luciferase activity and normalized to pAAV-Base knockdown.

Virus production and purification

Virus was generated and purified as previously described.[26] HEK293T cells were co-transfected in 15 15 x 15cm^2 dishes with pAAV-shRNA or pAAV-GFP and pDP1

(Plasmid factory, Bielefeld, Germany) using polyethylenimine. Sixty hours after transfection, cells were collected, pelleted and resuspended in ice-cold buffer (150mM NaCl, 50mM Tris, pH 8.4). Cells were lysed by three freeze-thaw cycles and incubated for 30min at 37°C with 50Uml^{-1} Benzonase (Sigma, Zwijndrecht, The Netherlands). The lysate was loaded onto a 15, 25, 40, and 60% iodixanol gradient. After centrifugation at 70.000r.p.m. for 60min at 18°C, the 40% layer was extracted and used for ion-exchange chromatography. AAV-positive fractions were determined by quantitative PCR for GFP RNA (Table 1) and concentrated using an Amicon Ultra 15ml filter (Millipore). Titer was determined by quantitative PCR for GFP RNA (Table 1).

Table 1 Oligonucleotides used in this study

Primer	Sequence
FTO#1 Top	TTTGCACCTACAAGTACTTGAACTTCCTGTCATTCAAGTACTTGTAGGTGCTTTTT
FTO#1 Bottom	CTAGAAAAAGCACCTACAAGTACTTGAATGACAGGAAGTTCAAGTACTTGTAGGTGC
FTO#2 Top	TTTGGCTATCAAAGAGAAGGCCAATGAACTTCCTGTCATTCATTGGCCTTCTCTTTGATAGCCTTTTT
FTO#2 Bottom	CTAGAAAAAGGCTATCAAAGAGAAGGCCAATGAATGACAGGAAGTTCATTGGCCTTCTCTTTGATAGCC
FTO#3 Top	TTTCCTGCGATGATGAAGTGGACCTTAACTTCCTGTCATTAAGGTCCACTTCATCATCGCAGGTTTTT
FTO#3 Bottom	CTAGAAAAACCTGCGATGATGAAGTGGACCTTAATGACAGGAAGTTAAGGTCCACTTCATCATCGCAGG
FTO#4 Top	TTTCAACGTGACTTTGCTAAACTTCTTCCTGTCAAAGTTTAGCAAAGTCACGTTGTTTTT
FTO#4 Bottom	CTAGAAAAACAACGTGACTTTGCTAAACTTTGACAGGAAGAAGTTTAGCAAAGTCACGTTG
FTO#5 Top	TTTCCAGGGAGACTGCTATTTCATCTTCCTGTCAATGAAATAGCAGTCTCCCTGGTTTTT
FTO#5 Bottom	CTAGAAAAACCAGGGAGACTGCTATTTCATTGACAGGAAGAATGAAATAGCAGTCTCCCTGG
FTO B1	GGGGACAAGTTTGTACAAAAAAGCAGGCTTCGAAGGAGATACCACCATGAAGCGCGTCCAGACCGCGGA
FTO B2	GGGGACCACTTTGTACAAGAAAGCTGGGTCGGATCTTGCTTCCAGAAGCTG
GFP Forward	CACATGAAGCAGCACGACTT
GFP Reverse	GAAGTTCACCTTGATGCCGT

Animals

Male Wistar rats (Charles River, Germany) were housed in filter top cages in a temperature- and humidity-controlled room temperature (RT) 21±2°C and humidity 55±5%) with a 12-h light/dark cycle. All experimental procedures were approved by the Committee for Animal Experimentation of the University of Utrecht (Utrecht, the Netherlands).

Surgical procedures

Rats were anesthetized using fentanyl/fluanisone and midazolam and mounted onto a stereotaxic apparatus. Virus was administered by placing syringe needles into the VMH (coordinates from Bregma: -2.1 AP, +1.5 ML, -9.9 DV, at a 5° angle). A total of 1,5µl of virus (8.4×10^{11} $gcml^{-1}$) was injected at a rate of 0.2 $\mu lmin^{-1}$.

ISH

For the ISH, cryostat sections of 20 µm thickness from fresh frozen brains were mounted onto slides. Sections were fixed in 4% paraformaldehyde (PFA) for 20 min, washed in phosphate-buffered saline (PBS), acetylated for 10 min and washed again. The following steps differed between the ISH and the LNA ISH.

For the ISH, sections were pre-hybridized in hybridization solution (50% formamide, 5 x SSC, 5 x Denhardts, 250μgml^{-1} tRNA Baker's yeast, 500μgml^{-1} sonicated salmon sperm DNA) for 2h at RT. The hybridization solution containing 400$ngml^{-1}$ 720-bp long digoxigenin (DIG)-labeled enhanced GFP riboprobe (antisense to NCBI gene DQ768212) was then applied to the slides followed by overnight incubation at 68°C.

After a quick wash in 68°C pre-warmed 2 x SSC, slides were transferred to 68°C pre-warmed 0.2 x SSC for 2h. After blocking for 1h with 10% FCS in B1 (0.1M Tris pH 7.5/0.15M NaCl), DIG was detected with an alkaline phosphatase-labeled antibody (1:5000, Roche, Mannheim, Germany) after overnight incubation at RT using NBT/BCIP as a substrate. Sections were dehydrated in ethanol, cleared in xylene and embedded in Entellan.

The LNA ISH hybridization is performed as previously described.[28] Briefly, sections were pre hybridized in hybridization solution (50% formamide, 5 x SSC, 5 x Denhardts, 200$mgml^{-1}$ tRNA Baker's yeast, 500$mgml^{-1}$ sonicated salmon sperm DNA, 0.02gml^{-1} Roche blocking reagent) for 1h at RT. Hybridization was performed with 10nM double-DIG (3' and 5')-labeled LNA probe for human miR-124 or miR-138 (Exiqon, Denmark) or with 20nM double-DIG (3' and 5')-labeled LNA probe for the shFTO (Exiqon, Vedbaek, Denmark) for 2h at 55°C. After a quick wash in 60°C pre-warmed 5 x SSC, slides were transferred to 60°C pre warmed 0.2 x SSC for 2h. After blocking for 1h with

10% FCS in B1 (0.1M Tris pH 7.5/0.15M NaCl), DIG was detected with an alkaline phosphatase labeled antibody (1:2500, Roche, Germany) after overnight incubation at RT using NBT/BCIP as a substrate. Slides were further processed for immunohistochemistry.

Immunofluorescent labeling

Sections were blocked using 1% FCS in PBS/0.2% TritonX100 for 1h at RT. Next, mouse anti-NeuN (1:200, Millipore) diluted in blocking solution was applied to the sections for overnight incubation at 4°C. After washing in PBS, sections were incubated in secondary antibody goat-anti-mouse Alexa 594 (1:600, Invitrogen) in blocking solution. Images were taken using Axioscope A1 fluorescence and Axioskop 2 microscopes (Carl Zeiss, Göttingen, Germany).

ImageJ Software (National Institutes of Health, Bethesda, MD, USA) was used to quantify miR-124 expression in VMH neurons.

Acknowledgements

This work was supported by TIPharma, project T5-210-1, and by a VIDI grant from the Netherlands Organization for Health Research and Development and a grant from Neuroscience and Cognition Utrecht (to RJP). We acknowledge Eljo van Battum, Rudolf Magnus Institute of Neuroscience, for her technical assistance and Dr. Joost Verhaagen, Netherlands Institute for Neuroscience, for critically reading the manuscript.

References

1. Bish LT, Sleeper MM, Reynolds C, Gazzara J, Withnall E, Singletary GE, et al. Cardiac gene transfer of short hairpin RNA directed against phospholamban effectively knocks down gene expression but causes cellular toxicity in canines. Hum Gene Ther. 2011 Aug;22(8):969–77.
2. Grimm D, Streetz KL, Jopling CL, Storm TA, Pandey K, Davis CR, et al. Fatality in mice due to oversaturation of cellular microRNA/short hairpin RNA pathways. Nature. 2006 May 25;441(7092):537–41.
3. Borel F, van Logtenstein R, Koornneef A, Maczuga P, Ritsema T, Petry H, et al. *In vivo* knock-down of multidrug resistance transporters ABCC1 and ABCC2 by AAV-delivered shRNAs and by artificial miRNAs. J Rnai Gene Silenc Int J Rna Gene Target Res. 2011 Jun 17;7:434–42.
4. Ahn M, Witting SR, Ruiz R, Saxena R, Morral N. Constitutive Expression of Short Hairpin RNA *in Vivo* Triggers Buildup of Mature Hairpin Molecules. Hum Gene Ther. 2011 Dec;22(12):1483–97.
5. McBride JL, Boudreau RL, Harper SQ, Staber PD, Monteys AM, Martins I, et al. Artificial miRNAs mitigate shRNA-mediated toxicity in the brain: Implications for the therapeutic development of RNAi. Proc Natl Acad Sci. 2008 Apr 15;105(15):5868–73.
6. Martin JN, Wolken N, Brown T, Dauer WT, Ehrlich ME, Gonzalez-Alegre P. Lethal toxicity caused by expression of shRNA in the mouse striatum: implications for therapeutic design. Gene Ther. 2011 Jul;18(7):666–73.
7. Boudreau RL, Martins I, Davidson BL. Artificial MicroRNAs as siRNA Shuttles: Improved Safety as Compared to shRNAs *In vitro* and *In vivo*. Mol Ther J Am Soc Gene Ther. 2009 Jan;17(1):169–75.
8. Ulusoy A, Sahin G, Björklund T, Aebischer P, Kirik D. Dose Optimization for Long-term rAAV-mediated RNA Interference in the Nigrostriatal Projection Neurons. Mol Ther J Am Soc Gene Ther. 2009 Sep;17(9):1574–84.
9. Khodr CE, Sapru MK, Pedapati J, Han Y, West NC, Kells AP, et al. An alpha-synuclein AAV gene silencing vector ameliorates a behavioral deficit in a rat model of Parkinson's disease, but displays toxicity in dopamine neurons. Brain Res. 2011 Jun 13;1395:94–107.
10. Ehlert EM, Eggers R, Niclou SP, Verhaagen J. Cellular toxicity following application of adeno-associated viral vector-mediated RNA interference in the nervous system. Bmc Neurosci. 2010 Feb 18;11(1):20.
11. Sledz CA, Holko M, Veer MJ de, Silverman RH, Williams BRG. Activation of the interferon system by short-interfering RNAs. Nat Cell Biol. 2003;5(9):834–9.
12. Jackson AL, Bartz SR, Schelter J, Kobayashi SV, Burchard J, Mao M, et al. Expression profiling reveals off-target gene regulation by RNAi. Nat Biotechnol. 2003;21(6):635–7.
13. Tiesjema B, la Fleur SE, Luijendijk MCM, Adan RAH. Sustained NPY overexpression in the PVN results in obesity via temporarily increasing food intake. Obes Silver Spring Md. 2009 Jul;17(7):1448–50.
14. De Backer MWA, la Fleur SE, Adan RAH. Both overexpression of agouti-related peptide or neuropeptide Y in the paraventricular nucleus or lateral hypothalamus induce obesity in a neuropeptide- and nucleus specific manner. Eur J Pharmacol. 2011 Jun 11;660(1):148–55.
15. Frayling TM, Timpson NJ, Weedon MN, Zeggini E, Freathy RM, Lindgren CM, et al. A common variant in the *FTO* gene is associated with body mass index and predisposes to childhood and adult obesity. Science. 2007 May 11;316(5826):889–94.
16. Bridge AJ, Pebernard S, Ducraux A, Nicoulaz A-L, Iggo R. Induction of an interferon response by RNAi vectors in mammalian cells. Nat Genet. 2003 Jul;34(3):263–4.
17. Yi R, Doehle BP, Qin Y, Macara IG, Cullen BR. Overexpression of exportin 5 enhances RNA interference mediated by short hairpin RNAs and microRNAs. Rna New York N. 2005 Feb;11(2):220–6.

18. Tung Y-CL, Ayuso E, Shan X, Bosch F, O'Rahilly S, Coll AP, et al. Hypothalamic-Specific Manipulation of *Fto*, the Ortholog of the Human Obesity Gene *FTO*, Affects Food Intake in Rats. Plos One. 2010 Jan 19;5(1):e8771.
19. Hayes MR, Skibicka KP, Leichner TM, Guarnieri DJ, DiLeone RJ, Bence KK, et al. Endogenous leptin signaling in the caudal nucleus tractus solitarius and area postrema is required for energy balance regulation. Cell Metab. 2010 Jan;11(1):77–83.
20. Choi DL, Davis JF, Magrisso IJ, Fitzgerald ME, Lipton JW, Benoit SC. Orexin signaling in the paraventricular thalamic nucleus modulates mesolimbic dopamine and hedonic feeding in the rat. Neuroscience. 2012 May 17;210:243–8.
21. Hommel JD, Trinko R, Sears RM, Georgescu D, Liu Z-W, Gao X-B, et al. Leptin receptor signaling in midbrain dopamine neurons regulates feeding. Neuron. 2006 Aug 21;51(6):801–10.
22. Yi R, Qin Y, Macara IG, Cullen BR. Exportin-5 mediates the nuclear export of pre-microRNAs and short hairpin RNAs. Genes Dev. 2003 Dec 15;17(24):3011–6.
23. Lund E, Güttinger S, Calado A, Dahlberg JE, Kutay U. Nuclear export of microRNA precursors. Science. 2004 Jan 2;303(5654):95–8.
24. Diederichs S, Jung S, Rothenberg SM, Smolen GA, Mlody BG, Haber DA. Coexpression of Argonaute-2 enhances RNA interference toward perfect match binding sites. Proc Natl Acad Sci U S A. 2008 Jul 8;105(27):9284–9.
25. Grimm D, Wang L, Lee JS, Schürmann N, Gu S, Börner K, et al. Argonaute proteins are key determinants of RNAi efficacy, toxicity, and persistence in the adult mouse liver. J Clin Invest. 2010 Sep;120(9):3106–19.
26. Backer MWA de, Brans M a D, Rozen AJ van, Zwaal EM van der, Luijendijk MCM, Garner KG, et al. Suppressor of cytokine signaling 3 knockdown in the mediobasal hypothalamus: counterintuitive effects on energy balance. J Mol Endocrinol. 2010 Nov 1;45(5):341–53.
27. Broekman MLD, Comer LA, Hyman BT, Sena-Esteves M. Adeno-associated virus vectors serotyped with AAV8 capsid are more efficient than AAV-1 or -2 serotypes for widespread gene delivery to the neonatal mouse brain. Neuroscience. 2006;138(2):501–10.
28. Kan AA, van Erp S, Derijck AAHA, de Wit M, Hessel EVS, O'Duibhir E, et al. Genome-wide microRNA profiling of human temporal lobe epilepsy identifies modulators of the immune response. Cell Mol Life Sci Cmls. 2012 Sep;69(18):3127–45.

CHAPTER 4

A cautionary note: shRNA-induced toxicity in the ventral tegmental area induces a behavioral phenotype

van Gestel MA*
Pandit R*
Roelofs TJ
Sanders LE
de Jong JW
Luijendijk MC
Garner KM
Boender AJ
Adan RA

**Authors contributed equally to this work*

Abstract

Eight years ago, serious side effects were reported after *in vivo* short hairpin (sh) RNA expression. Despite this toxicity, knockdown studies continue to be published without proper controls for toxicity. One must be careful in interpreting results from RNA interference experiments as toxic responses to the shRNA overexpression might lead to (behavioral) phenotypes that are not related to the targeted gene. This study highlights that an shRNA-induced adverse tissue response instead of gene knockdown itself in the ventral tegmental area of the rat can result in a behavioral phenotype.

Introduction

RNA interference (RNAi) was first described in 1998 by Fire et al. and serves as a mechanism for the inhibition of gene expression.[1] The introduction of double-stranded RNA in a cell directs gene-specific, post-transcriptional depletion of the target gene. Besides its potential therapeutic application, RNAi is a promising tool to study gene function and to validate drug targets. Although RNAi has been successfully applied in cell culture and *in vivo* studies, evidence has accumulated the past eight years that vector-mediated gene silencing can result in severe toxicity. Grimm et al. (2006) were the first to report about dose-dependent hepatotoxicity in mice after viral vector-mediated RNAi.[2] The study showed that almost half of the short hairpin RNA (shRNA) sequences tested eventually resulted in death of the animals. The observed morbidity was associated with a downregulation of endogenous microRNAs, which implies a possible competition for a limiting cellular factor involved in the shRNA/microRNA pathway. The shRNA-induced adverse effects can occur in multiple tissues and is not species-specific, as they have been reported in dog heart, mouse liver and brain (striatum and cerebellum) and rat brain (ventral tegmental area (VTA)/ substantia nigra, red nucleus and ventromedial hypothalamus (VMH)). [2–12]

Although it has been eight years since the first report about shRNA-induced toxicity, RNAi is still applied often without extensively ruling out toxicity. Care should be taken in the interpretation of the results in these reports, as adverse tissue responses might lead to phenotypes that are not related to the targeted gene (e.g. false positives). This study highlights that an RNAi-induced toxic response instead of the gene knockdown itself may be responsible for a behavioral phenotype. The leptin receptor (*LepR*) in the VTA was targeted, as this brain area is known to be vulnerable to shRNA-induced toxicity.[9,10] Leptin mediates its effects through the LepR. Leptin is an adipose-derived hormone and circulating leptin concentrations are directly proportional to body fat.[13,14] Leptin has anorexic properties by increasing energy expenditure and decreasing food intake.[15–17] Loss of leptin signaling results in hyperphagia and subsequently obesity in mice and rats.[13,18–20] Although the arcuate nucleus is a major hub in transmitting leptin signaling further into the brain,[21] LepR is expressed in the VTA and 75-90% of LepR-positive cells are dopamine neurons.[22–24] In rats exposed to the activity-based anorexia model, peripheral and central leptin administration reduces hyperactivity.[25,26] Direct leptin injections into the VTA also reduces activity levels in rats exposed to the activity-based anorexia model, indicating a role of the VTA in the effects of leptin on locomotor activity in this animal model.[27] In animals on a normal diet, direct administration of leptin to the VTA has been shown to attenuate dopamine neuronal activity.[22] Leptin injected into the ventricle or the VTA results in a decreased food intake, while locomotor activity remains unchanged.[24,28,29] Transgenic animals lacking *LepR* in the dopaminergic neurons of the VTA show no changes in body weight, food

intake or locomotor activity.[30] Viral knockdown of *LepR* in the VTA increases food intake and increases locomotor activity.[22] These differences between transgenic animals lacking *LepR* in the dopaminergic neurons of the VTA and VTA knockdown animals might be explained by the specificity of the knockdown in the VTA (only dopaminergic neurons vs. all neurons), but could also result from a toxicity-related aspect arising from an shRNA-induced adverse tissue response.

Motivation for food reward as assessed by the extent of lever pressing for sucrose, implicates VTA dopaminergic neurons projecting to the nucleus accumbens.[31] Ventricular administration of leptin decreases progressive ratio performance for food, which implies a decreased motivation for food reward.[32] Knockdown of *LepR* in the midbrain of rats increases progressive ratio responding, suggesting that leptin acts to suppress increased dopaminergic neuronal activity in rats motivated to work for a sucrose reward.[33]

In this study, rats were injected with an adeno-associated virus (AAV) vector encoding an shRNA targeting the *LepR* into the VTA (AAV-shLepR), using the same vector that has been used in recent other studies as well.[22,34–36] Effects on energy balance and progressive ratio performance were compared to animals injected with an AAV vector containing no shRNA (AAV-GFP), a *LepR* antagonist (AAV-antaLepR) or an AAV vector containing an shRNA placed in a microRNA background (AAV-miLepR). Placing an shRNA in a microRNA background has been shown to mitigate the shRNA-induced toxicity.[6,8,37]

Material & Methods

Cell lines

Human embryonic kidney (HEK) 293T cells were maintained at 37ºC with 5% CO_2 in growth medium (Dulbecco's modified Eagle medium, DMEM) (Invitrogen, USA) supplemented with 10% fetal calf serum (FCS) (Lonza, Switzerland), 2mM glutamine (PAA, Germany), 100Uml^{-1} penicillin (PAA, Germany), 100Uml^{-1} streptomycin (PAA, Germany) and non-essential amino acids (PAA, Germany).

Construction of plasmids

Experiments were conducted using AAVs containing an shRNA placed in a microRNA background targeting *LepR* (experiment 1 and 2), an shRNA targeting *LepR* (experiment 2), a control AAV containing no targeting sequence (experiment 1, 2 and 3) and an AAV containing the sequence for a *LepR* antagonist (experiment 3). Rat leptin antagonist (pAAV-antaLepR) was obtained by mutating wildtype leptin gene with several point mutations as previously described.[38] For *in vitro* knockdown efficiency, a control shRNA not targeting the *LepR* was placed in a microRNA background. The pAAV expressing

microRNA was generated using the Gateway cloning technology (Invitrogen, USA) as previously described.[39] Briefly, microRNA sequences targeting *LepR* were designed using the 'Block-iT RNAi Designer' (Invitrogen, USA). The oligos (Table 1) were annealed and ligated into the synthetic intron of PSM155.[40] A cassette containing the intronic microRNA upstream of enhanced green fluorescent protein (EGFP) was then amplified using B3 and B4 primers and recombined to generate the entry vectors pENTR-R4-miLepR-EGFP-R3 and pENTR-R4-miCNTRL-EGFP-R3. The entry vector was recombined with pENTR-L1-ESYN-L4, pENTR-L3-oPRE-L2 and pAAV-R1-R2 to generate pAAV-ESYN-miLepR-EGFP (pAAV-miLepR) and pAAV-ESYN-miCNTRL-EGFP (pAAV-miCNTRL). The pBabe-LepR-Renilla construct was generated as previously described (LepR cDNA, Table 1).[12] pAAV-GFP and pAAV-shLepR were a kind gift from R. DiLeone.[22] AAV-OxR#1, AAV-OxR#2, AAV-ETV5#1 and ETV5#2 were constructed using oligos as described before (Table 1).[41]

Table 1 Oligonucleotides used in this study

Primer	Sequence
miLepR Top	TGCTGATGACATTCGCATTCCCGAACGTTTTGGCCACTGACTGACGTTCGGGAGCGAATGTCAT
miLepR Bottom	CCTGATGACATTCGCTCCCGAACGTCAGTCAGTGGCCAAAACGTTCGGGAATGCGAATGTCAC
miControl Top	TGCTGTTTAGGATATTTCAGCTGCCAGTTTTGGCCACTGACTGACTGGCAGCTAATATCCTAAA
miControl Bottom	CCTGTTTAGGATATTAGCTGCCAGTCAGTCAGTGGCCAAAACTGGCAGCTGAAATATCCTAAAC
LepR Forward	ATGACGTGTCAGAAATTCTAT
LepR Reverse	TGATGTAGGACGAATAGATGG
OxR#1 Top	TTTCCCTATCATCTACAACTTCCTCTTCCTGTCAAGGAAGTTGTAGATGATAGGGTTTTT
OxR#1 Bottom	CTAGAAAAACCCTATCATCTACAACTTCCTTGACAGGAAGAGGAAGTTGTAGATGATAGGG
OxR#2 Top	TTTGCGATTATCTCTATCCGAAGCAGTACTTCCTGTCATACTGCTTCGGATAGAGATAATCGCTTTTT
OxR#2 Bottom	CTAGAAAAAGCGATTATCTCTATCCGAAGCAGTATGACAGGAAGTACTGCTTCGGATAGAGATAATCGC
ETV5#1 Top	TTTGACAACTATTGTGCCTACGATACTCGAGTATCGTAGGCACAATAGTTGTTTTT
ETV5#1 Bottom	CTAGAAAAACAACTATTGTGCCTACGATACTCGAGTATCGTAGGCACAATAGTTGTC
ETV5#2 Top	TTTGAGGAAGTTTGTGGACACAGATCTCGAGATCTGTGTCCACAAACTTCCTTTTT
ETV5#2 Bottom	CTAGAAAAAGGAAGTTTGTGGACACAGATCTCGAGATCTGTGTCCACAAACTTCCTC
GFP Forward	CACAGACTTGTGGGAGAAGC
GFP Reverse	AGCCACTCGTCTTGGCAGT
LepRanta Forward	AGACCCCAGCGAGGAAAATG
LepRanta Reverse	TACCGACTGCGTGTGTGAAA

Luciferase assay

HEK293T cells in a 24-well plate were transfected with 5ng pcDNA4/TO-luc, 500ng pBabe-LepR-Renilla and 0, 250, 500 or 750ng pAAV-miCNTRL or pAAV-miLepR using polyethylenimine (PEI) (Polysciences, Germany). Three days after transfection, cells were lysed in passive lysis buffer and analyzed with a dual luciferase reporter assay according to manufacturer's protocol (Promega, USA). Firefly and Renilla luciferase activity were assessed; values were corrected for transfection efficiency using Firefly Luciferase activity and normalized to pAAV-miCNTRL knockdown.

Virus production and purification

Virus was generated and purified as previously described.[41] Briefly, HEK293T cells were co-transfected with pAAV-miLepR, pAAV-shLepR, pAAV-antaLepR or pAAV-GFP and pDP1 (Plasmid factory, Germany) in fifteen 15 x 15cm dishes using PEI. Sixty hours after transfection, cells were collected, pelleted and resuspended in ice-cold buffer (150mM NaCl, 50mM Tris, pH 8.4). Cells were lysed by three freeze-thaw cycles and incubated for 30min at 37°C with 50Uml^{-1} benzonase (Sigma, The Netherlands). The lysate was loaded onto a 15%, 25%, 40%, and 60% iodixanol gradient. After centrifugation at 70.000rpm for 60 minutes at 18°C, the 40% layer was extracted and used for ion-exchange chromatography. AAV positive fractions were determined by quantitative PCR (qPCR) on GFP or leptin antagonist primers (Table 1) and concentrated using an Amicon Ultra 15ml filter (Millipore). Titer was determined by qPCR on GFP.

Animal studies

Male Wistar rats (Charles River, Germany) of 220-250g were housed in filter top cages in a temperature- and humidity-controlled room (temperature 21±2°C and humidity 55±5%) with a 12h light/dark cycle. Animals had *ad libitum* access to chow and water. After one week of acclimatization, virus was administered stereotactically in the VMH (experiment 1) or VTA (experiment 2 and 3).

Surgical procedures

Rats were anesthetized using fentanyl/fluanisone and midazolam and mounted onto a stereotaxic apparatus. Virus was administered by placing a syringe needle into the VMH (experiment 1) (coordinates from Bregma: -2.1 AP, +1.5 ML, -9.9 DV, at a 5° angle), VTA (experiment 2 and 3) (coordinates from Bregma: -5.4 AP, +2.2 ML, -8.9 DV, at a 10° angle) or LH (experiment 3) (coordinates from Bregma: -2.8 AP, +1.8 ML, -9.4 DV). A total of 1µl virus (1 x 10^{12} genomic copies(gc)ml^{-1}) was injected at a rate of 0.2µlmin^{-1}. Rats received a transmitter in the abdominal cavity for the recording of locomotor activity and body temperature (TA10TA-F40, Data Science International, USA).

pSTAT3 staining

Animals from experiment 1 were killed 6 weeks after injection. One hour before decapitation animals received an i.p. injection of 2mgkg^{-1} leptin. Brains were removed, overnight post-fixed with 4%PFA and immersed in 30% sucrose solution in phosphate-buffered saline. Immunohistochemistry was performed on 40µm coronal free-floating slices as described previously.[42] Phosphorylated STAT3 (pSTAT$_3$) staining was performed using rabbit anti-pSTAT$_3$ (1:1000, rabbit monoclonal, Cell Signaling, USA). After overnight incubation, sections were washed and incubated with biotinylated antirabbit antibody (1:1000), followed by avidin-biotin-complex labeling. For analysis, sections were photographed using a bright-field microscope with a digital camera (Axiocam, Zeiss, Germany). Sections were matched using the stereotaxic brain atlas from Paxinos and Watson (1998).

Progressive ratio schedule of reinforcement

Animals (experiment 2 and 3) were trained under a progressive ratio schedule of reinforcement (PR) and had to meet a response requirement on the active lever, which increased progressively (1, 2, 4, 6, 9, 12, 15, 20, 25, etc.)[43] with every reward earned being one sucrose pellet. Each session started with illumination of the house light (signaling availability of the reward) and insertion of both levers. One of these levers functioned as active lever and the other as inactive lever. Meeting response requirement on the active lever resulted in retraction of both levers, illumination of the cue light above the active lever for 10sec and delivery of one sucrose pellet. After a 5sec timeout, a new cycle started. The session ended when the animals failed to earn a reward within 30min. Animals were trained on 1 shaping session, 5 fixed ratio (FR) sessions and 5 PR sessions. Animals in experiment 3 were trained on 1 shaping session, 5 FR sessions and 15 PR sessions. The average of the last three sessions was used for the outcome of the study. Animals were labeled as bad learners if they had less than 50 active lever presses (ALPs) and were excluded from the PR study.

In situ hybridization (ISH)

Animals were sacrificed 5 weeks (experiment 2) or 6 weeks (experiment 1) after virus injection. For the ISH, cryostat sections of 20µm thickness from fresh, frozen brains were mounted onto slides. Sections were fixed in 4% paraformaldehyde (PFA) for 20min, washed in phosphate-buffered saline, acetylated for 10 min and washed again. The following steps differed between the ISH and the locked nucleic acid (LNA) ISH. For the ISH, sections were pre hybridized in hybridization solution (50% formamide, 5 × SSC, 5 × Denhardts, 250µgml^{-1} tRNA Baker's yeast, 500µgml^{-1} sonicated salmon sperm DNA) for 2h at room temperature. The hybridization solution containing 400ngml^{-1} 720-bp long digoxigenin (DIG)-labeled EGFP riboprobe (antisense to NCBI gene DQ768212) was then applied to the slides followed by overnight incubation at 68°C.

After a quick wash in 68°C pre warmed 2 × SSC, slides were transferred to 68°C pre warmed 0.2 × SSC for 2h. After blocking for 1h with 10% FCS in B1 (0.1M Tris pH 7.5/0.15M NaCl), DIG was detected with an alkaline phosphatase-labeled antibody (1:5000, Roche, Mannheim, Germany) after overnight incubation at RT using NBT/BCIP as a substrate. Sections were dehydrated in ethanol, cleared in xylene and embedded in Entellan.

The LNA ISH hybridization is performed as previously described.[44] Briefly, PFA-fixed sections were pre hybridized in hybridization solution (50% formamide, 5 × SSC, 5 × Denhardts, 200mgml^{-1} tRNA Baker's yeast, 500mgml^{-1} sonicated salmon sperm DNA, 0.02gml^{-1} Roche blocking reagent) for 1h at RT. Hybridization was performed with 10nM double-DIG (3 and 5)-labeled LNA probe for human microRNA-124 (Exiqon, Denmark) for 2h at 55°C. After a quick wash in 60°C pre warmed 5 × SSC, slides were transferred to 60°C pre warmed 0.2 × SSC for 2h. After blocking for 1h with 10% FCS in B1 (0.1M Tris pH 7.5/0.15M NaCl), DIG was detected with an alkaline phosphatase-labeled antibody (1:2500, Roche) after overnight incubation at RT using NBT/BCIP as a substrate. Slides were further processed for immunohistochemistry.

Results

Experiment 1: In vitro and in vivo knockdown

A microRNA sequence targeting *LepR* was cloned into an AAV2 vector (pAAV-miLepR) and its *in vitro* knockdown efficiency was determined using a dual luciferase assay. pAAV-miCNTRL was used as a control. Increasing amounts of pAAV-miLepR (250, 500 and 750ng) resulted in an 84%, 85% and 85% silencing efficacy, respectively (Figure 1).

The plasmids were encapsidated into an AAV1 coat and AAV-miLepR was unilaterally injected into the VMH (n=4) to determine *in vivo* knockdown efficiency. As a control, AAV-GFP was injected on the other side of the brain in the VMH. After 6 weeks, the animals were killed and *in vivo* knockdown efficiency was determined using leptin signaling marker, phosphorylated-STAT3 (pSTAT3), which showed a clear unilateral

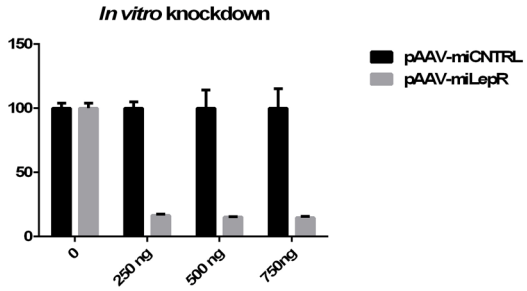

Figure 1 *In vitro* knockdown of *LepR*.

LepR was efficiently downregulated *in vitro* by pAAV-miLepR calculated as a percentage relative to pAAV-miCNRTL.

decline (Figure 2b), indicating decreased leptin signaling (n=2) and correct localization of the virus was determined using a GFP ISH (n=2)(Figure 2a).

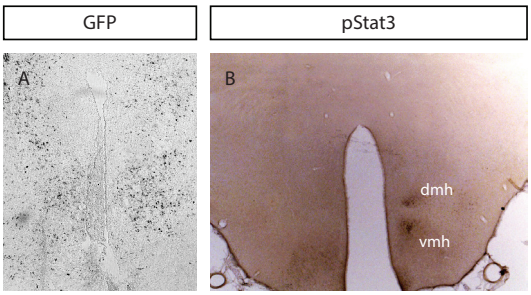

Figure 2 *In vivo* knockdown of *LepR*.

Rats (n=8) received a unilateral injection with AAV-miLepR and were killed 6 weeks after injection. AAV-GFP was injected on the other side as a control. pSTAT3, a leptin signaling marker showed a clear unilateral decline, indicating decreased leptin signaling (b). The VMH area was efficiently transduced as shown by ISH on GFP (a).

Experiment 2: Bodyweight, energy balance and progressive ratio

AAV-shLepR was designed as described.[22] AAV-shLepR (n=8), AAV-miLepR (n=8) and AAV-GFP (n=8) were stereotactically bilaterally injected into the VTA. Groups were matched for bodyweight, chow intake and locomotor activity prior to surgery. After injection of the AAVs into the VTA, bodyweight, chow intake and locomotor activity were measured for three weeks. No difference was observed for relative bodyweight (two-way ANOVA, interaction: $F(4, 40) = 0.4771$, $p = 0.75$; weeks: $F(2, 40) = 391.0$, $p < 0.01$; group: $F(2, 20) = 2.296$, $p = 0.1266$) or chow intake (two-way ANOVA, interaction: $F(4, 40) = 0.7575$, $p = 0.5591$; weeks: $F(2, 40) = 0.8621$, $p = 0.4300$; group $F(2, 20) = 0.8124$, $p = 0.4579$). Average locomotor activity prior to surgery was set at 100%. Relative locomotor activity in the dark phase of the AAV-shLepR group increased significantly compared to the AAV-miLepR and AAV-GFP group (two-way ANOVA, interaction: $F(6, 60) = 3.645$, $p < 0.01$; weeks: $F(3, 60) = 0.7453$, $p = 0.5293$; group: $F(2, 20) = 12.63$, $p < 0.01$) (Figure 3a). No differences in locomotor activity in the dark phase were observed between AAV-miLepR and AAV-GFP. We have also targeted other genes in the VTA with AAV-shRNAs and observed that many of them induced increased locomotor activity compared to AAV-GFP (Figure 3b). Three out of four shRNAs targeting E-twenty-six version 5 (ETV5) or the orexin receptor 1 (Ox1R) in the VTA resulted in increased dark phase locomotor activity.

Next, the animals injected with shRNAs targeting the leptin receptor (and controls) were trained and tested in a progressive ratio reinforcement schedule. Animals with less than 50 active lever presses were excluded from the experiment, as these animals did not learn the task. For the remaining animals (AAV-shLepR (n=5), AAV-miLepR (n=6) and AAV-GFP (n=5)) a trend was observed towards an increase in active lever presses in AAV-shLepR injected rats ($\chi 2=4.940$, $p=0.08$) (Figure 3c).

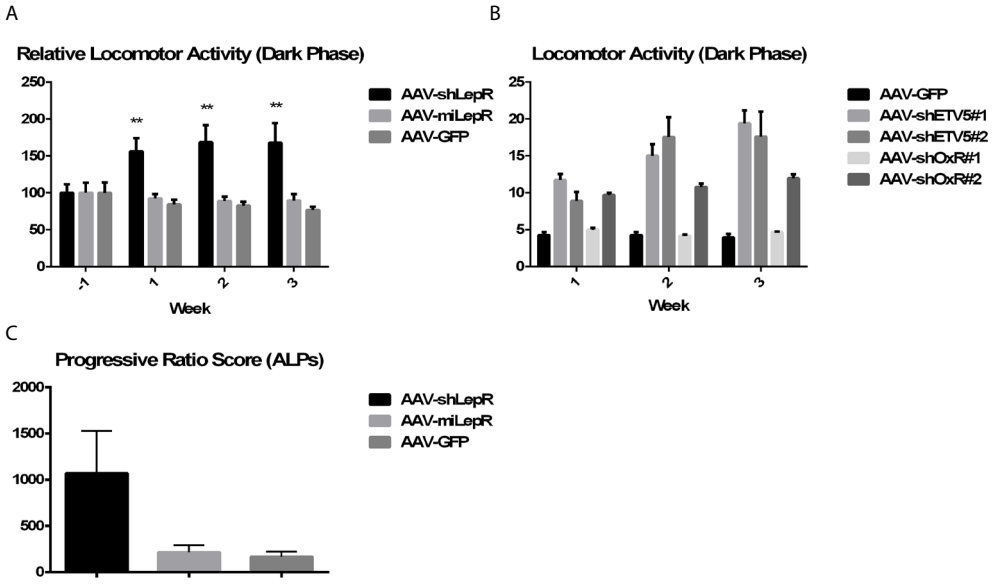

Figure 3 Locomotor activity and progressive ratio.
Rats received a bilateral injection with AAV-shLepR (n=8), AAV-miLepR (n=8) or AAV-GFP (n=8). Animals that received AAV-shLepR showed increased relative locomotor activity in the dark phase compared to the other groups ($p<0.01$)(a). Other shRNAs injected in the VTA induced the same increase in locomotor activity. Rats (n=8) received a bilateral injection in the VTA with AAV-GFP, AAV-shETV5#1, AAV-shETV5#2, AAV-shOxR#1 or AAV-shOxR#2 and locomotor activity was recorded for three weeks. Similar to observations in animals injected with AAV-shLepR, injection of three out of four shRNAs resulted in increased locomotor activity in the dark phase (b). Animals that received AAV-shLepR in the VTA showed a trend towards significance for the number of active lever pressing (ALP) on a progressive ratio schedule ($p=0.08$)(c).

Experiment 2: Virus localization and toxicity

Five weeks after virus injection, animals were killed and their brains were analyzed for the correct placement of the injections. As the viral vector contained a GFP cassette, the transduced area was precisely identified. An *in situ* hybridization to detect GFP mRNA expression was used to analyze transduction efficiency. Figures 4a, c and e represent typical examples of injections targeting the VTA. To ensure that the injections did not result in toxicity due to saturation of the microRNA pathway as observed after AAV-mediated short hairpin RNA expression in the VMH, we performed a microRNA-124 LNA ISH.[12] MicroRNA-124 is a ubiquitous microRNA expressed in neurons. AAV-GFP was previously shown not to cause a decrease in microRNA-124 expression.[12] Injections with AAV-miLepR did not result in shRNA-induced decreases in microRNA-124 expression compared to AAV-GFP (Figure 4d and f). A decrease of 78% in microRNA-124 levels was observed in regions transduced by AAV-shRNA (Figure 4b), indicating saturation of the microRNA pathway.

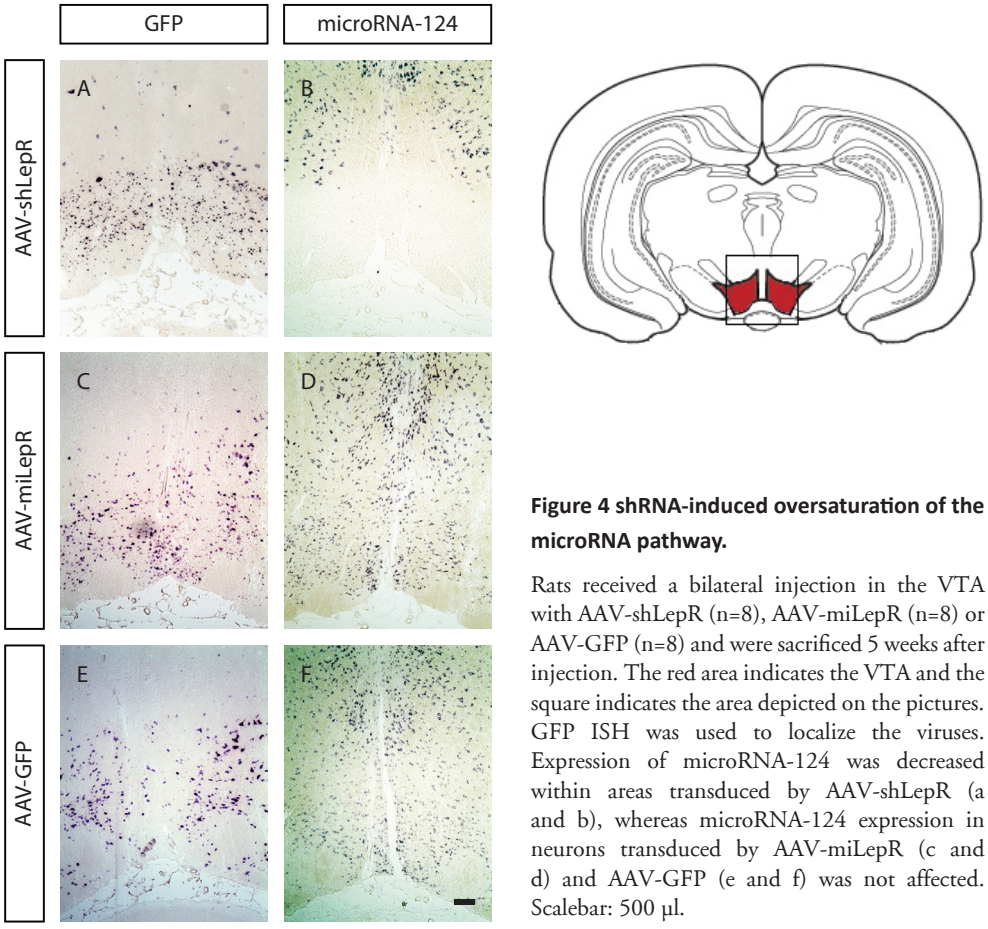

Figure 4 shRNA-induced oversaturation of the microRNA pathway.

Rats received a bilateral injection in the VTA with AAV-shLepR (n=8), AAV-miLepR (n=8) or AAV-GFP (n=8) and were sacrificed 5 weeks after injection. The red area indicates the VTA and the square indicates the area depicted on the pictures. GFP ISH was used to localize the viruses. Expression of microRNA-124 was decreased within areas transduced by AAV-shLepR (a and b), whereas microRNA-124 expression in neurons transduced by AAV-miLepR (c and d) and AAV-GFP (e and f) was not affected. Scalebar: 500 µl.

Experiment 3: Effect LepR antagonist on energy balance and progressive ratio

Animals (n=8) received a bilateral injection into the VTA with either AAV-GFP or AAV-antaLepR. After injection of the AAVs into the VTA, bodyweight, chow intake and locomotor activity were measured for 3 weeks. No differences between groups were observed in relative body weight (two-way ANOVA, interaction: $F(3, 42) = 1.930$, $p = 0.1393$; weeks: $F(3, 42) = 295.9$, $p < 0.01$; group: $F(1, 14) = 2.638$, $p = 0.1266$) (Figure 5c) or chow intake (two-way ANOVA, interaction: $F(2, 28) = 0.9657$, $p = 0.3930$; weeks: $F(2, 28) = 3.080$, $p = 0.0618$; group: $F(1, 14) = 2.747$, $p = 0.1197$). No differences in dark phase locomotor activity were observed (two-way ANOVA, interaction: $F(2, 10) = 0.2038$, $p = 0.8190$; weeks: $F(2, 10) = 0.3269$, $p = 0.7286$; group: $F(1, 5) = 1.690$, $p = 0.0.2503$)(Figure 5a). No significant effect was observed for the active lever presses on the progressive ratio procedure (Mann-Whitney U test, $p = 0.10$)(Figure 5b).

To ensure efficacy of the AAV-antaLepR, animals were injected bilaterally with AAV-antaLepR or AAV-GFP into the lateral hypothalamus and relative bodyweight was measured for three weeks. As mentioned before, AAV-antaLepR administration to the VTA did not result in changes in bodyweight (Figure 5c). Animals that received AAV-antaLepR showed a significant increase in bodyweight compared to controls. This difference in bodyweight was already observed one week after injection (two-way ANOVA, interaction: $F(3, 21) = 16.04$, $p < 0.01$; weeks: $F(3, 21) = 436.2$, $p < 0.01$; group: $F(1, 7) = 13.14$, $p < 0.01$)(Figure 5d).

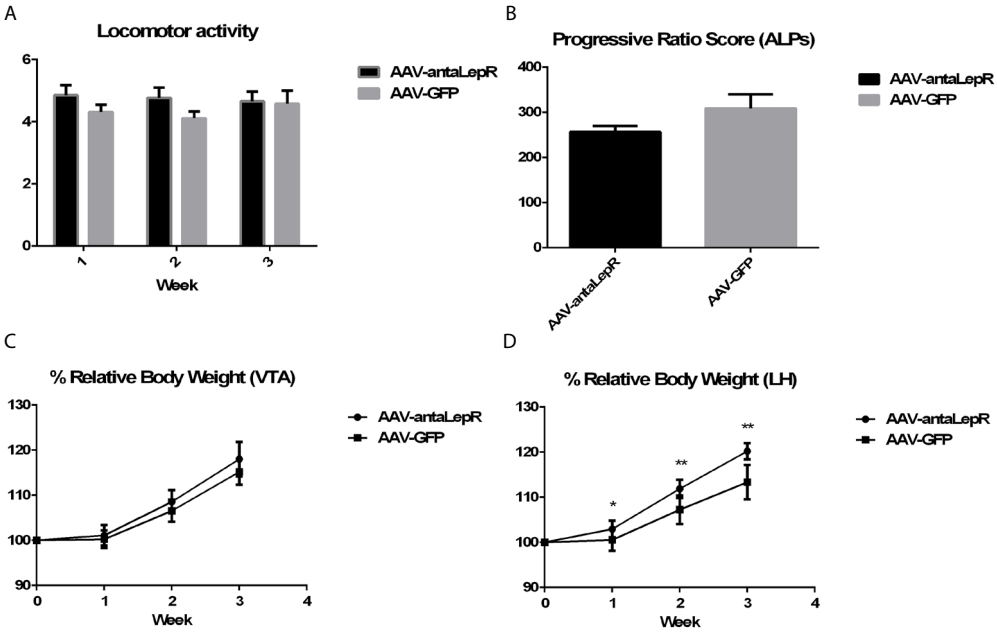

Figure 5 Effect LepR antagonist on energy balance and progressive ratio.

Rats received a bilateral injection of AAV-antaLepR or AAV-GFP in the VTA. No difference was observed in locomotor activity (a), active lever pressing (ALP)(b) or bodyweight (c). To ensure efficacy of the *LepR* antagonist, animals received a bilateral injection of AAV-LepR or AAV-GFP in the lateral hypothalamus (LH). Animals that received AAV-antaLepR showed a significant increase in bodyweight ($p<0.01$)(d).

Discussion

In the past eight years several studies have reported toxicity due to saturation of the endogenous microRNA pathway after AAV-mediated shRNA expression.[2,12] It is still unknown whether these observed adverse effects contribute to a toxicity-related behavioral phenotype. Recently, it was reported that shRNA expression resulted in a phenotype at a cellular level.[37] In this study, we investigated whether an RNAi-induced adverse tissue response in the VTA, a brain area known to be vulnerable to the shRNA-induced saturation of the microRNA pathway,[9,10] could result in a behavioral phenotype. The effects of an AAV carrying an shRNA against the LepR (AAV-shLepR)

and an AAV carrying an shRNA placed in a microRNA background against the LepR (AAV-miLepR) were compared.

To determine whether AAV-miLepR was able to knockdown LepR *in vivo*, animals were unilaterally injected with an AAV-miLepR and AAV-GFP served as a control (experiment 1). Immunohistochemical analysis of leptin-induced STAT3 phosphorylation showed unilateral staining, indicating decreased leptin signaling. In experiment 2, animals were bilaterally injected into the VTA with AAV-shLepR, AAV-miLepR or AAV-GFP. The effect on energy balance was measured for three weeks. No changes in bodyweight or chow intake were observed. Relative locomotor activity in the dark phase was increased in the AAV-shLepR group. Hommel et al. also found an increased locomotor activity after injection of this AAV carrying an shRNA targeting the *LepR*.[22] Both results are counterintuitive as transgenic animals lacking the *LepR* in dopaminergic neurons of the VTA do not show an increase in locomotor activity and leptin is known to have anorexic properties by increasing energy expenditure.[17,30] Furthermore, animals that received *LepR* antagonist in the VTA (experiment 3) did not show increased locomotor activity compared to controls. Animals were also tested for their performance on a PR schedule of reinforcement. A trend towards significance was observed for active lever presses for animals that received AAV-shLepR compared to controls. This trend was not observed for animals that received AAV-miLepR. In animals that received the LepR antagonist (experiment 3) no significant difference was observed compared to the controls, when tested for motivation to press a lever to obtain a sucrose reward under a progressive ratio schedule. These results are in contrast to a study in which viral knockdown of the LepR in the midbrain, using the same shRNA sequence targeting leptin receptor, was shown to result in an increased responding in a PR task.[33] The efficacy of the AAV-antaLepR used in this study was shown in the lateral hypothalamus, where its administration resulted in increased bodyweight.

When staining for neuronal microRNA-124 expression in the VTA, a decrease in microRNA-124 expression was observed in neurons transduced with AAV-shLepR, indicating a saturation of the microRNA pathway. No changes in microRNA expression were observed after transduction with AAV-miLepR or AAV-GFP. Both AAV-shLepR and AAV-miLepR resulted in *in vivo* downregulation of LepR expression.[22] It is very likely that the phenotype that is only observed after injections with AAV-shLepR and not after injections with AAV-miLepR was caused by saturation of the microRNA pathway and not (only) by knockdown of the *LepR*. Furthermore, previous experiments in our lab showed that shRNAs targeting different mRNAs show similar phenotypes. Only one shRNA targeting the orexin receptor 1 did not result in increased locomotor activity, which might be explained by a less efficient expression of this shRNA. To further exclude the possible role of the VTA LepR in locomotor activity, we examined

the effects after administration of a *LepR* antagonist expressed as cDNA from an AAV vector in the VTA. Animals receiving the LepR antagonist in the VTA did not show an increase in locomotor activity, confirming a role of shRNA-induced adverse tissue response in inducing the phenotype.

The vector encoding the shRNA targeting *LepR* was also used in other studies. As mentioned before, Hommel et al. (2006) observed a similar increase in locomotor activity after injection into the VTA.[22] Although the timeline of increased locomotor activity after virus administration is not clear from the description in the paper, this increase probably happened before the peak of AAV expression, making it very likely that the increased locomotor activity resulted from an adverse tissue response. In the Hayes et al. (2010) study, increased consumption of high caloric food was observed after expression of the shRNA targeting *LepR* in the medial nucleus tractus solitarius.[36] Similar observations were seen in rats with lesions in this brain area.[45] Without proper controls for toxicity, it cannot be excluded that the observations were due to RNAi-induced toxicity. Finally, Davis et al. (2011) used the same shRNA sequence in a lentiviral context to knockdown *LepR* in the VTA, resulting in increased responding for sucrose in a progressive ratio reinforcement schedule.[33] This study showed a trend towards increased active lever pressing for sucrose in rats with a decreased microRNA expression in the VTA. Although there is no evidence for *in vivo* lentiviral-induced toxicity and it was shown that transduction using lentiviral vectors is less efficient than transduction using AAV vectors,[46] controls for toxicity should exclude a toxicity-related behavioral phenotype.

The results from this study caution for the interpretation of shRNA results and one should take into account that proper controls for toxicity caused by saturation of the endogenous RNAi pathway need to be included when designing RNAi experiments. Since a variety of shRNAs expressed in the VTA induced increased locomotor activity, likely caused by saturation of the endogenous RNAi pathway, these data suggest that an endogenous microRNA in the VTA acts to suppress locomotor activity. A decrease in expression of this microRNA, due to saturation by shRNAs expressed from the AAV vector, may have caused the observed increased locomotor activity.

References

1. Fire, A. *et al.* Potent and specific genetic interference by double-stranded RNA in Caenorhabditis elegans. *Nature* **391,** 806–811 (1998).
2. Grimm, D. *et al.* Fatality in mice due to oversaturation of cellular microRNA/short hairpin RNA pathways. *Nature* **441,** 537–541 (2006).
3. Bish, L. T. *et al.* Cardiac gene transfer of short hairpin RNA directed against phospholamban effectively knocks down gene expression but causes cellular toxicity in canines. *Hum. Gene Ther.* **22,** 969–977 (2011).
4. Borel, F. *et al.* In vivo knock-down of multidrug resistance transporters ABCC1 and ABCC2 by AAV-delivered shRNAs and by artificial miRNAs. *J. RNAi Gene Silenc. Int. J. RNA Gene Target. Res.* **7,** 434–442 (2011).
5. Ahn, M., Witting, S. R., Ruiz, R., Saxena, R. & Morral, N. Constitutive Expression of Short Hairpin RNA in Vivo Triggers Buildup of Mature Hairpin Molecules. *Hum. Gene Ther.* **22,** 1483–1497 (2011).
6. McBride, J. L. *et al.* Artificial miRNAs mitigate shRNA-mediated toxicity in the brain: Implications for the therapeutic development of RNAi. *Proc. Natl. Acad. Sci.* **105,** 5868–5873 (2008).
7. Martin, J. N. *et al.* Lethal toxicity caused by expression of shRNA in the mouse striatum: implications for therapeutic design. *Gene Ther.* **18,** 666–673 (2011).
8. Boudreau, R. L., Martins, I. & Davidson, B. L. Artificial MicroRNAs as siRNA Shuttles: Improved Safety as Compared to shRNAs In vitro and In vivo. *Mol. Ther. J. Am. Soc. Gene Ther.* **17,** 169–175 (2009).
9. Ulusoy, A., Sahin, G., Björklund, T., Aebischer, P. & Kirik, D. Dose Optimization for Long-term rAAV-mediated RNA Interference in the Nigrostriatal Projection Neurons. *Mol. Ther. J. Am. Soc. Gene Ther.* **17,** 1574–1584 (2009).
10. Khodr, C. E. *et al.* An alpha-synuclein AAV gene silencing vector ameliorates a behavioral deficit in a rat model of Parkinson's disease, but displays toxicity in dopamine neurons. *Brain Res.* **1395,** 94–107 (2011).
11. Ehlert, E. M., Eggers, R., Niclou, S. P. & Verhaagen, J. Cellular toxicity following application of adeno-associated viral vector-mediated RNA interference in the nervous system. *BMC Neurosci.* **11,** 20 (2010).
12. Van Gestel, M. A. *et al.* shRNA-induced saturation of the microRNA pathway in the rat brain. *Gene Ther.* **21,** 205–211 (2014).
13. Zhang, Y. *et al.* Positional cloning of the mouse obese gene and its human homologue. *Nature* **372,** 425–432 (1994).
14. Considine, R. V. *et al.* Serum immunoreactive-leptin concentrations in normal-weight and obese humans. *N. Engl. J. Med.* **334,** 292–295 (1996).
15. Campfield, L. A., Smith, F. J., Guisez, Y., Devos, R. & Burn, P. Recombinant mouse OB protein: evidence for a peripheral signal linking adiposity and central neural networks. *Science* **269,** 546–549 (1995).
16. Grill, H. J. *et al.* Evidence that the caudal brainstem is a target for the inhibitory effect of leptin on food intake. *Endocrinology* **143,** 239–246 (2002).
17. Pelleymounter, M. A. *et al.* Effects of the obese gene product on body weight regulation in ob/ob mice. *Science* **269,** 540–543 (1995).
18. Bahary, N., Leibel, R. L., Joseph, L. & Friedman, J. M. Molecular mapping of the mouse db mutation. *Proc. Natl. Acad. Sci. U. S. A.* **87,** 8642–8646 (1990).

19. Phillips, M. S. *et al.* Leptin receptor missense mutation in the fatty Zucker rat. *Nat. Genet.* **13,** 18–19 (1996).

20. Takaya, K. *et al.* Nonsense mutation of leptin receptor in the obese spontaneously hypertensive Koletsky rat. *Nat. Genet.* **14,** 130–131 (1996).

21. Schwartz, M. W., Woods, S. C., Porte, D., Seeley, R. J. & Baskin, D. G. Central nervous system control of food intake. *Nature* **404,** 661–671 (2000).

22. Hommel, J. D. *et al.* Leptin Receptor Signaling in Midbrain Dopamine Neurons Regulates Feeding. *Neuron* **51,** 801–810 (2006).

23. Figlewicz, D. P., Evans, S. B., Murphy, J., Hoen, M. & Baskin, D. G. Expression of receptors for insulin and leptin in the ventral tegmental area/substantia nigra (VTA/SN) of the rat. *Brain Res.* **964,** 107–115 (2003).

24. Leshan, R. L. *et al.* Ventral tegmental area leptin receptor neurons specifically project to and regulate cocaine- and amphetamine-regulated transcript neurons of the extended central amygdala. *J. Neurosci. Off. J. Soc. Neurosci.* **30,** 5713–5723 (2010).

25. Exner, C. *et al.* Leptin suppresses semi-starvation induced hyperactivity in rats: implications for anorexia nervosa. *Mol. Psychiatry* **5,** 476–481 (2000).

26. Hillebrand, J. J. G., Koeners, M. P., de Rijke, C. E., Kas, M. J. H. & Adan, R. A. H. Leptin treatment in activity-based anorexia. *Biol. Psychiatry* **58,** 165–171 (2005).

27. Verhagen, L. A. W., Luijendijk, M. C. M. & Adan, R. A. H. Leptin reduces hyperactivity in an animal model for anorexia nervosa via the ventral tegmental area. *Eur. Neuropsychopharmacol.* **21,** 274–281 (2011).

28. Morton, G. J., Blevins, J. E., Kim, F., Matsen, M. & Figlewicz, D. P. The action of leptin in the ventral tegmental area to decrease food intake is dependent on Jak-2 signaling. *Am. J. Physiol. Endocrinol. Metab.* **297,** E202–210 (2009).

29. Krügel, U., Schraft, T., Kittner, H., Kiess, W. & Illes, P. Basal and feeding-evoked dopamine release in the rat nucleus accumbens is depressed by leptin. *Eur. J. Pharmacol.* **482,** 185–187 (2003).

30. Liu, J., Perez, S. M., Zhang, W., Lodge, D. J. & Lu, X.-Y. Selective deletion of the leptin receptor in dopamine neurons produces anxiogenic-like behavior and increases dopaminergic activity in amygdala. *Mol. Psychiatry* **16,** 1024–1038 (2011).

31. Nowend, K. L., Arizzi, M., Carlson, B. B. & Salamone, J. D. D1 or D2 antagonism in nucleus accumbens core or dorsomedial shell suppresses lever pressing for food but leads to compensatory increases in chow consumption. *Pharmacol. Biochem. Behav.* **69,** 373–382 (2001).

32. Figlewicz, D. P., Bennett, J. L., Naleid, A. M., Davis, C. & Grimm, J. W. Intraventricular insulin and leptin decrease sucrose self-administration in rats. *Physiol. Behav.* **89,** 611–616 (2006).

33. Davis, J. F. *et al.* Leptin Regulates Energy Balance and Motivation Through Action at Distinct Neural Circuits. *Biol. Psychiatry* **69,** 668–674 (2011).

34. Simonds, S. E. *et al.* Leptin Mediates the Increase in Blood Pressure Associated with Obesity. *Cell* **159,** 1404–1416 (2014).

35. Kanoski, S. E. *et al.* Endogenous leptin receptor signaling in the medial nucleus tractus solitarius affects meal size and potentiates intestinal satiation signals. *Am. J. Physiol. - Endocrinol. Metab.* **303,** E496–E503 (2012).

36. Hayes, M. R. *et al.* Endogenous leptin signaling in the caudal nucleus tractus solitarius and area postrema is required for energy balance regulation. *Cell Metab.* **11,** 77–83 (2010).

37. Baek, S. T. *et al.* Off-Target Effect of doublecortin Family shRNA on Neuronal Migration Associated with Endogenous MicroRNA Dysregulation. *Neuron* **82,** 1255–1262 (2014).

38. Matheny, M., Strehler, K. Y. E., King, M., Tümer, N. & Scarpace, P. J. Targeted leptin receptor blockade: role of ventral tegmental area and nucleus of the solitary tract leptin receptors in body weight homeostasis. *J. Endocrinol.* **222,** 27–41 (2014).

39. White, M. D. & Nolan, M. F. A Molecular toolbox for rapid generation of viral vectors to up- or down-regulate neuronal gene expression in vivo. *Front. Mol. Neurosci.* **4,** 8 (2011).

40. Du, G., Yonekubo, J., Zeng, Y., Osisami, M. & Frohman, M. A. Design of expression vectors for RNA interference based on miRNAs and RNA splicing. *FEBS J.* **273,** 5421–5427 (2006).

41. De Backer, M. W. A., Brans, M. A. D., Luijendijk, M. C., Garner, K. M. & Adan, R. A. H. Optimization of adeno-associated viral vector-mediated gene delivery to the hypothalamus. *Hum. Gene Ther.* **21,** 673–682 (2010).

42. Münzberg, H., Huo, L., Nillni, E. A., Hollenberg, A. N. & Bjørbaek, C. Role of signal transducer and activator of transcription 3 in regulation of hypothalamic proopiomelanocortin gene expression by leptin. *Endocrinology* **144,** 2121–2131 (2003).

43. Richardson, N. R. & Roberts, D. C. Progressive ratio schedules in drug self-administration studies in rats: a method to evaluate reinforcing efficacy. *J. Neurosci. Methods* **66,** 1–11 (1996).

44. Kan, A. A. *et al.* Genome-wide microRNA profiling of human temporal lobe epilepsy identifies modulators of the immune response. *Cell. Mol. Life Sci. CMLS* (2012). doi:10.1007/s00018-012-0992-7

45. Hyde, T. M. & Miselis, R. R. Effects of area postrema/caudal medial nucleus of solitary tract lesions on food intake and body weight. *Am. J. Physiol.* **244,** R577–587 (1983).

46. De Backer, M. W. A. *et al.* An adeno-associated viral vector transduces the rat hypothalamus and amygdala more efficient than a lentiviral vector. *BMC Neurosci.* **11,** 81 (2010).

CHAPTER 5

FTO knockdown in rat ventromedial hypothalamus does not affect energy balance

van Gestel MA
Sanders LE
de Jong JW
Luijendijk MC
Adan RA

Physiol Rep. 2014 Dec 11;2(12). pii: e12152

Abstract

Single nucleotide polymorphisms (SNPs) clustered in the first intron of the fat mass and obesity-associated (*FTO*) gene have been associated with obesity. FTO expression is ubiquitous, with particularly high levels in the hypothalamic area of the brain. To investigate the region-specific role of *FTO*, AAV technology was applied to knockdown *FTO* in the ventromedial hypothalamus (VMH). No effect of *FTO* knockdown was observed on bodyweight or parameters of energy balance. Animals were exposed twice to an overnight fast, followed by a high-fat high-sucrose (HFHS) diet for one week. *FTO* knockdown did not result in a different response to the diets. A region-specific role for *FTO* in the VMH in the regulation of energy balance could not be found.

Introduction

Overweight and obesity are increasingly important health problems worldwide. The World Health Organization reports that 1.4 billion adults are overweight and approximately one-third of them are obese. During 1980 and 2008, obesity rates nearly doubled.[1] Obesity has been implicated as a major risk factor for cardiovascular diseases[2–4] and diabetes[5,6]. Furthermore, obesity was associated with depression.[7] An environment that promotes high caloric food intake and discourages physical activity contributes to the occurrence of obesity. Obesity-associated genes might explain why individuals respond differently to this obesogenic environment. Indeed, family, twin and adoptions studies point to a strong genetic basis for the development of obesity.[8–11]
In 2007, studies confirmed the fat mass and obesity-associated (*FTO*) gene as the first genome-wide association study (GWAS)-identified obesity susceptibility gene.[12–14] Common variants in the first intron of the *FTO* gene were associated with an increase in body mass index (BMI) of approximately 0.4 kg/m^2 per risk allele.[12] Variations in the *FTO* gene seem to influence energy balance by increased energy intake[15–20] and not by decreased physical activity[16,17,19,21–25]. FTO was identified as a 2-oxoglutarate-dependent nucleic acid demethylase and is involved in the demethylation of single stranded DNA and RNA.[26,27] It is suggested that FTO may regulate transcription of genes involved in energy balance by demethylation.[26]

FTO is widely expressed throughout the brain, especially in the hypothalamic arcuate (ARC), paraventricular, dorsomedial (DMH) and ventromedial (VMH) nuclei.[26,28] In this study, we focused on the role of *FTO* on energy balance in the VMH, a hypothalamic nucleus involved in obesity, fear and female reproductive behavior.[29–32] A microRNA-expressing AAV was injected into the VMH of rats and bodyweight, food intake, locomotor activity and body temperature were monitored. No effect of *FTO* knockdown was found on bodyweight or parameters of energy balance. We previously showed that exposure to a restricted feeding schedule results in increased expression of FTO in the ARC and the VMH.[33] To examine the effect of fasting on bodyweight and food intake, animals with *FTO* knockdown were exposed to an overnight fast twice. We did not observe an effect of fasting on bodyweight or on refeeding after restriction. Finally, a high-fat high-sucrose (HFHS) diet was introduced to the animals. Again, no differences were seen between the controls and the VMH *FTO* knockdown animals in their response to the HFHS diet. *FTO* in the VMH seems to have no impact on bodyweight or energy balance.

Material and Methods

Cell lines

Human embryonic kidney (HEK) 293T cells were maintained at 37ºC with 5% CO_2 in growth medium (Dulbecco's modified Eagle medium, DMEM) (Invitrogen, Carlsbad, CA) supplemented with 10% fetal calf serum (FCS) (Lonza, Basel, Switzerland), 2mM glutamine (PAA, Germany), 100Uml^{-1} penicillin (PAA, Germany), 100Uml^{-1} streptomycin (PAA, Germany) and non-essential amino acids (PAA, Germany).

Construction of plasmids

An FTO-Renilla fusion plasmid was constructed as previously described.[34] Experiments were conducted using miRNAs targeting *FTO,* a control miRNA targeting *Hcrtr1* and a control miRNA targeting Firefly Luciferase. pAAVs that express miRNAs were generated using the Gateway cloning technology (Invitrogen, USA) as previously described.[35] Briefly, miRNA sequences targeting *FTO* and *Hcrtr1* were designed using the 'Block-iT RNAi Designer' (Invitrogen) (Table 1). The oligos were annealed and ligated into the synthetic intron of PSM155.[36] A cassette containing the intronic miRNA upstream of enhanced green fluorescent protein (EGFP) was then amplified using B3 and B4 primers and recombined to generate the entry vectors pENTR-R4-miFTO1-EGFP-R3, pENTR-R4-miFTO2-EGFP-R3, pENTR-R4-miFTO3-EGFP-R3 and pENTR-R4-miHcrtr1-EGFP-R3. Each entry vectors was recombined with pENTR-L1-ESYN-L4, pENTR-L3-oPRE-L2 and pAAV-R1-R2 to generate pAAV-ESYN-miFTO1-EGFP (pAAV-miFTO#1), pAAV-ESYN-miFTO2-EGFP (pAAV-miFTO#2), pAAV-ESYN-miFTO3-EGFP (pAAV-miFTO#3) and pAAV-ESYN-miHcrtr1-EGFP (pAAV-miHcrtr1). pAAV-miLuc was a kind gift of M.F. Nolan.[35]

Luciferase assay

HEK293T cells in a 24-well plate were transfected with 5ng pcDNA4/TO-luc, 500ng pBabe-FTO-Renilla and 1500ng pAAV-miFTO or pAAV-miHcrtr1 using polyethylenimine (PEI) (Polysciences, Eppelheim, Germany). Three days after transfection, cells were lysed in passive lysis buffer and analyzed/ with a dual luciferase reporter assay according to manufacturer's protocol (Promega, USA). Firefly and Renilla luciferase activity were assessed; values were corrected for transfection efficiency using Firefly Luciferase activity and normalized to pAAV-miHcrtr1 knockdown.

Virus production and purification

Virus was generated and purified as previously described.[37] Briefly, HEK293T cells were co-transfected with pAAV-miRNA and pDP1 (Plasmid factory, Bielefeld, Germany) in fifteen 15 x 15 cm dishes using PEI. Sixty hours after transfection, cells were collected, pelleted and resuspended in ice-cold buffer (150mM NaCl, 50mM Tris, pH 8.4). Cells

were lysed by three freeze-thaw cycles and incubated for 30min at 37°C with 50Uml^{-1} benzonase (Sigma, Zwijndrecht, The Netherlands). The lysate was loaded onto a 15%, 25%, 40%, and 60% iodixanol gradient. After centrifugation at 70.000rpm for 60min at 18°C, the 40% layer was extracted and used for ion-exchange chromatography. AAV positive fractions were determined by quantitative PCR (qPCR) on GFP (Table 1) and concentrated using an Amicon Ultra 15ml filter (Millipore). Titer was determined by qPCR on GFP.

Table 1 Overview of oligonucleotides used in this study

Primer	Sequence
miFTO#1 Top	TGCTGTTTAGGATATTTCAGCTGCCAGTTTTGGCCACTGACTGACTGGCAGCTAATATCCTAAA
miFTO#1 Bottom	CCTGTTTAGGATATTAGCTGCCAGTCAGTCAGTGGCCAAAACTGGCAGCTGAAATATCCTAAAC
miFTO#2 Top	TGCTGTTAAGGTCCACTTCATCATCGGTTTTGGCCACTGACTGACCGATGATGGTGGACCTTAA
miFTO#2 Bottom	CCTGTTAAGGTCCACCATCATCGGTCAGTCAGTGGCCAAAACCGATGATGAAGTGGACCTTAAC
miFTO#3 Top	TGCTGAGCAAAGTCACGTTGTAGGCTGTTTTGGCCACTGACTGACAGCCTACAGTGACTTTGCT
miFTO#3 Bottom	CCTGAGCAAAGTCACTGTAGGCTGTCAGTCAGTGGCCAAAACAGCCTACAACGTGACTTTGCTC
miHcrtr Top	TGCTGATGAGAACCCACTCGTACTGCGTTTTGGCCACTGACTGACGCAGTACGTGGGTTCTCAT
miHcrtr Bottom	CCTGATGAGAACCCACGTACTGCGTCAGTCAGTGGCCAAAACGCAGTACGAGTGGGTTCTCATC
GFP Forward	CACAGACTTGTGGGAGAAGC
GFP Reverse	CCCCTGAACCTGAAACATAAA
FTO#1 Forward	GAGCGGGAAGCTAAGAAACTG
FTO#1 Reverse	CTTGTGCAGTGTGAGAAAGGC
FTO#3 Forward	CGCATGTCAGACCTTCCTCA
FTO#3 Reverse	AGTCACGTTGTAGGCTGCTC
CycA Forward	AGCCTGGGGAGAAAGGATT
CycA Reverse	AGCCACTCGTCTTGGCAGT

Overview of oligonucleotides that were used to obtain miRNAs targeting *FTO* and *Hcrtr1* mRNA and to perform a qPCR.

Animal studies

Male Wistar rats (Charles River, Germany) of 220-250g were housed in filter top cages in a temperature- and humidity-controlled room (temperature 21±2°C and humidity 55±5%) with a 12h light/dark cycle. Animals had *ad libitum* access to chow and water. After one week of acclimatization, pAAV-miRNA was administered stereotactically in the VMH. Animals were exposed to an overnight fast for 16h twice in the sixth week after surgery by food restricting them from 1700h to 900h. All animals had to be at their original weight before exposure to the second overnight fast. Refeeding was measured by calculating cumulative chow intake after 2, 4, 8 and 24h. In the seventh week after

surgery, animals were exposed to a HFHS diet. The HFHS diet consisted of *ad libitum* access to chow, saturated fat (Vandemoortele, Eeklo, Belgium) and a 30% sucrose solution (Suiker Unie, Oud Gastel, the Netherlands). All experimental procedures were approved by the Committee for Animal Experimentation of the University of Utrecht (Utrecht, the Netherlands).

Surgical procedures

Rats were anesthetized using fentanyl/fluanisone and midazolam and mounted onto a stereotaxic apparatus. Virus was administered by placing a syringe needle into the VMH (coordinates from Bregma: -2.1 AP, +1.5 ML, -9.9 DV, at a 5° angle). A total of 1µl virus (1 x 10^{12} genomic copies(gc)ml^{-1}) was injected at a rate of 0.2 µlmin^{-1}. Rats received a transmitter in the abdominal cavity for the recording of locomotor activity and body temperature (TA10TA-F40, Data Science International, New Brighton, USA).
In situ hybridization (ISH)

For the ISH, cryostat sections of 20µm thickness from fresh, frozen brains were mounted onto slides. Sections were fixed in 4% paraformaldehyde for 20min, washed in phosphate-buffered saline, acetylated for 10min and washed again. The following steps differed between the ISH and the locked nucleic acid (LNA) ISH.
For the ISH, sections were pre-hybridized in hybridization solution (50% formamide, 5 × SSC, 5 × Denhardts, 250µgml^{-1} tRNA Baker's yeast, 500µgml^{-1} sonicated salmon sperm DNA) for 2h at room temperature. The hybridization solution containing 400ngml^{-1} 720-bp long digoxigenin (DIG)-labeled EGFP riboprobe (antisense to NCBI gene DQ768212) was then applied to the slides followed by overnight incubation at 68°C. After a quick wash in 68°C pre-warmed 2 × SSC, slides were transferred to 68°C pre-warmed 0.2 × SSC for 2h. After blocking for 1h with 10% FCS in B1 (0.1M Tris pH 7.5/0.15M NaCl), DIG was detected with an alkaline phosphatase-labeled antibody (1:5000, Roche, Mannheim, Germany) after overnight incubation at RT using NBT/BCIP as a substrate. Sections were dehydrated in ethanol, cleared in xylene and embedded in Entellan.

The LNA ISH hybridization is performed as previously described.[38] Briefly, sections were pre hybridized in hybridization solution (50% formamide, 5 × SSC, 5 × Denhardts, 200mgml^{-1} tRNA Baker's yeast, 500 mgml^{-1} sonicated salmon sperm DNA, 0.02gml^{-1} Roche blocking reagent) for 1h at RT. Hybridization was performed with 10nM double-DIG (3' and 5')-labeled LNA probe for human miR-124 (Exiqon, Denmark) for 2h at 55°C. After a quick wash in 60°C pre-warmed 5 × SSC, slides were transferred to 60°C pre-warmed 0.2 × SSC for 2h. After blocking for 1h with 10% FCS in B1 (0.1M Tris pH 7.5/0.15M NaCl), DIG was detected with an alkaline

phosphatase-labeled antibody (1:2500, Roche) after overnight incubation at RT using NBT/BCIP as a substrate. Slides were further processed for immunohistochemistry.

RNA isolation and qPCR in vivo knockdown

The VMH was dissected from fresh frozen cryostat sections. RNA was extracted by adding 0.5mL Trizol to the tissue. After 5min incubation at RT, 100µl chloroform was added followed by 2min incubation at RT. After centrifugation for 15min at 13.000rpm, RNA was precipitated from the aqueous layer by adding 0.25mL isopropanol. After 10min incubation at RT, samples were centrifuged for 10min at 13.000rpm. Next, the pellet was washed with 0.5mL 100% ethanol. After another centrifugation step, the pellet was dissolved in water. Expression of FTO was detected using quantitative PCR using primers for each miRNA sequence and a housekeeping gene, CycA (Table 1). The difference between Ct values of FTO and CycA was calculated for each sample. Next, the difference between the AAV-mirFTO#1/2 samples and the AAV-mirLuc samples was calculated to determine fold change.

Statistical analyses

All data were presented as means ± SEM. Statistical analyses were performed using GraphPad Prism 5 software. A P-value of <0.05 was considered to be significant.

Results

In vitro knockdown efficiency

Three different miRNA sequences targeting *FTO* were cloned into an AAV2 vector and their *in vitro* knockdown efficiency was determined using a dual luciferase assay. pAAV-miHcrtr1 was used as a control. pAAV-miFTO#1 and pAAV-miFTO#2 were selected for further study because of their 69% and 74% silencing efficacy, respectively (Figure 1a).

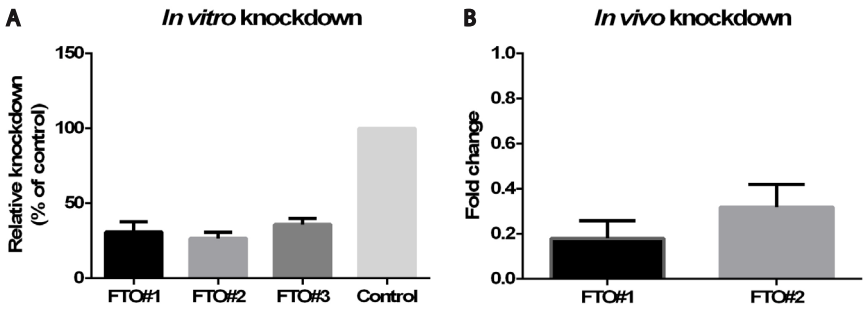

Figure 1 *In vitro* and *in vivo* knockdown efficiency of FTO constructs
In vitro knockdown efficiency of a cDNA FTO-Renilla fusion construct by pAAV-miFTO(1-3) relative to the control pAAV-miHcrtr1. pAAV-miFTO#1 and pAAV-miFTO#2 were selected for in vivo use based on their silency efficacy of 69% and 74%, respectively (a.) In vivo knockdown efficiency of pAAV-FTO#1 and pAAV-FTO#2 in the VMH as measured by qPCR for FTO (b.).

In vivo knockdown efficiency and hypothalamic injections

The plasmids were encapsidated into an AAV1 coat and AAV-miFTO#1 (n=8), AAV-miFTO#2 (n=8) and AAV-miLuc (n=8) were stereotactically injected into the ventromedial hypothalamus. After five weeks their brains were analyzed for *in vivo* knockdown efficiency and the placement of the hypothalamic injection. *In vivo* knockdown of *FTO* in the VMH was confirmed by qPCR. Due to technical problems, tissue from four animals could not be studied for knockdown efficiency. AAV-miFTO#1 (n=6) and AAV-miFTO#2 (n=8) decreased *FTO* mRNA levels by 82% and 68% compared to controls (n=6), respectively (Figure 1b). The viral vector contained a GFP cassette allowing the transduced area to be precisely identified. An ISH to detect GFP mRNA expression was used to analyze transduction efficiency. Figures 2a and c represent typical examples of injections targeting the ventromedial hypothalamus. To ensure that the hypothalamic injections did not result in toxicity due to saturation of the microRNA pathway as observed after AAV-mediated short hairpin RNA expression in the VMH,[34] we performed a miRNA 124 LNA ISH, as described previously.[34] No decreased miRNA 124 levels were observed after AAV transduction (Figure 2b and d), indicating no saturation of the miRNA pathway.

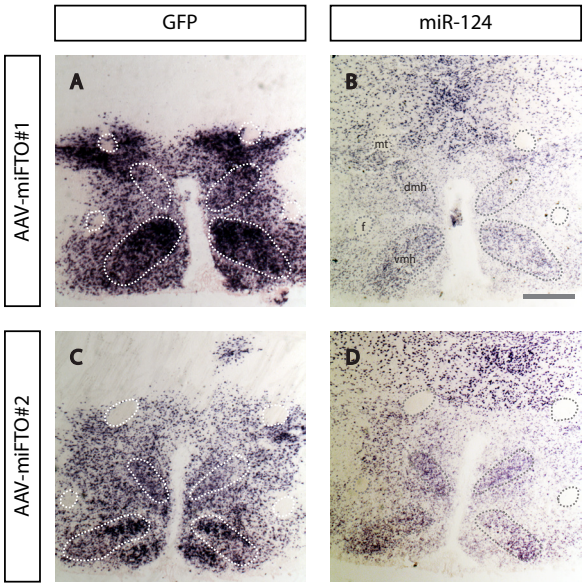

Figure 2 VMH transduction and miR-124 expression

Both AAV-miFTO#1 and #3 efficiently transduced the VMH (a. and c.). MiR-124 expression was not affected by transduction (b. and d.). mt = mammillary tract; f = fornix; dmh = dorsomedial hypothalamus; vmh = ventromedial hypothalamus. Scale bar: 500 µm

Bodyweight and energy balance

Groups were matched for bodyweight and chow intake prior to surgery. After injection of the AAVs into the VMH, bodyweight and chow intake were measured for five weeks. No effect of *FTO* knockdown was found on bodyweight (two-way ANOVA, f=1.363,

p=0.2057) or chow intake (two-way ANOVA, f=1.215, p=0.2992) (Figure 3a and b). Locomotor activity and body temperature were measured in the third week after surgery and used as a measure for energy expenditure. No differences in locomotor activity (dark phase: two-way ANOVA, f=1.452, p=0.1371; light phase: two-way ANOVA, f=0.8037, p=0.6640) or body temperature were observed (dark phase: two-way ANOVA, f=0.5881, p=0.8709; light phase: two-way ANOVA, f=1.015, p=0.4420) (Figure 3c and d).

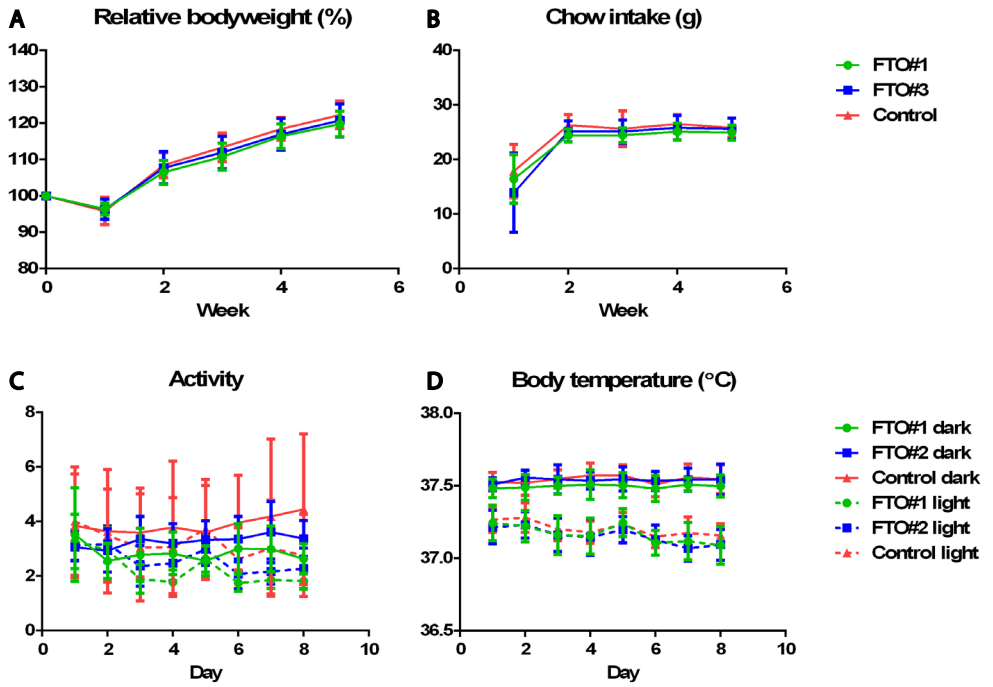

Figure 3 Bodyweight and parameters of energy balance after FTO knockdown in the VMH

Relative bodyweight (a.) and chow intake (b.) were measured for five weeks. No differences in relative bodyweight (two-way ANOVA, f=1.363, p=0.2057) or chow intake (two-way ANOVA, f=1.215, p=0.2992) were observed after FTO knockdown in the VMH. In the third week, locomotor activity (c.) and body temperature (d.) were assessed. FTO knockdown in the VMH did not affect locomotor activity (dark phase: two-way ANOVA, f=1.452, p=0.1371; light phase: two-way ANOVA, f=0.8037, p=0.6640) or body temperature (dark phase: two-way ANOVA, f=0.5881, p=0.8709; light phase: two-way ANOVA, f=1.015, p=0.4420) in the dark phase or in the light phase.

High-fat high-sucrose diet and fasting

Animals were fasted two times for 16 hours and refeeding was measured. Fasting had no effect on bodyweight (two-way ANOVA, f=1.845, p=0.1393) and no differences were observed in refeeding (two-way ANOVA, f=0.3633, p=0.8329) (Figure 4a and b). To examine the effect VMH *FTO* knockdown on high caloric food intake, animals were exposed to a HFHS diet for one week. No effect was observed on bodyweight (two-way

ANOVA, f=0.9387, p=0.4743) and total caloric intake (two-way ANOVA, f=0.4805, p=0.7499) (Figure 5a and b).

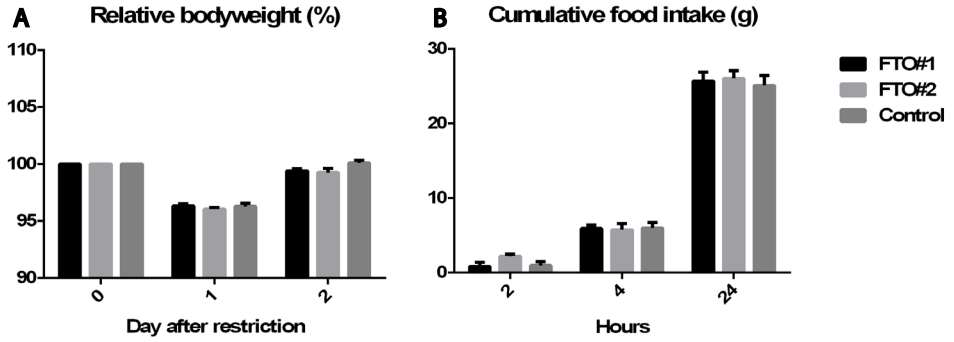

Figure 4 Overnight fasting

Animals were exposed to an overnight fast twice. Food was removed for 16h from 1700h to 900h. Bodyweight at day 0 (the day before the overnight fast) was set at 100%. Fasting had no effect on relative bodyweight (two-way ANOVA, f=1.845, p=0.1393) (a.). Cumulative food intake was measured 2, 4 and 24 hours after refeeding. No effect of FTO knockdown in the VMH was found on refeeding (two-way ANOVA, f=0.3633, p=0.8329) (b.).

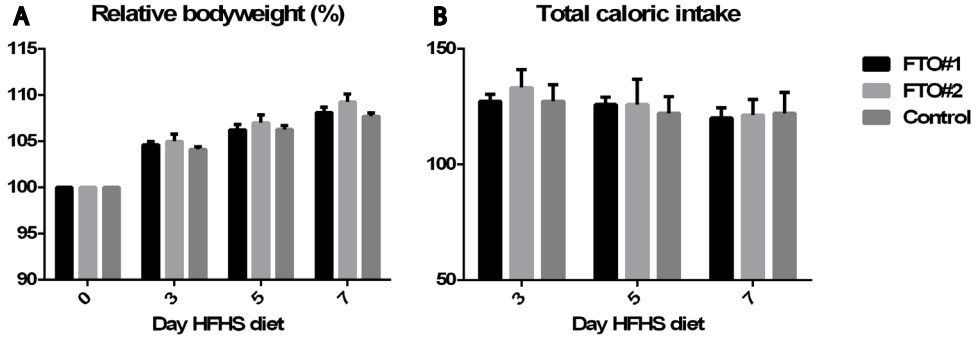

Figure 5 HFHS diet

In the seventh week after surgery, animals received a HFHS diet for one week. FTO knockdown in the VMH had no implications for bodyweight (two-way ANOVA, f=0.9387, p=0.4743) (a.) or total caloric intake (two-way ANOVA, f=0.4805, p=0.7499) (b.) on a HFHS diet.

Discussion

In 2007, single nucleotide polymorphisms in the first intron of *FTO* were associated with body mass index. *FTO* is ubiquitously expressed in the brain, with high levels in the hypothalamic nuclei, which are important contributors to energy homeostasis. Previously, we have shown that VMH *FTO* is upregulated after exposure to a restricted

feeding schedule. In this study, we investigated whether *FTO* knockdown in the VMH affects energy balance.

AAV-miFTO was bilaterally injected in the VMH and the effect on energy balance was measured for five weeks. *FTO* knockdown in the VMH did not affect bodyweight, food intake, body temperature or locomotor activity. Next, animals were exposed twice to an overnight fast, which did not result in differences in bodyweight or refeeding. Finally, animals received a HFHS diet for one week. Animals did not show a difference in caloric intake, nor was their bodyweight differently affected by the diet.

Mouse models with an (in)complete *FTO* loss-of-function demonstrate reduced body weight and fat mass, without a decrease in energy intake.[39,40] Consistent with these findings, mice overexpressing *FTO* show increased bodyweight and fat mass on both chow and high fat diet.[41] In contrast to the *FTO* deficient models, this effect on body weight was the result of an increase in food intake. Although it was shown that *FTO*-mediated regulation of energy balance is located in the brain,[42] *FTO* knockdown in the VMH did not result in a change in bodyweight or parameters of energy balance. Despite the very efficient *in vivo* knockdown of 84% in this study, it seems that *FTO* in the VMH does not affect energy homeostasis. *FTO* knockdown in the arcuate nucleus or mediobasal hypothalamus resulted in a modest reduction in food intake in the first week[43] and a reduction in food intake and bodyweight gain[44], respectively. In this study, *FTO* knockdown was not limited to the VMH and parts of the DMH and ARC were transduced as well in some rats. In this region, *FTO* expression is highest in the VMH[33] and therefore we targeted the VMH. As we did not observe a phenotype in any of the rats, we did not find evidence for a role of *FTO* in the DMH and ARC in energy balance. However, we cannot exclude that knockdown of *FTO* in these structures might counteract the consequences of *FTO* knockdown in the VMH. The latter seems less likely considering the outcome after *FTO* knockdown in the ARC.[43] Furthermore, although the virus spread could be observed throughout the whole mediobasal hypothalamus, some regions in the rostro-caudal extent of the VMH might be spared or have an incomplete transduction. Although these regions are relatively small, theoretically these might compensate for the loss of FTO. Possibly, other factors implicated in transcription and translation can compensate for a reduction in FTO, resulting in the absence of an effect of *FTO* knockdown. Although AAV-mediated knockdown was very effective, we cannot rule out that there are still functional levels of FTO protein.
Animals did not respond differently to exposure to overnight fasting, although we previously observed upregulation of FTO after exposure to a restricted feeding schedule. An overnight fast might not be enough for the development of a phenotype, secondary to the altered mRNA levels. Although effects of diet manipulation on *FTO* levels vary a

lot in general, we cannot rule out the possibility that *FTO* knockdown in the VMH will result in a different outcome after exposure to a restricted feeding schedule.

One of the limitations of a GWA study is that SNPs are associated that may link to a more distant gene than to the nearest gene. Recent studies have shown that the obesity-associated SNPs embedded in the first intron of *FTO* are influencing expression of different, distant genes, called *RPGRIP1L* and *IRX3*, instead of affecting *FTO* itselfs.[45,46] This might explain the absence of a phenotype after *FTO* knockdown. More research needs to be conducted to clarify the role of *RPGRIP1L* and *IRX3* in obesity and their relation to FTO.

References

1. Finucane MM, Stevens GA, Cowan MJ, Danaei G, Lin JK, Paciorek CJ, et al. National, regional, and global trends in body-mass index since 1980: systematic analysis of health examination surveys and epidemiological studies with 960 country-years and 9·1 million participants. Lancet. 2011 Feb 12;377(9765):557–67.
2. Garrison RJ, Kannel WB, Stokes J 3rd, Castelli WP. Incidence and precursors of hypertension in young adults: the Framingham Offspring Study. Prev Med. 1987 Mar;16(2):235–51.
3. Manson JE, Willett WC, Stampfer MJ, Colditz GA, Hunter DJ, Hankinson SE, et al. Body weight and mortality among women. N Engl J Med. 1995 Sep 14;333(11):677–85.
4. Ogden CL, Yanovski SZ, Carroll MD, Flegal KM. The epidemiology of obesity. Gastroenterology. 2007 May;132(6):2087–102.
5. Field AE, Coakley EH, Must A, Spadano JL, Laird N, Dietz WH, et al. Impact of overweight on the risk of developing common chronic diseases during a 10-year period. Arch Intern Med. 2001 Jul 9;161(13):1581–6.
6. Oguma Y, Sesso HD, Paffenbarger RS Jr, Lee I-M. Weight change and risk of developing type 2 diabetes. Obes Res. 2005 May;13(5):945–51.
7. Luppino FS, de Wit LM, Bouvy PF, Stijnen T, Cuijpers P, Penninx BWJH, et al. Overweight, obesity, and depression: a systematic review and meta-analysis of longitudinal studies. Arch Gen Psychiatry. 2010 Mar;67(3):220–9.
8. Stunkard AJ, Sørensen TI, Hanis C, Teasdale TW, Chakraborty R, Schull WJ, et al. An adoption study of human obesity. N Engl J Med. 1986 Jan 23;314(4):193–8.
9. Stunkard AJ, Foch TT, Hrubec Z. A twin study of human obesity. JAMA J Am Med Assoc. 1986 Jul 4;256(1):51–4.
10. A MacDonald AS. Body-mass indexes of British separated twins. N Engl J Med. 1990;322(21):1530.
11. Maes HH, Neale MC, Eaves LJ. Genetic and environmental factors in relative body weight and human adiposity. Behav Genet. 1997 Jul;27(4):325–51.
12. Frayling TM, Timpson NJ, Weedon MN, Zeggini E, Freathy RM, Lindgren CM, et al. A common variant in the FTO gene is associated with body mass index and predisposes to childhood and adult obesity. Science. 2007 May 11;316(5826):889–94.
13. Dina C, Meyre D, Gallina S, Durand E, Körner A, Jacobson P, et al. Variation in FTO contributes to childhood obesity and severe adult obesity. Nat Genet. 2007 Jun;39(6):724–6.
14. Scuteri A, Sanna S, Chen W-M, Uda M, Albai G, Strait J, et al. Genome-Wide Association Scan Shows Genetic Variants in the FTO Gene Are Associated with Obesity-Related Traits. PLoS Genet. 2007 Jul 20;3(7):e115.
15. Cecil JE, Tavendale R, Watt P, Hetherington MM, Palmer CNA. An obesity-associated FTO gene variant and increased energy intake in children. N Engl J Med. 2008 Dec 11;359(24):2558–66.
16. Haupt A, Thamer C, Staiger H, Tschritter O, Kirchhoff K, Machicao F, et al. Variation in the FTO gene influences food intake but not energy expenditure. Exp Clin Endocrinol Diabetes Off J Ger Soc Endocrinol Ger Diabetes Assoc. 2009 Apr;117(4):194–7.
17. Speakman JR, Rance KA, Johnstone AM. Polymorphisms of the FTO gene are associated with variation in energy intake, but not energy expenditure. Obes Silver Spring Md. 2008 Aug;16(8):1961–5.
18. Timpson NJ, Emmett PM, Frayling TM, Rogers I, Hattersley AT, McCarthy MI, et al. The fat mass- and obesity-associated locus and dietary intake in children. Am J Clin Nutr. 2008 Oct;88(4):971–8.
19. Wardle J, Llewellyn C, Sanderson S, Plomin R. The FTO gene and measured food intake in children. Int J Obes 2005. 2009 Jan;33(1):42–5.

20. Tanofsky-Kraff M, Han JC, Anandalingam K, Shomaker LB, Columbo KM, Wolkoff LE, et al. The FTO gene rs9939609 obesity-risk allele and loss of control over eating. Am J Clin Nutr. 2009 Dec;90(6):1483–8.
21. Berentzen T, Kring SII, Holst C, Zimmermann E, Jess T, Hansen T, et al. Lack of association of fatness-related FTO gene variants with energy expenditure or physical activity. J Clin Endocrinol Metab. 2008 Jul;93(7):2904–8.
22. Do R, Bailey SD, Desbiens K, Belisle A, Montpetit A, Bouchard C, et al. Genetic variants of FTO influence adiposity, insulin sensitivity, leptin levels, and resting metabolic rate in the Quebec Family Study. Diabetes. 2008 Apr;57(4):1147–50.
23. Goossens GH, Petersen L, Blaak EE, Hul G, Arner P, Astrup A, et al. Several obesity- and nutrient-related gene polymorphisms but not FTO and UCP variants modulate postabsorptive resting energy expenditure and fat-induced thermogenesis in obese individuals: the NUGENOB study. Int J Obes 2005. 2009 Jun;33(6):669–79.
24. Hakanen M, Raitakari OT, Lehtimäki T, Peltonen N, Pahkala K, Sillanmäki L, et al. FTO genotype is associated with body mass index after the age of seven years but not with energy intake or leisure-time physical activity. J Clin Endocrinol Metab. 2009 Apr;94(4):1281–7.
25. Liu G, Zhu H, Lagou V, Gutin B, Stallmann-Jorgensen IS, Treiber FA, et al. FTO variant rs9939609 is associated with body mass index and waist circumference, but not with energy intake or physical activity in European- and African-American youth. BMC Med Genet. 2010;11:57.
26. Gerken T, Girard CA, Tung Y-CL, Webby CJ, Saudek V, Hewitson KS, et al. The obesity-associated FTO gene encodes a 2-oxoglutarate-dependent nucleic acid demethylase. Science. 2007 Nov 30;318(5855):1469–72.
27. Jia G, Yang C-G, Yang S, Jian X, Yi C, Zhou Z, et al. Oxidative demethylation of 3-methylthymine and 3-methyluracil in single-stranded DNA and RNA by mouse and human FTO. FEBS Lett. 2008 Oct 15;582(23-24):3313–9.
28. McTaggart JS, Lee S, Iberl M, Church C, Cox RD, Ashcroft FM. FTO Is Expressed in Neurones throughout the Brain and Its Expression Is Unaltered by Fasting. PLoS ONE. 2011 Nov 30;6(11):e27968.
29. Brobeck JR, Tepperman J, Long CNH. Experimental Hypothalamic Hyperphagia in the Albino Rat. Yale J Biol Med. 1943 Jul;15(6):831–53.
30. Satoh N, Ogawa Y, Katsuura G, Tsuji T, Masuzaki H, Hiraoka J, et al. Pathophysiological significance of the obese gene product, leptin, in ventromedial hypothalamus (VMH)-lesioned rats: evidence for loss of its satiety effect in VMH-lesioned rats. Endocrinology. 1997 Mar;138(3):947–54.
31. Trogrlic L, Wilson YM, Newman AG, Murphy M. Context fear learning specifically activates distinct populations of neurons in amygdala and hypothalamus. Learn Mem Cold Spring Harb N. 2011;18(10):678–87.
32. Mathews D, Edwards DA. The ventromedial nucleus of the hypothalamus and the hormonal arousal of sexual behaviors in the female rat. Horm Behav. 1977 Feb;8(1):40–51.
33. Boender AJ, van Rozen AJ, Adan RAH. Nutritional state affects the expression of the obesity-associated genes Etv5, Faim2, Fto, and Negr1. Obes Silver Spring Md. 2012 Dec;20(12):2420–5.
34. Van Gestel MA, van Erp S, Sanders LE, Brans MAD, Luijendijk MCM, Merkestein M, et al. shRNA-induced saturation of the microRNA pathway in the rat brain. Gene Ther. 2014 Feb;21(2):205–11.
35. White MD, Nolan MF. A Molecular toolbox for rapid generation of viral vectors to up- or down-regulate neuronal gene expression in vivo. Front Mol Neurosci. 2011;4:8.
36. Du G, Yonekubo J, Zeng Y, Osisami M, Frohman MA. Design of expression vectors for RNA interference based on miRNAs and RNA splicing. FEBS J. 2006;273(23):5421–7.

37. De Backer MWA, Brans MAD, Luijendijk MC, Garner KM, Adan RAH. Optimization of adeno-associated viral vector-mediated gene delivery to the hypothalamus. Hum Gene Ther. 2010 Jun;21(6):673–82.

38. Kan AA, van Erp S, Derijck AAHA, de Wit M, Hessel EVS, O'Duibhir E, et al. Genome-wide microRNA profiling of human temporal lobe epilepsy identifies modulators of the immune response. Cell Mol Life Sci CMLS [Internet]. 2012 Apr 26 [cited 2012 Jul 13]; Available from: http://www.ncbi.nlm.nih.gov/pubmed/22535415

39. Fischer J, Koch L, Emmerling C, Vierkotten J, Peters T, Brüning JC, et al. Inactivation of the Fto gene protects from obesity. Nature. 2009 Apr 16;458(7240):894–8.

40. Church C, Lee S, Bagg EAL, McTaggart JS, Deacon R, Gerken T, et al. A mouse model for the metabolic effects of the human fat mass and obesity associated FTO gene. PLoS Genet. 2009 Aug;5(8):e1000599.

41. Church C, Moir L, McMurray F, Girard C, Banks GT, Teboul L, et al. Overexpression of Fto leads to increased food intake and results in obesity. Nat Genet. 2010 Dec;42(12):1086–92.

42. Gao X, Shin Y-H, Li M, Wang F, Tong Q, Zhang P. The Fat Mass and Obesity Associated Gene FTO Functions in the Brain to Regulate Postnatal Growth in Mice. PLoS ONE. 2010 Nov 16;5(11):e14005.

43. Tung Y-CL, Ayuso E, Shan X, Bosch F, O'Rahilly S, Coll AP, et al. Hypothalamic-Specific Manipulation of Fto, the Ortholog of the Human Obesity Gene FTO, Affects Food Intake in Rats. PLoS ONE. 2010 Jan 19;5(1):e8771.

44. McMurray F, Church CD, Larder R, Nicholson G, Wells S, Teboul L, et al. Adult onset global loss of the fto gene alters body composition and metabolism in the mouse. PLoS Genet. 2013;9(1):e1003166.

45. Stratigopoulos G, Martin Carli JF, O'Day DR, Wang L, LeDuc CA, Lanzano P, et al. Hypomorphism for RPGRIP1L, a Ciliary Gene Vicinal to the FTO Locus, Causes Increased Adiposity in Mice. Cell Metab. 2014 Jun 5;19(5):767–79.

46. Smemo S, Tena JJ, Kim K-H, Gamazon ER, Sakabe NJ, Gómez-Marín C, et al. Obesity-associated variants within FTO form long-range functional connections with IRX3. Nature. 2014 Mar 20;507(7492):371–5.

CHAPTER 6

General discussion

This thesis aimed to optimize adeno-associated virus (AAV)-mediated knockdown of genes implicated in energy balance. In this chapter, the major outcomes will be described and some recommendations for future research will be provided.

RNA interference

RNA interference for drug target validation and gene function

As mentioned in **chapter 1**, there are several methods to introduce RNA interference (RNAi)-mediating molecules into a cell. Transfection of synthetic double-stranded RNAs is often unsatisfactory for long-term studies as the effect is only transient. Vector-based siRNA delivery tools provide a means to study long-term loss-of-function phenotypes. Adeno-associated virus (AAV) currently is one of the most attractive gene transfer tools for RNAi and AAV vectors have been shown to be able to maintain transgene expression for at least 25 months in rats.[1]

Optimization of AAV-mediated RNA interference

Cell-type-specific characteristics can modulate the transduction efficiency of AAV. The mode of entrance into the cell, intracellular viral trafficking, nuclear transport, uncoating and second strand DNA synthesis are aspects of AAV infection that influence the transduction rate.[2–16] It has been reported that AAV vectors can transduce specific cell types both *in vitro* and *in vivo* by pseudotyping the AAV vector to alter its tropism.[17–21] In **chapter 2**, recombinant AAV vector pseudotyped with viral capsids from serotypes 1, 2, 5 and 8 display differential efficiency after delivery to the ventromedial hypothalamus (VMH). AAV2/1 and AAV2/5 were more efficient than AAV2/2 and AAV2/8 in transducing the VMH. As only serotypes most commonly used in the central nervous system were tested, additional experiments could be performed to study VMH transduction efficiency of other serotypes. This study showed the benefit of pseudotyping AAV vectors as this may improve transduction efficiency.

When using different serotypes, it is important to take serotype-specific biodistribution into account. One hour after injection of AAV2/1, AAV2/2, AAV2/5 or AAV2/8 in the VMH no viral particles could be traced in the blood (**chapter 2**). This indicates that the virus is not able to cross the blood-brain barrier or that the number of genomic copies is too low to detect. If the latter is the case, than probably the number of genomic copies crossing the blood-brain barrier is also too low to exert an unwanted side effect in the periphery. In the final part of **chapter 2**, half-lives were calculated for AAV1, AAV2, AAV5 and AAV8. AAV1 and AAV2 were rapidly cleared from the blood, 4 hours after systemic injection less than 3% of the starting material was left. Differences between serotypes in clearance rates might be explained by the number of genomic copies lost to phagocytic cells in the liver and serotype-specific transcytosis of AAV across the endothelial cells.[22,23] AAV2 was shown to have a very short half-life of 4.2

minutes. If large numbers of AAV2 genomic copies had crossed the blood-brain barrier, these numbers wouldn't be detected in a blood sample collected one hour after injection because of the short half-life. AAV1 and AAV5 were shown to safely and efficiently transduce the VMH. With a half-life of 0.55 (AAV1) and 1.67 (AAV5) hours, a systemic injection of 10^9 genomic copies of AAV1 and AAV5 would be fully cleared from blood after 16 hours and 2 days, respectively.

RNAi-induced toxicity

Despite the exceptional utility that RNAi technology seemed to offer for drug target validation, a study by Grimm et al. (2006) casted a shadow over the use of this promising technique.[24] Fatal side effects were observed after abundant short hairpin (sh)RNA expression in the livers of adult mice. Since then a series of other studies made clear that the shRNA-induced adverse effects are independent of species or tissue types.[25–34] **Chapters 3 and 4** show that microRNA expression was decreased in areas transduced by an AAV encoding an shRNA after injection into the VMH. In these chapters in situ hybridization was used to detect microRNAs. In situ hybridization is a very powerful technique allowing spatial information about gene expression. This way, it was possible to detect whether the decrease in microRNA expression was restricted to the transduced area. Indeed, cells infected with a virus encoding an shRNA showed decreased expression of microRNA-124, a neuronal microRNA, whereas there was ubiquitous expression of microRNA-124 in non-infected regions. The observed adverse effects were not due to knockdown of the target gene, expression of the marker gene (green fluorescence protein) or infection by the virus itself (**chapter 3**). Furthermore, the decreased microRNA expression was not limited to only microRNA-124 as microRNA-138 was also decreased in transduced cells (**chapter 3**).

Chapter 4 further elaborates on these findings. This chapter focused on the consequences of RNAi toxicity for the behavioral phenotype *in vivo* by injection of an AAV encoding an shRNA targeting the leptin receptor (*LepR*) in the ventral tegmental area (VTA). Several studies showed that LepR is expressed in the VTA and 75-90% of *LepR*-positive neurons are dopaminergic.[35–39] Leptin injections into the VTA or ventricle resulted in inhibition of dopamine neuronal activity and a decreased food intake, but no changes in locomotor activity.[35,37,40,41] Surprisingly, shRNA-mediated knockdown of *LepR* in the VTA resulted in increased locomotor activity in the dark phase (**chapter 4**). Injections with an AAV encoding an shRNA placed in a microRNA background targeting *LepR* or a *LepR* antagonist did not lead to an increase in dark phase locomotor activity. In situ hybridization showed decreased microRNA-124 expression in areas transduced by the AAV encoding an shRNA, whereas the brains of animals injected with an AAV encoding an shRNA placed in a microRNA background and with the *LepR* antagonist were unaffected. These results might explain the counterintuitive finding of increased

locomotor activity after transduction with the same viral vector in the VTA by Hommel et al.[35] Knockdown of *LepR* in the VTA is not likely to result in increased locomotor activity as transgenic animals lacking the *LepR* in dopaminergic neurons of the VTA do not show increased locomotor activity and leptin is known to have anorexic properties by increasing energy expenditure.[42,43] Lesions in the VTA were shown to result in increased locomotor activity in the dark phase.[44] An endogenous microRNA might be responsible for inhibition of locomotor activity in the VTA. Expression of this endogenous microRNA could be inhibited by saturation of the microRNA pathway leading to increased locomotor activity.

Cellular mechanisms underlying RNAi toxicity

shRNA-induced adverse effects have been attributed to induction of an interferon response, massive off-target effects and saturation of the microRNA pathway.[24,45–47] The experiments described in **chapter 3 and 4** point towards saturation of the microRNA pathway as a cause of the toxic side effects observed after shRNA expression. Support for this concept is provided by numerous *in vitro* studies as reviewed by Grimm (2011).[48] Primary human lymphocytes infected with U6-shRNA-encoding lentiviral vectors showed cytotoxicity, which could be alleviated by replacing the U6 promoter with the weaker H1 promoter.[49] Decreased expression of hepatic microRNAs was observed after infection of a liver cell line with U6-shRNA-encoding lentiviral vectors.[50] A meta-analysis of over 150 siRNA of shRNA transfection experiments describes frequent upregulation of microRNA-controlled genes upon abundant siRNA and/or shRNA overexpression.[51] Exportin-5 and Argonaute-2 have been observed *in vitro* as possible limiting cellular factors involved in the shRNA/ microRNA pathway.[24,52–55] Coexpression of hepatic Exportin-5 and Argonaute-2 from AAV vectors *in vivo* was shown to increase shRNA potency in the livers of adult mice and to partly relieve RNAi-induced toxicity.[24,54]

Despite the wealth of evidence indicating saturation of the microRNA pathway as the underlying mechanism, it cannot be ruled out that induction of an interferon response or off-target effects also attribute to the RNAi-induced adverse effects. In this thesis, those mechanisms have not been studied.

Possible solutions for toxicity

As reviewed by Grimm (2011) there are several strategies towards alleviating RNAi toxicity (Table 1).[48] These approaches include improvement of the RNAi vector itself by the use of a weaker promoter, lowering the applied vector dose, the use of a specific serotype, the use of an shRNA placed in a microRNA background or combining low-copy RNAi strategies with further inhibitors of gene expression.[24,28,30,31,33,54,56–59] Other approaches include mathematical modeling of all rate-limiting factors in mammalian cells, cell-based screening for potent and safe shRNA sequences prior to application *in*

vivo and controlled overexpression of known rate-limiting cellular components, together with the RNAi vector.[24,54,60–62]

Solution for toxicity	Advantage	Possible disadvantage
1. Weaker (tissue-specific) promoter	Target tissue transduction efficiency will not be affected	Increased chance of incomplete knockdown of the target gene. To overcome this limitation it can be combined with solution 5.
2. Lowering vector dose	Less genomic copies per cell	Increased chance of incomplete target tissue transduction. One genomic copy might already overload the microRNA machinery.
3. Using specific serotype	Less genomic copies per cell	Increased chance of incomplete target tissue transduction. One genomic copy might already overload the microRNA machinery.
4. Use of microRNA context	Target tissue transduction efficiency will not be affected	Increased chance of incomplete knockdown of the target gene. To overcome this limitation it can be combined with solution 5.
5. Use of shRNA sequences effective at low concentrations	Less genomic copies per cell	Only effective when applied in combination with other solutions mentioned.

Table 1 Recommendations for solutions to RNAi-induced toxicity.

This table offers some solutions to RNAi-induced toxicity. Each solution has its own advantages and disadvantages. Combining the use of very potent shRNA sequences with a weaker promoter or with the use of a microRNA context might overcome possible disadvantages

A disadvantage of lowering the dose or switching to another serotype is that it might interfere with complete target tissue transduction. Both **chapter 4 and 5** describe experiments in which an shRNA is placed in a microRNA background. In situ hybridizations showed that this shRNA expression did not result in decreased microRNA-124 expression. Both vectors did not result in a phenotype, which could indicate that RNAi from a microRNA scaffold is not able to sufficiently knockdown the target genes. However, resemblance with data from transgenic animals and with animals that received antagonist (**chapter 4**) and efficient *in vivo* knockdown as determined by qPCR (**chapter 5**) make it very likely that these vectors encode potent RNAi inducers effectively knocking down target genes, however with no detected effect.

Implications to the field

Despite increasing evidence that shRNA overexpression can result in an adverse tissue response, RNAi is still applied often without proper controls for toxicity. The vector encoding the shRNA targeting *LepR* (**chapter 4**) was also used in other studies published in several high impact journals.[35,63–65] Hommel et al. (2006) studied the role of midbrain dopamine neuron leptin signaling in energy homeostasis by leptin administration to the VTA and by knockdown of *LepR* in the VTA.[35] Leptin administration into the VTA resulted in decreased food intake and no changes in locomotor activity. Knockdown of *LepR* in the VTA resulted in increased food intake between the second and third week following viral delivery. According to the author this was consistent with the time peak of AAV expression and RNAi-mediated knockdown within VTA neurons. Interestingly, an increase in locomotor activity was observed as well. Although the paper offers no exact information about the timeline of increased locomotor activity after viral administration, a remark in the discussion section indicates that the locomotor behavior preceded the increased feeding behavior and would thus occur before the time peak of AAV expression and RNAi-mediated knockdown. Results from this paper heavily rely on *in vivo* experiments with the shRNA targeting the *LepR* and it is very likely that the increased locomotor activity resulted from an adverse tissue reaction as the same vector was used as described in **chapter 4**. The subsequent increase in food intake might be compensatory behavior for the increased energy expenditure.

In the Hayes et al. (2010) study, all results and conclusions completely rely on experiments with animals receiving the shRNA targeting *LepR* in the medial nucleus tractus solitarius.[65] Lesions in this area caused transient hypophagia and body weight loss.[66] *LepR* knockdown in the Hayes study resulted in an increased decline in bodyweight directly after surgery. This greater decrease in bodyweight was attributed to viral delivery. It is not likely that an adverse tissue response was responsible for this transient body weight loss as lesioned animals resumed normophagia after 2 to 3 weeks and *LepR* knockdown animals resumed normophagia already after 1 week. Overconsumption of highly palatable food by lesioned rats was observed during exposure to high-fat diets.[66] Therefore, it cannot be excluded that the observed increased intake of high caloric food in the Hayes study did not result from an adverse tissue reaction instead of *LepR* knockdown. The study from Kanoski et al. (2012) replicated, extended and refined these findings with AAV-mediated knockdown and pharmacological studies. Although results from these studies were complementary, results still heavily rely on experiments using shRNA-mediated knockdown. Without proper controls, one needs to be careful interpreting these results.[64]

Davis et al. (2011) used the same shRNA sequence to knockdown *LepR* in the VTA, but the shRNA was expressed using a lentiviral vector.[67] *LepR* knockdown in the VTA resulted

in increased progressive ratio responding for sucrose. AAV-mediated shRNA expression in the VTA resulted in a trend towards increased active lever presses. Although, there is no evidence for *in vivo* toxicity after lentiviral-mediated shRNA expression and our group previously showed lower transduction efficiency of lentiviral vectors compared to AAV,[68] proper controls need to exclude saturation of the microRNA pathway.

The study using the shRNA targeting the *LepR* in the dorsomedial hypothalamus (DMH) to examine obesity-associated increased blood pressure used shRNA-mediated knockdown of *LepR* complemented with studies using administration of a *LepR* antagonist and selective depletion of leptin signaling using the Cre recombinase technique.[63] Results from these different methods of *LepR* depletion are conclusive. If the shRNA expression had resulted in an adverse tissue response, this would not have affected the major outcomes of this study.

In these studies the AAV vector was encapsidated into AAV2 serotype capsids. It was reported that changing from AAV1 to AAV2 alleviated shRNA-induced toxicity in the red nucleus.[33] This reduction in adverse effects was determined by neuronal morphology. However, this thesis shows that lack of morphological changes or neuronal loss does not implicate that there is no shRNA-induced toxicity on microRNA level (**chapter 3**). Furthermore, changing from AAV1 to AAV2 not only alleviated the RNAi-induced adverse effects, it also abolished knockdown of the target gene. Therefore, although these studies make use of the less potent AAV serotype 2, results obtained from this vector remain questionable without proper controls for toxicity.

Furthermore, the studies mentioned above have injected a lower dose than 10^9 infectious particles. Figure 2 from **chapter 3** shows that the virus spread far beyond the site of injection. Although this spread diluted the viral particles, especially at the borders, microRNA expression is decreased in all transduced cells. It is therefore likely that infection of small numbers of particles per cell already overloads the microRNA pathway, because of the very potent U6 promotor. In that case, studies would greatly benefit from placing an shRNA in a microRNA background as this thesis confirmed that this alleviates the shRNA-mediated adverse effects (**chapter 4 and 5**).

AAV-mediated knockdown of genes implicated in obesity

Overweight and obesity are increasingly important health problems worldwide. An estimated 40 to 70% of the variation in response to an obesogenic environment is due to inter-individual genetic differences.[69,70] In 2007, two studies confirmed the fat mass and obesity-associated (*FTO*) gene as the first genome-wide association study-identified obesity-susceptibility gene.[71–73] SNPs located in the first intron of *FTO* showed an association for obesity traits of which the minor allele increased body mass index by

0.4kg/m^2.[71] Several studies indicated that these *FTO* SNPs are associated with obesity through changes in energy intake and not energy expenditure.[74–84] **Chapter 5** describes an experiment in which an shRNA placed in a microRNA background targeting *FTO* was injected into the VMH, a hypothalamic area involved in obesity, where FTO is widely expressed.[85–88] Despite a very efficient *in vivo* knockdown of 84%, no changes in energy balance were observed. *FTO* knockdown animals showed the same response after exposure to a high fat high sucrose diet or an overnight fast. These results are not consistent with mouse models lacking *FTO* or mouse models overexpressing *FTO*, which result in an reduced and increased bodyweight, respectively.[89–91] *FTO* knockdown in the arcuate nucleus or mediobasal hypothalamus resulted in a modest reduction in food intake only in the first week and a reduction in food intake and bodyweight gain, respectively.[92,93] In this study we could not find evidence for a role of *FTO* in the VMH in energy balance. Incomplete transduction of the VMH in the rostro-caudal extent of the VMH, compensation by other transcription factors or remaining functional levels of FTO protein might explain a lack of phenotype. An important limitation of a genome-wide association study is that SNPs associated to a phenotype may link to a more distant gene than to the nearest gene. Another explanation for the absence of a phenotype might be found in recent evidence, indicating that the obesity-associated SNPs in de first intron of *FTO* are influencing expression of different distant genes, called *RPGRIP1L* and *IRX3*, instead of affecting *FTO* itself.[94,95] Future experiments need to clarify the role of these genes in obesity and their relation to *FTO*. As mentioned before, this study confirms that placing an shRNA in a microRNA background alleviates an shRNA-mediated adverse tissue response. No decrease in microRNA-124 expression was observed in areas transduced by the virus.

Concluding remarks

Science is often romanticized as a flawless system of building knowledge and understanding, in which scientist work together towards the production of more and more accurate explanations for natural phenomena's. Unfortunately, this is not always the case. Unexpected results that do not fit with the current scientific thinking are more difficult to sell than positive results. Although RNAi seemed to be a promising technique for drug target validation, it is unsurprising, at least in retrospect, that such a massive overload of the endogenous machinery with RNAi inducers results in an adverse tissue response. Despite the overwhelming evidence that toxic side effects can occur after application of shRNA-mediated RNAi, it is unfortunate that many scientists seem to ignore these findings and still publish studies in high impact journals without applying proper controls. Although RNAi can be very effective, scientists need to test whether the endogenous machinery can manage the throughput of sequences and doses they wish to use in their study. Furthermore, the targeted tissue needs to be taken into account, as some tissues might be more vulnerable to the adverse effects than others. If

more data is accumulated about what sequences and doses are and are not toxic, RNAi can be applied more successfully and potential toxic side effects might be predicted in the future.

“To kill an error is as good a service as, and sometimes even better than, the establishing of a new truth or fact” - Charles Darwin.

References

1. Klein, R. L. *et al.* Dose and promoter effects of adeno-associated viral vector for green fluorescent protein expression in the rat brain. *Exp. Neurol.* **176,** 66–74 (2002).
2. Summerford, C. & Samulski, R. J. Membrane-associated heparan sulfate proteoglycan is a receptor for adeno-associated virus type 2 virions. *J. Virol.* **72,** 1438–1445 (1998).
3. Summerford, C., Bartlett, J. S. & Samulski, R. J. V 5 integrin: a co-receptor for adeno-associated virus type 2 infection. *Nat. Med.* **5,** 78–82 (1999).
4. Qing, K. *et al.* Human fibroblast growth factor receptor 1 is a co-receptor for infection by adeno-associated virus 2. *Nat. Med.* **5,** 71–77 (1999).
5. Kashiwakura, Y. *et al.* Hepatocyte growth factor receptor is a coreceptor for adeno-associated virus type 2 infection. *J. Virol.* **79,** 609–614 (2005).
6. Akache, B. *et al.* The 37/67-kilodalton laminin receptor is a receptor for adeno-associated virus serotypes 8, 2, 3, and 9. *J. Virol.* **80,** 9831–9836 (2006).
7. Rabinowitz, J. E. *et al.* Cross-Packaging of a Single Adeno-Associated Virus (AAV) Type 2 Vector Genome into Multiple AAV Serotypes Enables Transduction with Broad Specificity. *J. Virol.* **76,** 791–801 (2002).
8. Negishi, A. *et al.* Analysis of the interaction between adeno-associated virus and heparan sulfate using atomic force microscopy. *Glycobiology* **14,** 969–977 (2004).
9. Walters, R. W. *et al.* Binding of Adeno-associated Virus Type 5 to 2,3-Linked Sialic Acid Is Required for Gene Transfer. *J. Biol. Chem.* **276,** 20610–20616 (2001).
10. Kaludov, N., Brown, K. E., Walters, R. W., Zabner, J. & Chiorini, J. A. Adeno-Associated Virus Serotype 4 (AAV4) and AAV5 Both Require Sialic Acid Binding for Hemagglutination and Efficient Transduction but Differ in Sialic Acid Linkage Specificity. *J. Virol.* **75,** 6884–6893 (2001).
11. Chen, S. *et al.* Efficient Transduction of Vascular Endothelial Cells with Recombinant Adeno-Associated Virus Serotype 1 and 5 Vectors. *Hum. Gene Ther.* **16,** 235–247 (2005).
12. Wu, Z., Miller, E., Agbandje-McKenna, M. & Samulski, R. J. Alpha2,3 and alpha2,6 N-linked sialic acids facilitate efficient binding and transduction by adeno-associated virus types 1 and 6. *J. Virol.* **80,** 9093–9103 (2006).
13. Pasquale, G. D. *et al.* Identification of PDGFR as a receptor for AAV-5 transduction. *Nat. Med.* **9,** 1306–1312 (2003).
14. Hauck, B., Zhao, W., High, K. & Xiao, W. Intracellular Viral Processing, Not Single-Stranded DNA Accumulation, Is Crucial for Recombinant Adeno-Associated Virus Transduction. *J. Virol.* **78,** 13678–13686 (2004).
15. Thomas, C. E., Storm, T. A., Huang, Z. & Kay, M. A. Rapid Uncoating of Vector Genomes Is the Key to Efficient Liver Transduction with Pseudotyped Adeno-Associated Virus Vectors. *J. Virol.* **78,** 3110–3122 (2004).
16. Ferrari, F. K., Samulski, T., Shenk, T. & Samulski, R. J. Second-strand synthesis is a rate-limiting step for efficient transduction by recombinant adeno-associated virus vectors. *J. Virol.* **70,** 3227–3234 (1996).
17. Cearley, C. N. *et al.* Expanded repertoire of AAV vector serotypes mediate unique patterns of transduction in mouse brain. *Mol. Ther. J. Am. Soc. Gene Ther.* **16,** 1710–1718 (2008).
18. Howard, D. B., Powers, K., Wang, Y. & Harvey, B. K. Tropism and toxicity of adeno-associated viral vector serotypes 1, 2, 5, 6, 7, 8, and 9 in rat neurons and glia in vitro. *Virology* **372,** 24–34 (2008).
19. Shevtsova, Z., Malik, J. M. I., Michel, U., Bähr, M. & Kügler, S. Promoters and serotypes: targeting of adeno-associated virus vectors for gene transfer in the rat central nervous system in vitro and in vivo. *Exp. Physiol.* **90,** 53–59 (2005).

20. Büning, H., Perabo, L., Coutelle, O., Quadt-Humme, S. & Hallek, M. Recent developments in adeno-associated virus vector technology. *J. Gene Med.* **10,** 717–733 (2008).
21. Kwon, I. & Schaffer, D. V. Designer gene delivery vectors: molecular engineering and evolution of adeno-associated viral vectors for enhanced gene transfer. *Pharm. Res.* **25,** 489–499 (2008).
22. Di Pasquale, G. & Chiorini, J. A. AAV transcytosis through barrier epithelia and endothelium. *Mol. Ther. J. Am. Soc. Gene Ther.* **13,** 506–516 (2006).
23. Alemany, R., Suzuki, K. & Curiel, D. T. Blood clearance rates of adenovirus type 5 in mice. *J. Gen. Virol.* **81,** 2605–2609 (2000).
24. Grimm, D. *et al.* Fatality in mice due to oversaturation of cellular microRNA/short hairpin RNA pathways. *Nature* **441,** 537–541 (2006).
25. Bish, L. T. *et al.* Cardiac gene transfer of short hairpin RNA directed against phospholamban effectively knocks down gene expression but causes cellular toxicity in canines. *Hum. Gene Ther.* **22,** 969–977 (2011).
26. Borel, F. *et al.* In vivo knock-down of multidrug resistance transporters ABCC1 and ABCC2 by AAV-delivered shRNAs and by artificial miRNAs. *J. RNAi Gene Silenc. Int. J. RNA Gene Target. Res.* **7,** 434–442 (2011).
27. Ahn, M., Witting, S. R., Ruiz, R., Saxena, R. & Morral, N. Constitutive Expression of Short Hairpin RNA in Vivo Triggers Buildup of Mature Hairpin Molecules. *Hum. Gene Ther.* **22,** 1483–1497 (2011).
28. McBride, J. L. *et al.* Artificial miRNAs mitigate shRNA-mediated toxicity in the brain: Implications for the therapeutic development of RNAi. *Proc. Natl. Acad. Sci.* **105,** 5868–5873 (2008).
29. Martin, J. N. *et al.* Lethal toxicity caused by expression of shRNA in the mouse striatum: implications for therapeutic design. *Gene Ther.* **18,** 666–673 (2011).
30. Boudreau, R. L., Martins, I. & Davidson, B. L. Artificial MicroRNAs as siRNA Shuttles: Improved Safety as Compared to shRNAs In vitro and In vivo. *Mol. Ther. J. Am. Soc. Gene Ther.* **17,** 169–175 (2009).
31. Ulusoy, A., Sahin, G., Björklund, T., Aebischer, P. & Kirik, D. Dose Optimization for Long-term rAAV-mediated RNA Interference in the Nigrostriatal Projection Neurons. *Mol. Ther. J. Am. Soc. Gene Ther.* **17,** 1574–1584 (2009).
32. Khodr, C. E. *et al.* An alpha-synuclein AAV gene silencing vector ameliorates a behavioral deficit in a rat model of Parkinson's disease, but displays toxicity in dopamine neurons. *Brain Res.* **1395,** 94–107 (2011).
33. Ehlert, E. M., Eggers, R., Niclou, S. P. & Verhaagen, J. Cellular toxicity following application of adeno-associated viral vector-mediated RNA interference in the nervous system. *BMC Neurosci.* **11,** 20 (2010).
34. Baek, S. T. *et al.* Off-Target Effect of doublecortin Family shRNA on Neuronal Migration Associated with Endogenous MicroRNA Dysregulation. *Neuron* **82,** 1255–1262 (2014).
35. Hommel, J. D. *et al.* Leptin Receptor Signaling in Midbrain Dopamine Neurons Regulates Feeding. *Neuron* **51,** 801–810 (2006).
36. Figlewicz, D. P., Evans, S. B., Murphy, J., Hoen, M. & Baskin, D. G. Expression of receptors for insulin and leptin in the ventral tegmental area/substantia nigra (VTA/SN) of the rat. *Brain Res.* **964,** 107–115 (2003).
37. Leshan, R. L. *et al.* Ventral tegmental area leptin receptor neurons specifically project to and regulate cocaine- and amphetamine-regulated transcript neurons of the extended central amygdala. *J. Neurosci. Off. J. Soc. Neurosci.* **30,** 5713–5723 (2010).
38. Elmquist, J. K., Bjørbaek, C., Ahima, R. S., Flier, J. S. & Saper, C. B. Distributions of leptin receptor mRNA isoforms in the rat brain. *J. Comp. Neurol.* **395,** 535–547 (1998).

39. Fulton, S. *et al.* Leptin regulation of the mesoaccumbens dopamine pathway. *Neuron* **51,** 811–822 (2006).
40. Morton, G. J., Blevins, J. E., Kim, F., Matsen, M. & Figlewicz, D. P. The action of leptin in the ventral tegmental area to decrease food intake is dependent on Jak-2 signaling. *Am. J. Physiol. Endocrinol. Metab.* **297,** E202–210 (2009).
41. Krügel, U., Schraft, T., Kittner, H., Kiess, W. & Illes, P. Basal and feeding-evoked dopamine release in the rat nucleus accumbens is depressed by leptin. *Eur. J. Pharmacol.* **482,** 185–187 (2003).
42. Pelleymounter, M. A. *et al.* Effects of the obese gene product on body weight regulation in ob/ob mice. *Science* **269,** 540–543 (1995).
43. Liu, J., Perez, S. M., Zhang, W., Lodge, D. J. & Lu, X.-Y. Selective deletion of the leptin receptor in dopamine neurons produces anxiogenic-like behavior and increases dopaminergic activity in amygdala. *Mol. Psychiatry* **16,** 1024–1038 (2011).
44. Oades, R. D., Taghzouti, K., Rivet, J. M., Simon, H. & Le Moal, M. Locomotor activity in relation to dopamine and noradrenaline in the nucleus accumbens, septal and frontal areas: a 6-hydroxydopamine study. *Neuropsychobiology* **16,** 37–42 (1986).
45. Sledz, C. A., Holko, M., Veer, M. J. de, Silverman, R. H. & Williams, B. R. G. Activation of the interferon system by short-interfering RNAs. *Nat. Cell Biol.* **5,** 834–839 (2003).
46. Jackson, A. L. *et al.* Expression profiling reveals off-target gene regulation by RNAi. *Nat. Biotechnol.* **21,** 635–637 (2003).
47. Bridge, A. J., Pebernard, S., Ducraux, A., Nicoulaz, A.-L. & Iggo, R. Induction of an interferon response by RNAi vectors in mammalian cells. *Nat. Genet.* **34,** 263–264 (2003).
48. Grimm, D. The dose can make the poison: lessons learned from adverse in vivo toxicities caused by RNAi overexpression. *Silence* **2,** 8 (2011).
49. An, D. S. *et al.* Optimization and functional effects of stable short hairpin RNA expression in primary human lymphocytes via lentiviral vectors. *Mol. Ther. J. Am. Soc. Gene Ther.* **14,** 494–504 (2006).
50. Pan, Q. *et al.* Disturbance of the microRNA pathway by commonly used lentiviral shRNA libraries limits the application for screening host factors involved in hepatitis C virus infection. *FEBS Lett.* **585,** 1025–1030 (2011).
51. Khan, A. A. *et al.* Transfection of small RNAs globally perturbs gene regulation by endogenous microRNAs. *Nat. Biotechnol.* **27,** 549–555 (2009).
52. Castanotto, D. *et al.* Combinatorial delivery of small interfering RNAs reduces RNAi efficacy by selective incorporation into RISC. *Nucleic Acids Res.* **35,** 5154–5164 (2007).
53. Diederichs, S. *et al.* Coexpression of Argonaute-2 enhances RNA interference toward perfect match binding sites. *Proc. Natl. Acad. Sci. U. S. A.* **105,** 9284–9289 (2008).
54. Grimm, D. *et al.* Argonaute proteins are key determinants of RNAi efficacy, toxicity, and persistence in the adult mouse liver. *J. Clin. Invest.* **120,** 3106–3119 (2010).
55. Yi, R., Doehle, B. P., Qin, Y., Macara, I. G. & Cullen, B. R. Overexpression of exportin 5 enhances RNA interference mediated by short hairpin RNAs and microRNAs. *RNA N. Y. N* **11,** 220–226 (2005).
56. Giering, J. C., Grimm, D., Storm, T. A. & Kay, M. A. Expression of shRNA from a tissue-specific pol II promoter is an effective and safe RNAi therapeutic. *Mol. Ther. J. Am. Soc. Gene Ther.* **16,** 1630–1636 (2008).
57. Grimm, D. & Kay, M. A. Combinatorial RNAi: a winning strategy for the race against evolving targets? *Mol. Ther. J. Am. Soc. Gene Ther.* **15,** 878–888 (2007).
58. Abad, X., Razquin, N., Abad, A. & Fortes, P. Combination of RNA interference and U1 inhibition leads to increased inhibition of gene expression. *Nucleic Acids Res.* **38,** e136 (2010).

59. DiGiusto, D. L. *et al.* RNA-based gene therapy for HIV with lentiviral vector-modified CD34(+) cells in patients undergoing transplantation for AIDS-related lymphoma. *Sci. Transl. Med.* **2,** 36ra43 (2010).
60. Cuccato, G. *et al.* Modeling RNA interference in mammalian cells. *BMC Syst. Biol.* **5,** 19 (2011).
61. Arvey, A., Larsson, E., Sander, C., Leslie, C. S. & Marks, D. S. Target mRNA abundance dilutes microRNA and siRNA activity. *Mol. Syst. Biol.* **6,** 363 (2010).
62. Beer, S. *et al.* Low-level shRNA cytotoxicity can contribute to MYC-induced hepatocellular carcinoma in adult mice. *Mol. Ther. J. Am. Soc. Gene Ther.* **18,** 161–170 (2010).
63. Simonds, S. E. *et al.* Leptin Mediates the Increase in Blood Pressure Associated with Obesity. *Cell* **159,** 1404–1416 (2014).
64. Kanoski, S. E. *et al.* Endogenous leptin receptor signaling in the medial nucleus tractus solitarius affects meal size and potentiates intestinal satiation signals. *Am. J. Physiol. - Endocrinol. Metab.* **303,** E496–E503 (2012).
65. Hayes, M. R. *et al.* Endogenous leptin signaling in the caudal nucleus tractus solitarius and area postrema is required for energy balance regulation. *Cell Metab.* **11,** 77–83 (2010).
66. Hyde, T. M. & Miselis, R. R. Effects of area postrema/caudal medial nucleus of solitary tract lesions on food intake and body weight. *Am. J. Physiol.* **244,** R577–587 (1983).
67. Davis, J. F. *et al.* Leptin Regulates Energy Balance and Motivation Through Action at Distinct Neural Circuits. *Biol. Psychiatry* **69,** 668–674 (2011).
68. De Backer, M. W. A. *et al.* An adeno-associated viral vector transduces the rat hypothalamus and amygdala more efficient than a lentiviral vector. *BMC Neurosci.* **11,** 81 (2010).
69. Elks, C. E. *et al.* Variability in the heritability of body mass index: a systematic review and meta-regression. *Front. Endocrinol.* **3,** 29 (2012).
70. Maes, H. H., Neale, M. C. & Eaves, L. J. Genetic and environmental factors in relative body weight and human adiposity. *Behav. Genet.* **27,** 325–351 (1997).
71. Frayling, T. M. *et al.* A common variant in the FTO gene is associated with body mass index and predisposes to childhood and adult obesity. *Science* **316,** 889–894 (2007).
72. Scuteri, A. *et al.* Genome-Wide Association Scan Shows Genetic Variants in the FTO Gene Are Associated with Obesity-Related Traits. *PLoS Genet* **3,** e115 (2007).
73. Dina, C. *et al.* Variation in FTO contributes to childhood obesity and severe adult obesity. *Nat. Genet.* **39,** 724–726 (2007).
74. Cecil, J. E., Tavendale, R., Watt, P., Hetherington, M. M. & Palmer, C. N. A. An obesity-associated FTO gene variant and increased energy intake in children. *N. Engl. J. Med.* **359,** 2558–2566 (2008).
75. Haupt, A. *et al.* Variation in the FTO gene influences food intake but not energy expenditure. *Exp. Clin. Endocrinol. Diabetes Off. J. Ger. Soc. Endocrinol. Ger. Diabetes Assoc.* **117,** 194–197 (2009).
76. Speakman, J. R., Rance, K. A. & Johnstone, A. M. Polymorphisms of the FTO gene are associated with variation in energy intake, but not energy expenditure. *Obes. Silver Spring Md* **16,** 1961–1965 (2008).
77. Timpson, N. J. *et al.* The fat mass- and obesity-associated locus and dietary intake in children. *Am. J. Clin. Nutr.* **88,** 971–978 (2008).
78. Wardle, J., Llewellyn, C., Sanderson, S. & Plomin, R. The FTO gene and measured food intake in children. *Int. J. Obes. 2005* **33,** 42–45 (2009).
79. Tanofsky-Kraff, M. *et al.* The FTO gene rs9939609 obesity-risk allele and loss of control over eating. *Am. J. Clin. Nutr.* **90,** 1483–1488 (2009).
80. Berentzen, T. *et al.* Lack of association of fatness-related FTO gene variants with energy expenditure or physical activity. *J. Clin. Endocrinol. Metab.* **93,** 2904–2908 (2008).

81. Do, R. *et al.* Genetic variants of FTO influence adiposity, insulin sensitivity, leptin levels, and resting metabolic rate in the Quebec Family Study. *Diabetes* **57,** 1147–1150 (2008).

82. Goossens, G. H. *et al.* Several obesity- and nutrient-related gene polymorphisms but not FTO and UCP variants modulate postabsorptive resting energy expenditure and fat-induced thermogenesis in obese individuals: the NUGENOB study. *Int. J. Obes. 2005* **33,** 669–679 (2009).

83. Hakanen, M. *et al.* FTO genotype is associated with body mass index after the age of seven years but not with energy intake or leisure-time physical activity. *J. Clin. Endocrinol. Metab.* **94,** 1281–1287 (2009).

84. Liu, G. *et al.* FTO variant rs9939609 is associated with body mass index and waist circumference, but not with energy intake or physical activity in European- and African-American youth. *BMC Med. Genet.* **11,** 57 (2010).

85. Gerken, T. *et al.* The obesity-associated FTO gene encodes a 2-oxoglutarate-dependent nucleic acid demethylase. *Science* **318,** 1469–1472 (2007).

86. McTaggart, J. S. *et al.* FTO Is Expressed in Neurones throughout the Brain and Its Expression Is Unaltered by Fasting. *PLoS ONE* **6,** e27968 (2011).

87. Brobeck, J. R., Tepperman, J. & Long, C. N. H. Experimental Hypothalamic Hyperphagia in the Albino Rat. *Yale J. Biol. Med.* **15,** 831–853 (1943).

88. Satoh, N. *et al.* Pathophysiological significance of the obese gene product, leptin, in ventromedial hypothalamus (VMH)-lesioned rats: evidence for loss of its satiety effect in VMH-lesioned rats. *Endocrinology* **138,** 947–954 (1997).

89. Fischer, J. *et al.* Inactivation of the Fto gene protects from obesity. *Nature* **458,** 894–898 (2009).

90. Church, C. *et al.* A mouse model for the metabolic effects of the human fat mass and obesity associated FTO gene. *PLoS Genet.* **5,** e1000599 (2009).

91. Church, C. *et al.* Overexpression of Fto leads to increased food intake and results in obesity. *Nat. Genet.* **42,** 1086–1092 (2010).

92. Tung, Y.-C. L. *et al.* Hypothalamic-Specific Manipulation of Fto, the Ortholog of the Human Obesity Gene FTO, Affects Food Intake in Rats. *PLoS ONE* **5,** e8771 (2010).

93. McMurray, F. *et al.* Adult onset global loss of the fto gene alters body composition and metabolism in the mouse. *PLoS Genet.* **9,** e1003166 (2013).

94. Stratigopoulos, G. *et al.* Hypomorphism for RPGRIP1L, a Ciliary Gene Vicinal to the FTO Locus, Causes Increased Adiposity in Mice. *Cell Metab.* **19,** 767–779 (2014).

95. Smemo, S. *et al.* Obesity-associated variants within FTO form long-range functional connections with IRX3. *Nature* **507,** 371–375 (2014).

ADDENDUM

Curriculum Vitae
List of publications
Samenvatting in het Nederlands
Dankwoord

Curriculum Vitae

Marguérite Alexandra van Gestel was born on August 26th 1980 in Delft, the Netherlands. In 1998, she graduated from secondary school and became a student Physical Therapy at the Hogeschool Utrecht. After obtaining her bachelor's degree in 2003, she studied Psychobiology at the University of Amsterdam and acquired her bachelor's degree in 2006. In the same year she enrolled in the research master Neuroscience and Cognition at Utrecht University. During this Master she performed two scientific internships: 'Downregulation of the MC4 receptor in rats through lentiviral mediated transgenesis' at the laboratory of Prof. Roger Adan, PhD, Brain Center Rudolf Magnus, University Medical Center Utrecht and 'A potential role of the trace amine-associated receptor 1 in major depressive disorder' at the laboratory of Prof. Berend Olivier, PhD, Utrecht University. In November 2008, she started working on a PhD project under supervision of Prof. Roger Adan, PhD, Brain Center Rudolf Magnus, University Medical Center Utrecht. The results of the research she performed as a PhD student are presented in this thesis. In september 2014, she began working as policy advisor research at the Julius Center for Health Sciences and Primary Care, University Medical Center Utrecht.

List of publications

FTO knockdown in rat ventromedial hypothalamus does not affect energy balance.
van Gestel MA, Sanders LE, de Jong JW, Luijendijk MC, Adan RA.
Physiol Rep. 2014 Dec 11

Pharmacological manipulations in animal models of anorexia and binge eating in relation to humans.
van Gestel MA, Kostrzewa E, Adan RA, Janhunen SK.
Br J Pharmacol. 2014 Oct

The obesity-associated gene Negr1 regulates aspects of energy balance in rat hypothalamic areas.
Boender AJ, **van Gestel MA**, Garner KM, Luijendijk MC, Adan RA.
Physiol Rep. 2014 Jul 30

Recombinant adeno-associated virus: efficient transduction of the rat VMH and clearance from blood.
van Gestel MA, Boender AJ, de Vrind VA, Garner KM, Luijendijk MC, Adan RA.
PLoS One. 2014 May 23

GHS-R1a signaling in the DMH and VMH contributes to food anticipatory activity.
Merkestein M, **van Gestel MA**, van der Zwaal EM, Brans MA, Luijendijk MC, van Rozen AJ, Hendriks J, Garner KM, Boender AJ, Pandit R, Adan R.
Int J Obes (Lond). 2014 Apr

shRNA-induced saturation of the microRNA pathway in the rat brain.
van Gestel MA, van Erp S, Sanders LE, Brans MA, Luijendijk MC, Merkestein M, Pasterkamp RJ, Adan RA.
Gene Ther. 2014 Feb

Hypothalamic κ-opioid receptor modulates the orexigenic effect of ghrelin.
Romero-Picó A, Vázquez MJ, González-Touceda D, Folgueira C, Skibicka KP, Alvarez-Crespo M, **van Gestel MA**, Velásquez DA, Schwarzer C, Herzog H, López M, Adan RA, Dickson SL, Diéguez C, Nogueiras R.
Neuropsychopharmacology. 2013 Jun

Samenvatting in het Nederlands

Overgewicht en obesitas zijn in toenemende mate een wereldwijd gezondheidsprobleem. Volgens de Wereldgezondheidsorganisatie (WHO) hebben ongeveer 1.4 miljard mensen overgewicht en ongeveer een derde daarvan is obees. Tussen 1980 en 2008 is de wereldwijde prevalentie van obesitas bijna verdubbeld. Voedselinname en energieverbruik moeten in evenwicht zijn om een stabiel lichaamsgewicht te behouden. In obesitas is dit evenwicht verschoven door overmatige voedselinname en verminderd energieverbruik. Studies hebben aangetoond dat bepaalde hersengebieden maaltijdpatronen en energieverbruik kunnen beïnvloeden. Hoewel het duidelijk is dat omgevingsfactoren een belangrijke rol spelen bij de toenemende prevalentie van obesitas, reageren individuen verschillend op obesogene omstandigheden doordat ze genetische variatie vertonen. Twee genen die betrokken zijn bij obesitas zijn het leptine receptor gen, LepR, en het vetmassa en obesitas-geassocieerde gen, FTO. Deze genen komen ook tot expressie in de hersengebieden die geassocieerd zijn met energiebalans.

RNA interferentie

Om de functie van obesitas-gerelateerde genen in de hersenen te onderzoeken, kan gebruik gemaakt worden van RNA interferentie (RNAi). RNAi maakt gebruik van een cel-eigen mechanisme waarbij messenger RNA (mRNA) wordt afgebroken. mRNA speelt een centrale rol in het tot expressie brengen van genetische informatie: DNA wordt overgeschreven tot mRNA en mRNA wordt vervolgens vertaald naar een eiwit. Bij RNAi leidt de introductie van dubbelstrengs DNA in een cel tot sequentie-specifieke afbraak van endogeen mRNA, resulterend in verlaagde hoeveelheden eiwit (knockdown). Dit dubbelstrengs DNA kan zo worden ontworpen, dat het specifiek zal hechten aan het mRNA van het eiwit dat men wil verminderen. Om dubbelstrengs DNA in een cel te brengen kan men gebruik maken van een vector, een middel dat gebruikt wordt om genetisch materiaal in een cel te krijgen. In dit proefschrift is gebruik gemaakt van een vector bestaande uit een circulair stuk DNA. Deze vector brengt een short hairpin RNA (shRNA) tot expressie, een RNA sequentie die een haarspeldbocht maakt en zo dubbelstrengs DNA wordt. Deze shRNA kan worden gebruikt om expressie van het doelwit gen door RNAi te reduceren.

AAV-gemedieerde RNA interferentie

Voor RNAi biedt de adeno-geassocieerde virus (AAV)-vector momenteel de meeste voordelen. Eén van die voordelen is dat de vector verpakt kan worden in verschillende virusomhulsels. Het virusomhulsel kan van invloed zijn op de mate waarin het virus een bepaald celtype in kan komen. In **hoofdstuk 2** wordt gekeken naar de efficiëntie van verschillende virusomhulsels (AAV1, 2, 5 en 8) bij het infecteren van de ventromediale nucleus van de hypothalamus (VMH), een hersengebied dat betrokken is bij energie balans. Hoe meer virus partikels in de cellen kunnen komen, des te meer shRNA

(dubbelstrengs DNA) tot expressie zal komen in de geïnfecteerde cellen, waardoor er meer mRNA zal worden afgebroken. Met name AAV1 en 5 blijken erg efficiënt in het infecteren van neuronen in de VMH. Daarnaast wordt gekeken naar eventuele spreiding van het virus vanuit de hersenen naar het bloed. Indien het virus, na injectie in de hersenen, zich weet te verspreiden richting de rest van het lichaam, kan het daar cellen infecteren in bijvoorbeeld de lever. Als het gen dat je wilt downreguleren ook in de lever tot expressie komt, kan verspreiding van het virus richting lever je resultaten beïnvloeden. In **hoofdstuk 2** wordt ook aangetoond dat geen van de virusomhulsels wordt aangetroffen in het bloed na injectie in de VMH. Tevens wordt de halfwaardetijd van de verschillende virusomhulsels in bloed bepaald. Met een halfwaardetijd van 0.55 (AAV1) en 1.67 (AAV5) uur, zal een injectie in het bloed van 10^9 kopieën van het virale genoom volledig geklaard zijn uit het bloed na respectievelijk 16 uur en 2 dagen.

RNA interferentie-geïnduceerde toxiciteit

Ondanks het uitzonderlijke voordeel dat RNAi leek te bieden, wierp een studie van Grimm (2006) een schaduw over het gebruik van deze veelbelovende techniek. Fatale neveneffecten werden geobserveerd na het gebruik van shRNA expressie in de lever van volwassen muizen. Een reeks andere studies maakte duidelijk dat de shRNA-geïnduceerde bijwerkingen onafhankelijk zijn van diersoort of weefseltype. Voordat er na het afschrijven van de vector een mature shRNA is, moet het afgeschreven RNA door enkele eiwitten bewerkt worden. Deze eiwitten worden ook door de cel gebruikt om endogene microRNAs te bewerken tot mature microRNAs. Een microRNA is een cel-eigen RNA die de expressie van genen reguleert. In **hoofdstuk 3 en 4** wordt onderzocht of er sprake is van verzadiging van de eiwitten die betrokken zijn bij het vormen van mature microRNAs door de expressie van shRNAs uit de vector. Er wordt in **hoofdstuk 3** aangetoond dat cellen, die geïnfecteerd zijn door virussen met een vector die een shRNA tot expressie brengt, een verlaagde expressie van endogene microRNAs vertonen. Deze verlaging in endogene microRNAs wijst op saturatie van de enzymen die nodig zijn om deze endogene microRNAs te vormen. In **hoofdstuk 4** wordt verder ingegaan op deze bevindingen. Dit hoofdstuk heeft als doel de gevolgen van RNAi-geïnduceerde toxiciteit voor het gedragsfenotype te beschrijven. Hiervoor wordt een shRNA met als doelwit gen de LepR geïnjecteerd in het ventrale tegmentum. Een eerdere studie heeft aangetoond dat dit leidt tot een verhoging van activiteit. Gezien de functie van de LepR is dit echter een onverwacht resultaat. De studie beschreven in **hoofdstuk 4** laat óók zien dat injectie van een shRNA met de LepR als doelwit gen, verhoging van de activiteit geeft. MicroRNA expressie is verlaagd in cellen geïnfecteerd met het virus, hetgeen duidt op RNAi-geïnduceerde verzadiging van de eiwitten betrokken bij de vorming van mature microRNAs. Na injectie van een shRNA geplaatst in een microRNA achtergrond met als doelwit gen LepR, wordt geen verhoogde activiteit waargenomen en wordt ook geen toxiciteit gezien. Wel wordt aangetoond dat de LepR expressie verlaagd is. Hieruit

kan geconcludeerd worden dat LepR knockdown in het ventrale tegmentum niet zal leiden tot verhoogde activiteit, maar dat dit gedragsfenotype resulteert uit de RNAi-geïnduceerde toxiciteit. Dit komt overeen met het gedragsfenotype dat wordt gezien nadat een laesie in dit hersengebied is aangebracht.

Gevolgen voor het onderzoeksveld

Ondanks het toenemende bewijs dat shRNA overexpressie kan resulteren in afgenomen microRNA expressie, wordt RNAi nog steeds toegepast zonder dat er afdoende wordt gecontroleerd op toxiciteit. De vector, die gebruikt werd in de hier beschreven studies, werd ook gebruikt in andere studies welke gepubliceerd zijn in hoog aangeschreven tijdschriften. Voor veel van deze studies hangen de resultaten voornamelijk af van de experimenten waarbij gebruik is gemaakt van de shRNAs. Zonder de juiste controles, moet men voorzichtig zijn met de interpretatie van deze studies.

AAV-gemedieerde knockdown van genen betrokken bij obesitas

In 2007 identificeerden twee genoomwijde associatie studies het *FTO* gen: een transcriptiefactor die een rol zou spelen bij de totstandkoming van obesitas. In **hoofdstuk 5** wordt een shRNA tegen *FTO* geplaatst in een microRNA achtergrond. Het plaatsen van de shRNA in een microRNA achtergrond voorkomt shRNA-gemedieerde toxiciteit, zo blijkt uit **hoofdstuk 4**. Ondanks een efficiënte knockdown van 84%, resulteerde *FTO* knockdown in de VMH van de rat niet in veranderingen in energie balans in tegenstelling tot de resultaten gezien in muizen die het *FTO* gen geheel misten. Het gebrek aan een effect op energiebalans zou verklaard kunnen worden door een onvolledige transductie van de VMH, compensatie door andere transcriptiefactoren of resterende functionele niveaus van het *FTO* eiwit. Een belangrijke beperking van een genoomwijde associatie studie is dat de gevonden variaties in het DNA die geassocieerd zijn met een fenotype kunnen verwijzen naar een meer afgelegen gen dan naar het dichtstbijzijnde gen. Een andere verklaring voor de afwezigheid van een fenotype zou kunnen worden gevonden in recent bewijs dat obesitas-geassocieerde afwijkingen in het eerste intron van *FTO* de expressie beïnvloeden van twee verder weg gelegen genen, *RPGRIP1L* en *IRX3*, in plaats van *FTO* zelf. Toekomstige experimenten zullen de rol van deze genen in obesitas en hun relatie tot *FTO* moeten verduidelijken.

Slotbeschouwing

Wetenschap wordt vaak geromantiseerd als een vlekkeloos systeem van opbouw van kennis en inzicht, waarin wetenschappers samenwerken aan het produceren van accurate verklaringen voor natuurverschijnselen. Helaas is dit niet altijd het geval. Onverwachte resultaten die niet passen in het huidige wetenschappelijk denken zijn moeilijker te verkopen dan positieve resultaten. Hoewel RNAi een veelbelovende techniek leek, is het niet verwonderlijk, althans achteraf bezien, dat dergelijke overbelasting van de endogene

machinerie met RNAi inductoren resulteert in een ongunstige weefselreactie. Ondanks het overweldigende bewijs dat toxische bijwerkingen kunnen optreden na toepassing van shRNA-gemedieerde RNAi, lijken veel wetenschappers deze bevindingen te negeren en worden nog steeds studies gepubliceerd in vooraanstaande tijdschriften zonder toepassing van de juiste controles. Hoewel RNAi zeer effectief kan zijn, moeten wetenschappers testen of de endogene machinerie de doorvoer van de sequenties en doseringen die men wenst te gebruiken wel aankan. Als er meer data verzameld wordt over welke sequenties en doseringen wel of niet leiden tot een toxische weefselreactie, kan in de toekomst RNAi goed worden toegepast en kunnen eventuele potentiële toxische neveneffecten beter worden voorspeld.

Dankwoord

Met heel veel plezier kijk ik terug op de jaren dat ik heb gewerkt aan de studies beschreven in dit proefschrift. Vooral de grote verscheidenheid aan mensen waar ik mee heb mogen samenwerken, maakt het een periode waaraan ik mooie herinneringen zal blijven houden.

Allereerst wil ik mijn promotor **Roger** bedanken voor de begeleiding en het in mij gestelde vertrouwen. Het moet voor een promotor toch even slikken zijn als een promovendus tot driemaal toe aankondigt zwanger te zijn. Toch gaf je me alle vrijheid om het moederschap met het promotietraject te combineren. Ook denk ik met veel plezier terug aan de jaarlijkse etentjes bij Valentine en jou thuis. Deze avonden stonden elk jaar weer garant voor veel gezelligheid, lekker eten en heel veel wijn!

Mieneke, waar zou ik zijn geweest zonder jouw hulp. Voor mijn DEC aanvragen had ik altijd een 'mannetje' en dat 'mannetje' was jij. Nog steeds heb ik geen idee hoe ik zo'n aanvraag in zou moeten vullen. Ook voor de operaties en andere dier-gerelateerde zaken kon deze held op sokken altijd op jou rekenen. Mijn enige angst is dat je na mijn vertrek gaat vergeten dat je jongste kind toch écht een meisje is!

Dan was er nog een niet te missen persoon op de vijfde verdieping. Een grote glimlach en een bos rode krullen werden meestal voorafgegaan door veel lawaai en gelach. Wat heb ik met je gelachen, **Maike**, en hoe fijn was onze samenwerking. Ik vergeet nooit meer dat een bange rat mijn mouw inschoot en dat ik jou angstig aankeek 'wat nu?'. Jouw immer grote grijns werd nog groter en je antwoordde: 'Nu is het tijd voor koffie!'.

Keith, een virus maken was extra gezellig als jij naast me in het lab zat. Je hebt ooit zitten grappen dat je graag als een 'grumpy old man' bekend zou willen staan, zodat niemand je meer zou durven storen. Ik vrees dat je daarin faalt, want ik heb je al die jaren met veel plezier en succes lastiggevallen!

Na de aankoop van ons jaren 30 huis was ik zó blij toen ik hoorde dat ik een Poolse collega zou krijgen, **Ela**. Ik kreeg helaas al snel door dat ik voor timmeren, stuken, verven of slopen niet bij jou moest zijn. Wel voor veel gezelligheid, Poolse pannenkoeken en koekjes!! Toen ik je inwerkte noemde ik je liefkozend mijn 'lab rack'. Uiteindelijk heeft mijn 'lab rack' een mooie inhaalslag gemaakt en is ruimschoots voor mij gepromoveerd. Helaas woon je weer in het buitenland (ondanks de aan de haak geslagen Néderlandse man!), maar ik hoop dat we toch contact kunnen blijven houden!

Rahul, de laatste loodjes zijn het zwaarst en jij hebt heel wat van die laatste loodjes voor mij getild en daarvoor ben ik je erg dankbaar! Ook stond jouw naam steevast op de Excel lijstjes met 'wie doet wat' als ik weer eens op vakantie ging terwijl er een experiment liep. De taart die daar tegenover staat, heb je nog steeds van me tegoed!

In het lab hebben we nooit veel samen hoeven te werken, **Geoffrey**. Ik was druk met 'het creëren van hersenschade', zoals jij dat graag noemt en jij was bezig met...tja, wat doe je eigenlijk precies;) In de pauzes waren we vaak veroordeeld tot elkaar en eerlijkheid gebiedt me te zeggen dat ik het altijd erg gezellig heb gevonden (alhoewel ik dat natuurlijk nóóit in het echt zal toegeven!).

Arjen, dank je wel voor alle gezelligheid en hulp in het lab. Veel succes met je postdoc in Italië! **Han** en **Tessa**, dank jullie wel voor jullie hulp met het PR experiment! En dan nog een 'gekaapte' student, **Veronne**, dank voor je hulp met het klaringsexperiment! **Sanna**, although we haven't actually worked together in the Netherlands, our cross-border cooperation resulted in a great review!

Bij jou is het allemaal begonnen, **Marijke**, als student met jou het lab in! Heel even zijn we daarna collega's geweest, waarna ik het virusstokje van je heb overgenomen. Ik hoop dat we contact zullen blijven houden! Alle overige oud-collega's uit de groep Adan: **Edwin, Inge**, **Jan Willem, Judith, Linde, Marek, Olivier, Ralph, Rea, Ruud, Susanne**, **Tom**, **Yanina.** Dank jullie wel voor de fijne samenwerking de afgelopen jaren!

Het werken op de vijfde verdieping had niet mijn voorkeur, **Marjolein,** maar jij zorgde er wel voor dat het in ieder geval heel gezellig was! **Henk,** ontelbare keren betrapte je me zonder labjas. 'Je hebt ze óók in XL hoor!' gaf wel aan dat ook een zwangere buik geen genade kent in jouw bijzijn! **Leo**, samen met Henk onmisbaar op de vierde verdieping, bedankt voor het draaiend houden van het lab met de daarbij behorende humor! **Youri**, veel van de foto's in dit proefschrift zijn er dankzij jou en **Eljo**, zonder jouw geduldige Illustrator uitleg had ik die figuren nooit voor elkaar gekregen. Voor de niet-lab-gerelateerde ondersteuning wil ik **Krista, Ria, Roger, Sandra** en **Vicki** bedanken!

Mijn studenten **Kaoutar**, **Anne** en **Loek**, met veel plezier heb ik jullie mogen begeleiden! Kaoutar, veel succes met je studie geneeskunde. Anne, ik weet niet wie nu wie iets leerde tijdens jouw stage, maar ik heb genoten van je eerlijkheid (ik geef nooit meer mijn zwemtijden prijs) en de gezellige gesprekken. Veel succes met jouw promotietraject! Loek, als ik weer eens gestrest rondliep, was jouw 'dat komt wel goed!'-mentaliteit fantastisch. Ondanks het feit dat ik je belaagde met een 'zweep-app' op mijn telefoon als je 'niet hard genoeg' werkte, heb je me vanwege mijn zwangerschap zelfs ná je stage nog geholpen met ratten wegen. Met jou 'komt het zeker weten allemaal wel goed!'.

Mijn kamergenootjes dan. Het geitenwollensokken imago van de onderzoeker wordt door jou geheel teniet gedaan, **Susan (ven Urp)**. Fantastisch hoe jij als 'science geek in disguise' op je hakjes even een Science artikel bij elkaar pipetteert. Ook al verklaar jij jezelf niet als meest belangrijke persoon bij de totstandkoming van míjn boekje, hoofdstukken 3 en 4 zouden er zonder jou niet geweest zijn. Veel succes in Schotland en ik hoop nog veel van je te blijven horen! **Frank**, van pluche telefoons tot kakelende kippen, het is me niet gelukt je op de kast te krijgen. In stilte was je aan het broeden op een wraakactie en daarin ben je zeker geslaagd met het dichtlijmen van mijn ladekast! **Francesca** and **Sara**, I loved hearing your conversations in Italian, although I didn't understand one word of it. I think we had a great room for scientific conversations, but especially for chit-chat!

Pauline, ik vond het heel erg gezellig om tijdens onze wekelijkse lunch promotieperikelen uit te kunnen wisselen!

El van Leersum (www.vanleersumart.com), bedankt dat ik het mooie DikkeDamesSchilderij 'Sweet Dreams' mag gebruiken voor de omslag van mijn proefschrift. Daarnaast wil ik **Robert-Jan Egberts** (www.artline-holland.nl) graag bedanken voor het toesturen van een voor dit boekje geschikt formaat van het schilderij.

En dan het gouden duo dat mij over de eindstreep gaat helpen: de paranimfen! Na jullie vertrek werd het voor mij wel erg stil op het RMI. **Myrte**, wat heb jij een eeuwig optimisme en vooral aanstekelijke energie! Je hebt mij een paar keer zo ver gekregen mee te gaan hardlopen na het werk. Enigszins frustrerend werd het toen ik met mijn rode, bezwete hoofd zag dat jij uit verveling rondjes om mij heen kon lopen. Een kijkje in jouw VTA zou bij de vervolgstudies moeten staan;) Je was er altijd om me te helpen en, niet onbelangrijk, om me weer helemaal op de hoogte te brengen van alle 'nieuwtjes'. **Esther**, ik leerde je kennen tijdens mijn stage. Toen Roger naar je toe kwam met de vraag 'Ik wil Margriet de OIO baan aanbieden, wat denk jij?' heb je geantwoord 'Prima, zo'n rustig type, daar zullen we niet veel last van hebben!'. Ik geloof dat je daar al snel op terug moest komen! Met jou een kamer delen was super! Ik moet wel eerlijk opbiechten dat één van je plantjes (wat was jij fanatiek met je stekjes!) na je vertrek niet aan verwaarlozing ten onder is gegaan, maar door ethanol (het leek op water!). 'Jack' was een veelvoorkomend onderwerp op onze kamer en ik ben blij dat jij hem tijdens je 'Holiday' gevonden hebt!

Er is leven naast een promotie! En daarbij waren de volgende mensen voor mij erg belangrijk:

Ank, ik heb je leren kennen tijdens de studie fysiotherapie en je bent één van mijn meest dierbare vriendinnen geworden. In het begin moest je even wennen aan die lawaaierige Uf die ijsklontjes naar je gooide in de kroeg, maar uiteindelijk durfde je het zelfs aan om mijn huisgenootje te worden. Dankzij jou heb ik Gom leren kennen en ik kan nu zeggen: 'I returned (swiped) the favor!'. Je bent mijn favoriete meubelstuk in huis en ook Jasmijn en Elin zijn dol op hun 'tantAnk'!

Mirjam, al snel nadat je kwam hospiteren werden we beste vriendinnen! Met name door jou kan ik zeggen dat mijn studententijd niet mooier had kunnen zijn. Als Jut en Jul deden dezelfde studie, woonden in hetzelfde huis en zaten in dezelfde jaarclub. Wat hebben we veel meegemaakt: onze huisgenoot op Smaragdplein, opgesloten worden op de IBB, samenwonen op 11m^2, in een Porsche op volle snelheid over de A2 (we leven nog!), een riem ophalen in Amsterdam gevolgd door Chris Zegers en Bou(!) en vele avonden met gratis biertjes en taxi's. Ik vergeet nog een heleboel en ik hoop dat er nog een heleboel aan de lijst toegevoegd gaat worden! Om te beginnen met twee mooie kereltjes!

Als ik denk aan mijn middelbare school, denk ik aan jou **Debbie**. De vakken Latijn, Geschiedenis en Engels halen bij mij fantastische herinneringen op. Maar het lag natúúrlijk nooit aan ons:) Desondanks haalden we goede cijfers en konden we samen naar Utrecht. Na een moeizame start op de trap van het Stratenum hebben we onze uiteindelijke draai gevonden. Maar hoe heerlijk was het om af en toe het Utrechtse uitgaansleven af te wisselen met dat in Zundert! Na een paar biertjes was mijn Brabants weer vloeiend! Ook al woon je ver weg, als we elkaar weer zien, is het als vanouds!

Eline, jaren hebben we samen getennist en de honden uitgelaten. Je woont alweer ruime tijd op steenworp afstand van het Mastbos en mijn voornemen is dan ook om je weer veel vaker op te komen zoeken! **Elise**, soms lange tijd uit het oog, maar zeker niet uit het hart. We kennen elkaar al sinds de luier en ik hoop je met de rollator nog steeds te zien!

Pram, **Plof**, **Carmen**, **Sherry**, **Bennie**, **Kip**, **Marcella**, **Marieke**, **Blair**, **Britno**, **Stefanie**, **Ymkje** en **Viola**. Vriendinnetjes voor het leven, deze ouwe topper gaat eindelijk over de finish!

Tim en Marjolein, als bijna-buren en goede vrienden hebben jullie veel meegekregen van alle perikelen rondom mijn promotie. Om in NS termen te spreken: er was sprake van enige vertraging, maar het dossier kan nu officieel worden gesloten!

Mijn collega's op het **Julius Centrum**, kamer 7.101, bedankt voor jullie interesse en betrokkenheid.

Jos en **Celine**, bedankt voor jullie interesse in mijn promotie en fijn dat jullie het alweer zo lang volhouden binnen onze familie!

'Hi sis', zo beginnen altijd onze berichtjes. Lieve **Renske,** ondanks al je waarschuwingen moest ik toch zo nodig ook promoveren. En ik kan alleen maar zeggen, je had gelijk;) Vaak heb ik je ge-'hi-sis'-t om je om raad te vragen, dank voor de final touch aan de lekensamenvatting. En die schoenen... daar moeten we het nog maar eens over hebben. Mijn lieve broer(tje) **Rob**. Zo fanatiek als onze grote zus zijn wij alletwee nooit geweest, maar we komen er wel. Terwijl ik zat te ploeteren aan dit boekje, werkte jij hard aan je Master 'iets met internet en marketing'. Ik ben supertrots dat je ondanks je drukke leven die mastertitel bijna op zak hebt!

Lieve **papa** en **mama**, iedere keer als ik weer met de kinderen op de stoep stond om bij jullie in alle rust aan mijn proefschrift te kunnen werken, grapten jullie: 'Als we maar wel in je dankwoord komen!'. Wat is het ontzettend bijzonder hoe jullie keer op keer voor me klaar staan! Ik voel me gezegend dat ik in een gezin heb mogen opgroeien waarin we vrij gelaten werden in onze keuzes en waarbij humor de boventoon voert. Dank jullie wel voor alles!

En dan mijn lieve meisjes, **Jasmijn** en **Elin**. Zoals Dora zou zeggen: 'We did it, yes yes, we did it!'. Ik heb genoten van de 'thee en gebakjes' die jullie me vaak kwamen brengen tijdens het schrijven!

'Hoe houdt die jongen het toch met je uit?' Een vraag die me vaak voor de grap is gesteld. Lieve **Gom**, als iemand weet hoe zwaar het is om samen te leven met een promovendus ben jij het wel. 'Heeft die laptop van je vleugels?! Want ik ga hem nu leren vliegen!' riep ik vaak boos als iets weer niet lukte. Inmiddels zijn we talloze verbouwingen, twee (bijna drie) kinderen en een knievalletje-ringetje verder en is het boekje eindelijk daar. Dank je wel voor alles wat je voor me hebt gedaan! Bij jou ben ik thuis, drie emmertjes vol!